QC
1
.456
v.64A
no.5

Volume 64A

Number 5

Sept.–Oct. 1960

OCT
LIBRARY

Journal of Research

of the

NATIONAL BUREAU OF STANDARDS

A. PHYSICS AND CHEMISTRY

Journal of Research

of the

National Bureau of Standards

A. Physics and Chemistry

SEPT.–OCT. • 1960

VOLUME • 64A

NUMBER • 5

Editor: U. Fano

Associate Editors: L. M. Kushner
J. M. Richardson

Publication dates:
Feb. 1, Apr. 1, June 1, Aug. 1, Oct. 1, Dec. 1, 1960.

JOURNAL OF RESEARCH

The National Bureau of Standards Journal of Research reports research and development in the fields of activity shown at right. Also included from time to time are survey articles on topics closely related to the Bureau's scientific and technical program.

The Journal is published in four separate sections as follows:

A. Physics and Chemistry

Contains papers of interest primarily to scientists working in these fields. Issued six times a year. Annual subscription: domestic, $4.00; foreign, $4.75.

B. Mathematics and Mathematical Physics

Presents studies and compilations designed mainly for the mathematician and the theoretical physicist. Issued quarterly. Annual subscription: domestic, $2.25; foreign, $2.75.

C. Engineering and Instrumentation

Reports research and development results of interest chiefly to the engineer and the applied scientist. Issued quarterly. Annual subscription: domestic, $2.25; foreign, $2.75.

D. Radio Propagation

Reports work in radio propagation, upper atmospheric physics, and communications. Issued six times a year. Annual subscription: domestic, $4.00; foreign, $4.75.

U.S. DEPARTMENT OF COMMERCE
Frederick H. Mueller, Secretary

NATIONAL BUREAU OF STANDARDS
A. V. Astin, Director

Functions and Activities

The functions of the National Bureau of Standards are set forth in the Act of Congress, March 3, 1901, as amended. These include the development and maintenance of the national standards of measurement and the provision of means and methods for making measurements consistent with these standards; the determination of physical constants and properties of materials; the development of methods and instruments for testing materials, devices, and structures; advisory services to government agencies on scientific and technical problems; invention and development of devices to serve special needs of the Government; and the development of standard practices, codes, and specifications. The work includes basic and applied research, development, engineering, instrumentation, testing, evaluation, calibration services, and various consultation and information services. The Bureau also serves as the Federal technical research center in a number of specialized fields. The scope of activities of the National Bureau of Standards is suggested in the following listing of the divisions and sections engaged in technical work.

Washington, D.C.

Electricity. Resistance and Reactance. Electrochemistry. Electrical Instruments. Magnetic Measuments. Dielectrics.

Metrology. Photometry and Colorimetry. Refractometry. Photographic Research. Length. Engineering Metrology. Mass and Scale. Volumetry and Densimetry.

Heat. Temperature Physics. Heat Measurement. Cryogenic Physics. Rheology. Molecular Kinetics. Free Radicals Research. Equation of State. Statistical Physics. Molecular Spectroscopy.

Radiation Physics. X-ray. Radioactivity. High Energy Radiation. Radiological Equipment. Nucleonic Instrumentation. Neutron Physics. Radiation Theory.

Chemistry. Surface Chemistry. Organic Chemistry. Analytical Chemistry. Inorganic Chemistry. Electrodeposition. Molecular Structure and Properties of Gases. Physical Chemistry. Thermochemistry. Spectrochemistry. Pure Substances.

Mechanics. Sound. Pressure and Vacuum. Fluid Mechanics. Engineering Mechanics. Combustion Controls.

Organic and Fibrous Materials. Rubber. Textiles. Paper. Leather. Testing and Specifications. Polymer Structure. Plastics. Dental Research.

Metallurgy. Thermal Metallurgy. Chemical Metallurgy. Mechanical Metallurgy. Corrosion. Metal Physics.

Mineral Products. Engineering Ceramics. Glass. Refractories. Enameled Metals. Constitution and Microstructure.

Building Technology. Structural Engineering. Fire Protection. Air Conditioning, Heating, and Refrigeration. Floor, Roof, and Wall Coverings. Codes and Safety Standards. Heat Transfer. Concreting Materials.

Applied Mathematics. Numerical Analysis Computation. Statistical Engineering. Mathematical Physics.

Data Processing Systems. SEAC Engineering Group. Components and Techniques. Digital Circuitry. Digital Systems. Analog Systems. Applications Engineering.

Atomic Physics. Spectroscopy. Radiometry. Mass Spectrometry. Solid State Physics. Electron Physics. Atomic Physics.

Instrumentation. Engineering Electronics. Electron Devices. Electronic Instrumentation. Mechanical Instruments. Basic Instrumentation.

• Office of Weights and Measures.

Boulder, Colorado

Cryogenic Engineering. Cryogenic Equipment. Cryogenic Processes. Properties of Materials. Gas Liquefaction.

Radio Propagation Physics. Upper Atmosphere Research. Ionosphere Research. Regular Prediction Services. Sun-Earth Relationships. VHF Research. Radio Warning Services. Airglow and Aurora. Radio Astronomy and Arctic Propagation.

Radio Propagation Engineering. Data Reduction Instrumentation. Radio Noise. Tropospheric Measurements. Tropospheric Analysis. Propagation-Terrain Effects. Radio-Meteorology. Lower Atmospheric Physics.

Radio Standards. High-Frequency Electrical Standards. Radio Broadcast Service. Radio and Microwave Materials. Electronic Calibration Center. Microwave Circuit Standards.

Radio Communication and Systems. Low Frequency and Very Low Frequency Research. High Frequency and Very High Frequency Research. Modulation Systems. Antenna Research. Navigation Systems. Systems Analysis. Field Operations.

Order all publications from the Superintendent of Documents, U.S. Government Printing Office, Washington 25, D.C.

Use of funds for printing this publication approved by the Director of the Bureau of the Budget (June 24, 1958).

DEPOSITED BY THE
UNITED STATES OF AMERICA

JOURNAL OF RESEARCH of the National Bureau of Standards—A. Physics and Chemistry
Vol. 64, No. 5, September–October 1960

Infrared Spectrum of Hydrobromic Aid

Earle K. Plyler

(April 21, 1960)

A precise measurement of the infrared fundamental bands of HBr^{79} and HBr^{81} has been made. The two band centers have been found to be 2,558.94 and 2,558.56 cm^{-1}, respectively. Rotational and vibrational constants have been calculated from the observed data. The constants are in good agreement with previous reported values. The centers of the two harmonic bands were used to calculate $\omega_e x_e$ and $\omega_e y_e$ and they were found to be 45.58 and 0.072 cm^{-1}, respectively, for HBr^{79} and 45.56 and 0.072 cm^{-1} for HBr^{81}.

1. Introduction

Hydrobromic acid was one of the first molecules whose spectrum was determined with a spectrometer of good resolution.[1] The spectrum showed a series of lines which made up the P- and R-branches of the band. With improved instruments it was possible to partially resolve some of the lines of the fundamental band into two components.[2] These components arise from the two isotopes of bromine and the separation is about 0.4 cm^{-1}. Naudé and Verleger [3] measured the 4–0 band of HBr in the photographic region and separated the isotopic bands. They calculated the rotational constants and their values will be compared with the results reported in this paper. More recently Thompson, Williams, and Callomon [4] have measured the fundamental band with high resolution and have been able to separate the individual lines into two components. While the observed and calculated positions of the lines reported by them showed good agreement, it was thought that the absolute values of the line positions might be in error. A preliminary scan of the spectrum revealed that all the wavenumbers of the lines of HBr^{79} and HBr^{81} as measured by Thompson, Williams, and Callomon were too small by about 0.15 cm^{-1} and it was felt that a more precise measurement of the spectrum was needed so that this band could be used as a reference standard for calibration in the infrared region. Also, it was expected that a more accurate set of molecular constants could be obtained.

2. Experimental Results

The spectrum of HBr was observed on a high resolution spectrometer containing a grating with 10,000 lines/in. The ruled surface was 8¼ in. and was used double pass. A cool lead sulfide cell served as the detector and the resolution of the instrument was about 0.04 cm^{-1}. The components of a line arising from HBr^{79} and HBr^{81} were completely separated. Further details of the instrument are given in a previous paper.[5]

The spectrum was measured by using the fringe system of a Fabry-Perot interferometer as a comparison spectrum. Reference standards were also superimposed on the recorded spectrum. Higher orders of the atomic lines of krypton were found to be well suited for the comparison spectrum.

A further method of insuring the absolute positions of the lines was employed. This method consisted of overlapping a section of the spectrum of HBr with that of the spectrum of HCl by putting both gases in the absorption cell, and then using the accurately known HCl lines as standards for the measurement of the HBr spectrum.

Figure 1 shows a section of the HBr spectrum from $R5$ through $R10$ overlapping the HCl spectrum from $P8$ to $P10$. The wavenumbers for the HBr lines from $R5$ to $R10$ as found by the two methods of measurement agreed to ± 0.01 cm^{-1} and this result indicated that the absolute position of the band was well determined.

In order to have sufficient bands for determining the anharmonic terms $\omega_e x_e$ and $\omega_e y_e$ several lines of the first harmonic band were measured.

The calculated and observed positions of the rotational lines of the fundamental bands of HBr^{79} and HBr^{81} are listed in table 1. The values of the molecular constants were calculated and are listed in table 2. The following equation was used in determining the rotational constants:

$$\nu=\nu_0+(B_1+B_0)m+(B_1-B_0-D_1+D_0)m^2-(2D_1+2D_0-H_1-H_0)m^3-[(D_1-D_0)-3(H_1-H_0)]m^4+3(H_1+H_0)m^5 \quad (1)$$

where $m=J+1$ for the R-branch and $-J$ for the P-branch. The data of table 1 were reduced by means of an electronic computer.

The terms ω_e, $\omega_e x_e$, and $\omega_e y_e$ are found by using the following equations:

$$\left.\begin{aligned} \nu_{1-0}&=\omega_e-2\ \omega_e x_e+3¼\ \omega_e y_e, \\ 2\nu_{1-0}-\nu_{2-0}&=2\omega_e x_e-9\ \omega_e y_e, \\ 4\nu_{1-0}-\nu_{4-0}&=12\omega_e x_e-78\ \omega_e y_e. \end{aligned}\right\} \quad (2)$$

[1] H. M. Randall and E. S. Imes, Phys. Rev. **15,** 152 (1920).
[2] E. K. Plyler and E. F. Barker, Phys. Rev. **44,** 984 (1933).
[3] S. H. Naudé and H. Verleger, Proc. Phys. Soc. **63A,** 470 (1950).
[4] H. W. Thompson, R. L. Williams, and H. J. Callomon, Spectrochimica Acta **5,** 313 (1952).
[5] E. K. Plyler and L. R. Blaine, J. Research NBS **62,** 7 (1959) RP2922.

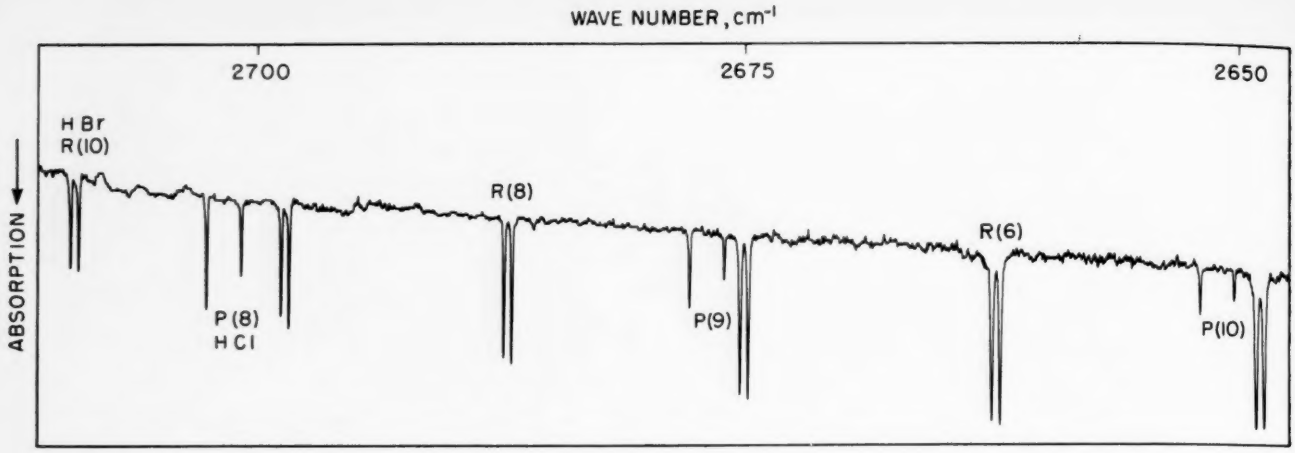

FIGURE 1. *The absorption spectrum of* HBr *from R5 to R10 and* HCl *from P8 to P10.*

The pressure of each gas was 2.5 mm with a cell length of 6 m.

TABLE 1. *The observed and calculated positions of the lines of the fundamental bands of* HBr^{79} *and* HBr^{81}

J	P_{obs}	P_{obs}	P_{calc}	P_{calc}	$P_{obs-calc}$	$P_{obs-calc}$
			HBr^{79}			
0	2,575.181	----------	2,575.176	----------	0.005	----------
1	2,590.945	2,542.240	2,590.939	2,542.237	.006	0.003
2	2,606.221	2,525.075	2,606.222	2,525.079	−.001	−.004
3	2,621.012	2,507.472	2,621.016	2,507.472	−.004	.000
4	2,635.314	2,489.423	2,635.314	2,489.427	.000	−.004
5	2,649.110	2,470.949	2,649.111	2,470.953	−.001	−.004
6	2,662.392	2,452.063	2,662.392	2,452.059	.000	.004
7	2,675.155	2,432.757	2,675.156	2,432.756	−.001	.001
8	2,687.393	2,413.060	2,687.395	2,413.055	−.002	.005
9	2,699.102	2,392.964	2,699.100	2,392.968	.002	−.004
10	2,710.266	----------	2,710.263	----------	.003	----------
11	2,720.876	----------	2,720.871	----------	.005	----------
12	2,730.928	----------	2,730.931	----------	−.003	----------
13	2,740.421	----------	2,740.420	----------	.001	----------
14	2,749.333	----------	2,749.333	----------	.000	----------
			HBr^{81}			
0	2,574.789	----------	2,574.790	----------	−0.001	----------
1	2,590.555	2,541.865	2,590.549	2,541.862	.006	0.003
2	2,605.831	2,524.710	2,605.827	2,524.709	.004	.001
3	2,620.612	2,507.102	2,620.616	2,507.108	−.004	−.006
4	2,634.907	2,489.062	2,634.909	2,489.068	−.002	−.006
5	2,648.701	2,470.598	2,648.699	2,470.598	.002	.000
6	2,661.976	2,451.718	2,661.977	2,451.709	−.001	.009
7	2,674.732	2,432.408	2,674.737	2,432.411	−.005	−.003
8	2,686.969	2,412.717	2,686.972	2,412.714	−.003	.003
9	2,698.674	2,392.628	2,698.678	2,392.630	−.004	−.002
10	2,709.842	----------	2,709.844	----------	−.002	----------
11	2,720.448	----------	2,720.444	----------	.004	----------
12	2,730.494	----------	2,730.498	----------	−.004	----------
13	2,739.988	----------	2,739.989	----------	−.001	----------
14	2,748.907	----------	2,748.906	----------	.001	----------

The observed wavenumbers of ν, 2ν, and 4ν and the calculated values of ω_e, $\omega_e x_e$, and $\omega_e y_e$ are given in table 3. The band centers for ν and 2ν have been determined in this work, but the value of 4ν has been taken from the work of Naudé and Verleger (see footnote 3, page 377).

The constants reported in table 2 are in good agreement with the results of Naudé and Verleger and

TABLE 2. *The calculated constants of* HBr^{79} *and* HBr^{81} *in* cm^{-1}

Constant	HBr^{79}	HBr^{81}
ν_0	2,558.939 ±.001	2,558.559 ±.001
B_1	8.1190 ±.0001	8.1165 ±.0002
B_0	8.3516 ±.0001	8.3490 ±.0002
D_1	3.37 ±.02 ×10⁻⁴	3.37 ±.02 ×10⁻⁴
D_0	3.49 ±.02 ×10⁻⁴	3.48 ±.02 ×10⁻⁴
H	6.8 ±1 ×10⁻⁸	5.8 ±1 ×10⁻⁸
α	0.2325 ±.00007	0.2325 ±.0001
B_e	8.4678 ±.0001	8.4652 ±.0001
B	1.12 ±.11 ×10⁻³	1.10 ±.11 ×10⁻³
D_e	3.54 ±.02 ×10⁻⁴	3.52 ±.02 ×10⁻⁴

those of Thompson, Williams, and Callomon, but the reported values differ more than the estimated accuracy given in the different reports. The greatest difference between the results reported in this paper and those of Thompson, Williams, and Callomon is the position of the band centers. They report ν_0= 2,558.76 cm^{-1} for HBr^{79} and ν_0=2,558.40 cm^{-1} for

TABLE 3. *The vibrational constants of* HBr^{79} *and* HBr^{81} *in* cm^{-1}

Constant	HBr^{79}	HBr^{81}
ν	2,558.939	2,558.559
2ν	5,027.378	5,026.636
4ν	9,694.495	9,693.151
ω_e	2,649.855	2,644.450
$\omega_e x_e$	45.576	45.564
$\omega_e y_e$	0.0724	0.0726

HBr^{81}, while our measurements give the band centers at 2,558.94 cm^{-1} and 2,558.56, respectively. Also, the B_0 values for the two molecules are greater by 0.0018 cm^{-1} in the measurements of Thompson, Williams, and Callomon than calculated from our measurements. It is believed that the molecular constants of HBr here presented are more precise than any previously reported. The probable error

of the constants have been calculated and are included in table 2.

On the condition that the ratio of the molecular constants for HBr^{79} and HBr^{81} are only a function of the masses, the constants listed in table 2 for HBr^{81} have been calculated from the values of HBr^{79}. The agreement between the molecular constants of HBr^{81} calculated from the measured lines listed in table 1 and the values calculated from HBr^{79} by the isotopic effect are all within the limit of the listed experimental error. This indicates that the relative values of the molecular constants for HBr^{79} and HBr^{81} are in excellent accord.

The error in the constants D and H is larger than in the B values. Only when a band has many lines which include large J values do these constants have a significant effect on a line position. That is, from eq (1) it is seen that the greatest contribution of H and D to the line position occurs in the terms m^3, m^4, and m^5.

There are relationships between the molecular constants so that some of them can be calculated from the known values of others. For example, D_e can be obtained from B_e and ω_e by the following relation:

$$D_e=4B_e^3/\omega_e^2. \tag{3}$$

From the above relation $D_e=3.459\times10^{-4}$ cm^{-1} for HBr^{79} and $D_e=3.457\times10^{-4}$ cm^{-1} for HBr^{81}. These calculated constants are about two percent smaller than those obtained from the experimental data.

The author is indebted to Jessie Kirkland and Mary C. Dannemiller for assistance in reducing the data.

(Paper 64A5–62)

JOURNAL OF RESEARCH of the National Bureau of Standards—A. Physics and Chemistry
Vol. 64A, No. 5, September–October 1960

Determination of the Value of the Faraday With a Silver-Perchloric Acid Coulometer

D. Norman Craig, James I. Hoffman, Catherine A. Law, and Walter J. Hamer

(June 2, 1960)

An accurate value of the faraday has been determined by the electrolytic dissolution of metallic silver in aqueous solutions of perchloric acid. Standards of electric current, mass, and time as maintained by the National Bureau of Standards were utilized in the determinations. The electric current was measured in terms of the standards of electromotive force and electrical resistance. Silver of high purity, freed from oxygen, was used.

The value of the faraday was found to be

faraday = 96516.5 ± 2.4 coulombs gram-equivalent^{-1} (physical scale),

faraday = 96490.0 ± 2.4 coulombs gram-equivalent^{-1} (chemical scale).

These values were obtained using 107.9028 ± 0.0013 and 107.8731 ± 0.0013, for the atomic weight of silver on the physical and chemical scales, respectively.

The electrochemical equivalent of silver was found to be

electrochemical equivalent of silver = 1.117972 ± 0.000019 milligram coulomb^{-1}.

This value may be used in an alternate method of defining the ampere in absolute value, namely, that steady current which will dissolve 1.117972 milligrams of silver per second and depends only on the standards of mass and time. The indicated uncertainties are overall limits of error based on 95 percent confidence limits for the mean and allowances for the effects of known sources of possible systematic error.

1. Introduction

The classic method for the determination of the faraday involves the electrolytic deposition of silver on platinum from an aqueous solution of silver nitrate. This method has been extensively studied and under closely specified conditions [1] [1] was used for many years in defining the international ampere. In the original work at the National Bureau of Standards the national standards of electric current, mass, and time were used, and great emphasis was placed on the reproducibility of the method as a check on the stability of the existing standards of electromotive force (Weston cell) and electrical resistance (mercury ohm). In 1916 Rosa and Vinal [2] summarized the work that had been done with the silver coulometer not only in yielding a value of the faraday but also in attaining conditions wherein reproducible results could be obtained. At that time the consensus was that the silver coulometer gave highly accurate as well as reproducible results and yielded a value of the faraday accurate to within 0.001 percent (10 ppm).

However, 4 years earlier (in 1912) Washburn and Bates [3] had proposed an improved [2] iodine coulometer for which high reproducibility and accuracy were claimed. In 1914 Vinal and Bates [8, 9] made a direct comparison of the silver and iodine coulometers in the laboratories of NBS and found that the two methods yielded different values for the faraday. Since the two types of coulometers were run in series the ratio of the results given by the two methods was independent of the electrical units and the durations of the runs. The result obtained with the iodine coulometer was 220 ppm higher than that given by the classic silver method. To date this discrepancy has not been resolved conclusively.[3]

In the ensuing years the silver coulometer has been criticized on two main counts: (1) a partial separation of the isotopes of silver may occur during the deposition, and (2) the silver deposits may contain occlusions of electrolyte (silver nitrate), acid (nitric acid), and water, alone or in combination. The first criticism does not appear to be valid judging from the results of the most precise determinations [12, 13] on the atomic weight of silver wherein in some cases the silver was reported to have been purified by repeated electrolysis. It will be shown later in this paper that no measurable separation of the isotopes of silver occurs on one, two, or three successive electrolyses; therefore, the first criticism is, in fact, not pertinent. Vinal and Bovard [14] studied the

[1] Figures in brackets indicate the literature references at the end of this paper.

[2] The iodine coulometer had been studied earlier by Herroun [4], Danneel [5], Kreider [6], and Gallo [7] but these experimenters did not claim high accuracy for their work.

[3] In recent years two new methods, one a physical method using an omegatron [10] and the other an electrochemical method involving the anodic oxidization of sodium oxalate [11] have been reported. These are not considered here.

occlusion problem at length and observed a loss in weight when the silver deposits were heated to slightly above 600° C. They attributed this loss in weight to occluded foreign matter which was released on heating. This loss in weight amounted to a correction of only 0.004 percent in the faraday and was insufficient to explain the discrepancy between the silver and iodine values. Others [15 to 18] who worked on the problem found occlusions, the amounts of which varied from 0.004 to 0.016 percent. In all this work it is evident that corrections for occlusions remain uncertain.

Although the iodine coulometer has received less criticism in the ensuing years, the iodine value for the faraday has not been generally accepted. Vinal and Bates discussed the possible sources of error in each method but did not indicate a preference for either method. Instead they recommended that a rounded value of the average of the values given by the two methods, namely 96,500 international coulombs per gram-equivalent, be adopted for general use. It is somewhat surprising that this situation has persisted more or less to the present time. One reason for this lies in the fact that the national standardizing laboratories were engaged in work leading to the conversion from international to absolute electrical units. Two World Wars had caused delays in the necessary experimental work. When this conversion was finally realized on January 1, 1948, it was then deemed an appropriate time to redetermine the faraday. Several electrochemical methods were considered and of all those considered the one presented here was considered to be the most promising.

Because of the two main criticisms of the silver coulometer a method wherein these would not be valid would be desirable. Electrolytic dissolution (or corrosion) of metallic silver at once suggests itself. Occlusions could play no part in electrolytic dissolution of pure silver. Also, isotopic separation would be eliminated a priori (see p. 393), since whole (or bulk) silver would be uniformly dissolved electrolytically. This method using an electrolyte of silver nitrate was used in a few qualitative experiments by Mascart [19] and Gray [20]. Also, Rosa, Vinal, and McDaniel [21] investigated the electrolytic dissolution of silver in silver nitrate in studies of the reversibility of the silver coulometer. Their results, although generally overlooked, indicate good reversibility. Their anode consisted of silver deposited electrolytically on platinum and the loss in weight agreed well indeed with the gain in weight in a conventional coulometer, run in series, wherein the silver was deposited electrolytically. In two runs, electrolytic deposition gave 96,494 whereas electrolytic dissolution of silver gave 96,488 international coulombs gram-equivalent^{-1}.

These two experiments of Rosa, Vinal, and McDaniel, therefore, showed that the silver coulometer was reversible to at least 6 parts in 100,000. However, the silver anodes that were corroded had been prepared by electrolytic deposition and were, therefore, subject to occlusion errors. Furthermore, Rosa, Vinal, and McDaniel stated that the amount of silver on the platinum bowl should not fall below a critical amount and that a large surface of silver should be used. If the current density became too high, or the amount of silver on the platinum too small, current flowed from the underlying platinum whereby simultaneous reactions occurred at the anode. Although not stated by Rosa, Vinal, and McDaniel, silver oxide or oxygen probably formed at the exposed platinum in the neutral silver nitrate solution if the current density became too high. Since silver oxide is not appreciably soluble in silver nitrate it would be included in the anode sediment (the silver that fell from the anode during the electrolysis) which must be weighed at the end of an experiment; this silver oxide would thus cause errors. Likewise, if oxygen were formed at the anode in neutral silver nitrate solution it would escape to the atmosphere also causing errors in faraday determinations.

It is obvious, therefore, if a method wherein silver is electrolytically dissolved is to be considered seriously for a determination of the faraday, these sources of error must be eliminated or reduced to a minimum. This may be done (1) by using silver anodes thereby eliminating platinum entirely, and (2) by using an acid electrolyte in which silver is highly stable but in which the silver salt is freely soluble. By using an acid solution the formation of silver oxide would be precluded as well as the formation of oxygen (see below). The problem then rested in finding the proper electrolyte to use with silver anodes so that the electrochemical reaction:

$$\text{Ag (metal)} \rightarrow \text{Ag}^{+} \text{ (ions)} + \epsilon\text{(electrons)}$$

would proceed quantitatively without any side reactions.

Of all the electrolytes considered or studied it was found that perchloric acid was the most suitable and was used in some preliminary studies by Craig and Hoffman [22]. The stability (or solubility) of silver in perchloric acid, in the absence of current flow, has recently been studied in detail [23]. It was found that silver is highly stable in perchloric acid (20 wt %), more stable in perchloric acid (20 wt %) containing a small amount (0.5 wt %) of silver perchlorate, and practically inert in conductivity water. The stability is such as to cause negligible errors in faraday determinations.

Although occlusion errors are eliminated in the method described herein, the purity of the silver remains a most important problem. The purity of deposits (old method) and the purity of silver used as anodes (new method) are equally important. Fortunately, however, extremely pure silver may be prepared for use in the present method whereas the determinations of the occlusions in silver deposits is extremely difficult. The most insidious impurity that is encountered in preparing pure silver is oxygen either as the element or combined as silver oxide. When it is present as free or uncombined oxygen it introduces an error which is proportional to its con-

centration. When combined as the oxide 16 parts of oxygen are equivalent to 232 parts of silver oxide which is chemically soluble in perchloric acid, and, accordingly, its presence as combined oxygen in the starting silver would cause appreciably larger errors in determining the faraday (this is discussed in more detail in appendix 1 to this paper).

2. Method and Coulometer

2.1. Method

The method consists simply of the electrolytic dissolution of metallic silver in aqueous solutions of perchloric acid (20 wt %) initially containing a small amount (0.5 wt %) of silver perchlorate according to the electrochemical reaction:

$$\text{Ag (metallic)} \xrightarrow{\text{HClO}_4 \text{ and } \text{AgClO}_4} \text{Ag}^+ \text{ (ions)} + \epsilon^- \text{(electrons)}$$

wherein silver (the anode) is electrolytically oxidized to argentous ions. Metallic silver, in sheet or rod form, is used. It is weighed before and after the passage of a known current through the coulometer for a known time. Platinum gauze is used as the cathode. Silver perchlorate is added to the perchloric acid in the small amount stated above to reduce the chemical solubility of silver in perchloric acid to an insignificant amount [23]. Sufficient silver oxide is initially added to the solution around the platinum cathode to provide silver ions so that silver is deposited throughout the run on the cathode and discharge of hydrogen ions and formation of hydrogen gas on the cathode are prevented; turbulence at the cathode and within the coulometer is thereby prevented.

2.2. Coulometer

A schematic view of the coulometer is given in figure 1 and a photograph in figure 2. The silver anode is housed in a Pyrex beaker, the platinum cathode in a separate Pyrex beaker, and the solutions in the two beakers are brought into contact by two siphons and an intermediate beaker. In some cases two intermediate beakers and three siphons were used (see photograph). The coulometer was housed in a plastic cabinet to minimize exposure of the solution to dust and fumes. The diagram as shown in figure 1 is self-explanatory except for the reference silver electrode shown at the extreme right. The silver anode, during electrolysis, exhibits a potential, the value of which depends on the voltage drop in the solution, the concentration of silver ions in its vicinity, and on electrode polarization. As silver goes into solution during the electrolysis these effects change in a systematic manner; evidence of side or undesirable electrode reactions would be indicated by abrupt changes in the potential of the silver anode with respect to the reference (non-corroding) silver electrode. No abrupt change in the potential of the silver anode was observed in any of the coulometric runs.

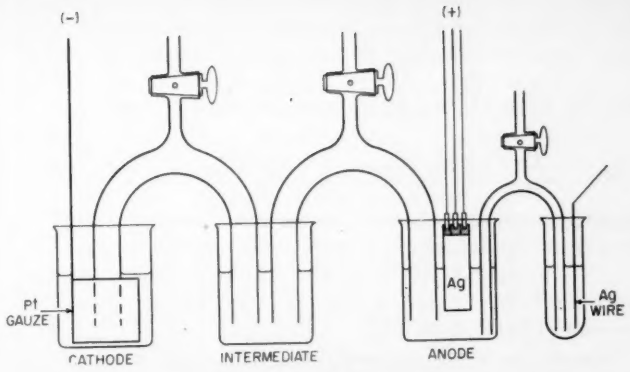

FIGURE 1. *Schematic view of the coulometer.*

FIGURE 2. *Photograph of coulometer with two intermediate beakers.*

Thermodynamic data may be used to show that the reaction at a silver anode in aqueous solutions of perchloric acid is the postulated one. The following electrochemical reactions may conceivably occur at silver anodes in aqueous solutions of perchloric acid containing a small amount of silver perchlorate (such solutions contain Ag^+, ClO_4^-, OH^-, and H^+ ions):

(a) $\text{Ag (metallic)} \longrightarrow \text{Ag}^+ + \epsilon^-$, $\quad E° = -0.799$ v

(b) $\text{Ag (metallic)} + \text{ClO}_4^-, (aq) \longrightarrow \text{AgClO}_4(aq) + \epsilon^-$, $\quad E° = -0.799$ v

[(c) $\text{Ag (metallic)} + \text{OH}^-, (aq) \longrightarrow (\tfrac{1}{2})\text{Ag}_2\text{O} + (\tfrac{1}{2})\text{H}_2\text{O}\ (l) + \epsilon^-$],

(d) $(\tfrac{1}{2})\text{H}_2\text{O}\ (l) \longrightarrow (\tfrac{1}{4})\text{O}_2(g) + \text{H}^+ + \epsilon^-$, $\quad E° = -1.229$ v

(e) $\text{H}_2\text{O}\ (l) \longrightarrow (\tfrac{1}{2})\text{H}_2\text{O}_2\ (aq) + \text{H}^+ + \epsilon^-$, $\quad E° = -1.77$ v

(f) $(\tfrac{1}{2})\text{Ag (metallic)} \longrightarrow (\tfrac{1}{2})\text{Ag}^{++} + \epsilon^-$, $\quad E° = -1.39$ v

where *aq* represents aqueous solution, *l* liquid, and *g* gas. Since $AgClO_4$ is completely dissociated into silver and perchlorate ions, reaction (b) is equivalent to reaction (a). Since Ag_2O dissolves or reacts readily with $HClO_4$ according to the reaction:

$$(g)\quad (\tfrac{1}{2})Ag_2O+HClO_4\longrightarrow AgClO_4+(\tfrac{1}{2})H_2O$$

reaction (c) combined with (g) is equivalent to reaction (b) which in turn is equivalent to reaction (a). The standard electrode (or oxidation-reduction) potentials are listed above for the pertinent eletrochemical processes [24].

Since the reaction requiring the least free energy will occur in preference to those of higher free energy, reactions other than reaction (a) will occur only to a negligible extent unless the overpotential for silver dissolution is high, of the order of 0.5 to 1.2 v. Measurements of the potentials of the silver anodes relative to the reference silver electrode throughout the experiments showed that these potentials, when concentration differences and *IR* drop were considered, were very close to the standard silver potential; accordingly, then, reaction (a) takes place in the electrolytic dissolution of silver in aqueous perchloric acid and the other reactions are negligible. In the above the standard potentials were used. Actually, the potentials corresponding to the perchloric acid-silver perchlorate solution should be used. However, the differences between the standard potentials and those corresponding to the solutions of perchloric acid-silver perchlorate are so small as not to alter the above conclusion.

Since the above electrode potentials relate to reactions in solutions free of oxygen some considerations must be given to errors that might have arisen from the oxygen dissolved in the solutions during the faraday determinations. Two reactions are involved, viz:

$$2Ag+(1/2)O_2\rightarrow Ag_2O,$$

followed by

$$(g)\quad Ag_2O+2HClO_4\rightarrow 2AgClO_4+H_2O.$$

Both of these reactions are thermodynamically spontaneous. The first reaction is rate controlling and has an extremely slow rate under the conditions prevailing in the faraday determinations. In a careful study the errors that could arise from these reactions were found to be extremely small and are given in a previous paper [23].

The dimensions of the coulometer used with the purified anodes were for the most part as follows:

(a) Anode beaker—5 cm in diameter and 8 cm in height, especially constructed with rounded bottom to facilitate removal of anode sediment; cathode and intermediate beakers 7 cm in diameter and 9 cm in height.

(b) Siphons—2.1 cm in bore, 2.3 cm in outside diameter, 5 cm between legs, 25 cm along center of bore.

(c) Silver anode (sheet form)—4 cm in width, 0.02 to 0.03 cm thick, 1 to 3.5 cm in solution at start of electrolysis.

(d) Silver anode (elliptical rod form)—1.0 to 1.2 cm, major axis; 0.4 to 0.6 cm, minor axis; 1 to 3 cm in solution at start of electrolysis.

(e) Cylindrical platinum cathode—5 cm in height and 4 cm in diameter; 0.1 cm thick gauze.

(f) Reference electrode vessel—glass tube 9 cm in height and 1.5 cm in inside diameter.

(g) Reference silver electrode—wire 10 cm in length and 0.2 cm in diameter.

(h) Siphon (to reference electrode)—0.3 cm in inside diameter, 0.5 cm in outside diameter, 7 cm between legs, 24 cm along center of bore.

During the electrolysis the silver anode dissolves electrolytically and means had to be provided to lower the anode at intervals into the solution. The means by which this was done for sheet anodes is shown in figure 3. The silver anode sheet was suspended in the solution by gold-plated clips. A piece of thin silver foil was bent over the entire top edge of the silver anode so that it was between the anode and the gold-plated clips. In all cases the silver foil and gold-plated clips were above the solution. These gold-plated clips were fastened to other clips by copper wires. The latter clips were clasped to a sheet of brass (⅛ in. thick) which was soldered at the upper middle edge to a brass rod, threaded at its

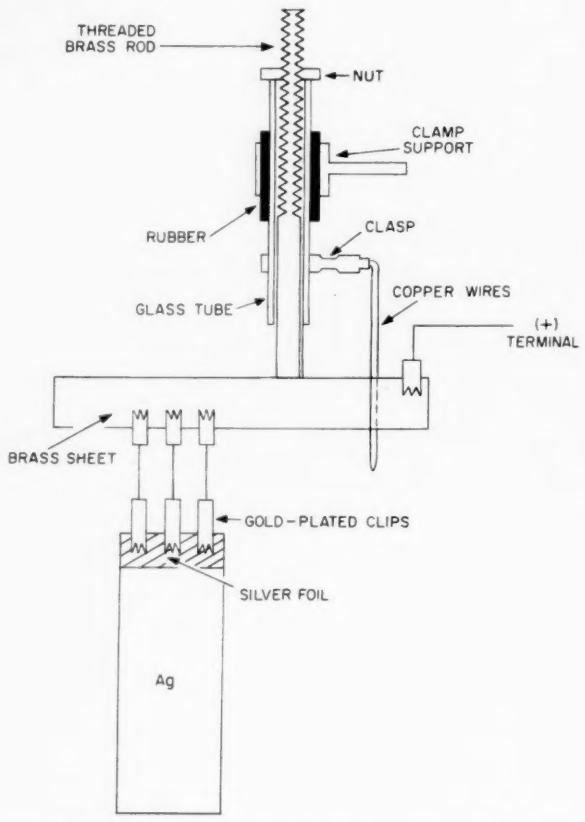

FIGURE 3. *Schematic view of support for silver anode showing the method for lowering the anode into the coulometer solution.*

upper end. The threaded end protruded through a glass tube and the location (height) of the sheet brass and, therefore, the silver anode was adjusted by a nut on the thread placed over the upper end of the glass tube. The glass tube was housed in a rubber stopper supported by a clamp on a ring stand. A clasp was placed around the glass tube and at the outer end of the clasp a copper wire was attached which looped around the sheet of brass; this wire prevented the silver anode from rotating during the lowering process. Current and potential leads were connected to the sheet of brass as indicated in figure 3.

Silver anodes of the elliptical rod form were supported in a different manner. Silver wires were inserted through holes bored in the upper end of the silver rods as shown in figure 4. These wires were looped through the holes several times and were covered with a sheet of silver foil at their upper parts. This silver foil was covered with a second foil and then clasped by gold-plated clips; the rest of the support was identical to that described above. Here also, the wires, silver foil, and gold-plated clips were above the solution.

In these arrangements the question may arise as to whether the electrolyte creeps up the anode and onto the silver foil and gold-plated clips during the electrolysis causing errors in the final results. Repeated checks were made on this possibility by weighing the silver foil over the period of time during which it had been used in experiments. Typical results on the constancy of the weight of the silver foil which was used with sheet anodes are given in table 1. No trend in the weight of the silver foil was observed over a period of 2 months. These data show that any creepage that occurred was insignificant. Similar results were found for the foil used with anodes of the rod type.

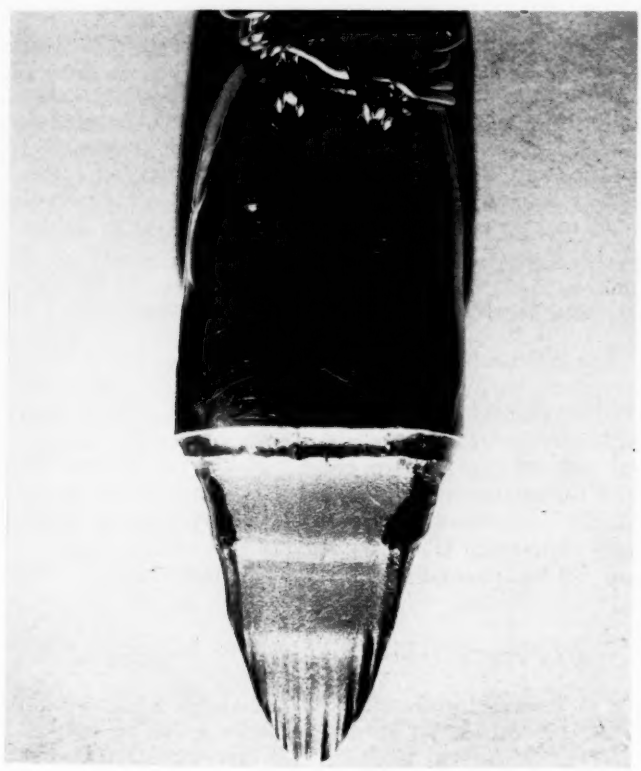

FIGURE 4. *View of a silver anode showing the means of support and corrosion pattern.*

TABLE 1. *Data on the constancy in weight of silver foil used in the support of silver anodes*

Date	Hour	Electrolyses	Weight of silver foil (after electrolyses)
1956			*g*
Aug. 27	4:15 p.m.	None	1.937572
Aug. 29	10:00 a.m.	One	1.937568
Aug. 30	4:00 p.m.	One	1.937556
Aug. 30	8:15 p.m.	None	1.937568
Sept. 16	7:55 p.m.	None	1.937567
Sept. 17	4:00 p.m.	One	1.937558
Sept. 19	4:10 p.m.	One	1.937553
Sept. 23	9:50 p.m.	None	1.937554
Sept. 25	2:15 p.m.	One	1.937572
Sept. 28	3:00 p.m.	One	1.937561
Oct. 25	4:30 p.m.	Three	1.937556

3. Coulometer Circuit

The circuit, sketched in figure 5, consisted of the coulometer with an alternate circuit of equal resistance, approximately 25 ohms (labeled Sub. res.) for use in adjusting the current prior to an actual run; a standard resistor (or resistors), SR; a battery, B; a double pole switch, BS, for connecting the battery to the circuit; two fixed resistors, FR; suitable rheostats, CC, for adjusting the current during the run.

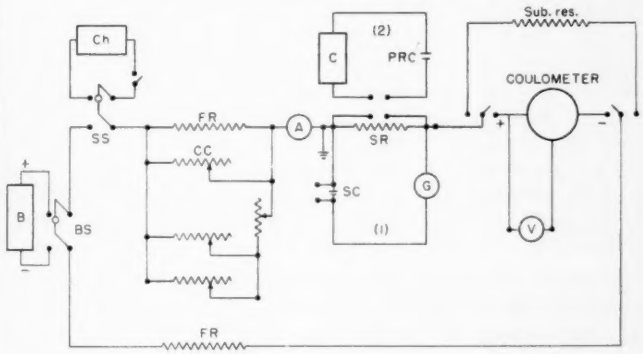

FIGURE 5. *Coulometer circuit.*

(These were in parallel with one of the fixed resistors, FR, which carried approximately 95% of the current.) The circuit also contained an ammeter, A; a chronograph, Ch; a reference silver electrode with a voltmeter, V (25,000 ohms), for measuring the potential of the silver anode during the electrolysis; and a large double-pole switch, SS, for simultaneously closing the coulometer and chronograph circuits. Two parallel circuits, 1 and 2, were used in measuring the *IR* drop across the standard resistors during the run.

4. Constancy and Magnitude of *IR*

The constancy of the *IR* drop across the NBS standard resistor or resistors was maintained by balancing the *IR* drop against the electromotive

force of NBS saturated standard cell No. 1064 using a sensitive galvanometer as null detector (circuit No. 1). Thus, the *IR* drop should be equal to the electromotive force of the standard cell. The galvanometer key was always closed except when opened momentarily from time to time to check the zero. The galvanometer had a nominal sensitivity of 0.0007 μa/mm of scale; actual experimental checks were made during each run and gave 3.5 ppm/mm for the current sensitivity at 0.2 amp for circuit No. 1. Circuit No. 2 consisted of NBS saturated standard cell No. 1073 (PRC) and a Brooks standard cell comparator [25]. Suitable leads and connectors were used so that the emf of cell No. 1064 and the potential across the standard resistors could be measured *independently* of one another.

Electromotive force readings on NBS standard cell No. 1064 (in circuit No. 1) were made prior to, during, and after a run using NBS saturated standard cell No. 1073 (in circuit No. 2) as the reference cell. These readings were made to verify that the emf of 1064 remained constant throughout the run. Illustrative data, obtained in a run on May 22, 1958, are given in table 2.

TABLE 2. *Electromotive force of NBS standard cell No. 1064 during a coulometric run (May 22, 1958)*

Time	emf	Time	emf
	v		*v*
8:45 a.m.	1.0182103	12:10 p.m.	1.0182103
8:47 a.m.	1.0182103	12:18 p.m.	1.0182102
8:59 a.m.	1.0182103	12:51 p.m.	1.0182102
9:20 a.m.	start	12:54 p.m.	1.0182102
9:36 a.m.	1.0182103	1:26 p.m.	1.0182102
9:39 a.m.	1.0182103	1:29 p.m.	1.0182103
10:11 a.m.	1.0182103	2:06 p.m.	1.0182103
10:14 a.m.	1.0182103	2:09 p.m.	1.0182103
10:51 a.m.	1.0182103	2:20 p.m.	end
10:54 a.m.	1.0182103	2:28 p.m.	1.0182103
11:28 a.m.	1.0182103	2:29 p.m.	1.0182103
11:31 a.m.	1.0182103		
Mean value			1.0182103

A direct and more accurate measure of the *IR* drop across the standard resistors was also made at intervals by means of circuit No. 2. With the Brooks comparator, in circuit No. 2, the actual *IR* drop across the standard resistors was measured against cell No. 1073. The sensitivity for these measurements was checked before each run and was 5 μv/cm on the galvanometer scale. As an illustration, data taken on May 22, 1958 are given in table 3. The *IR* drop was 1.0182103 v which agrees exactly with that given by circuit No. 1 and no correction was necessary. In all cases the agreement was within 3 ppm; the *IR* drop as given by circuit No. 2 was always used in calculating the faraday.

Saturated standard cells No. 1064 and No. 1073 were in a well-stirred oil bath maintained during the run to ±0.002° C. The temperature of the bath during all the runs was 28.00°±0.01° C. The temperature of the bath was measured with a platinum resistance thermometer using a Mueller Temperature Bridge. Both cell No. 1064 and cell No. 1073 were

TABLE 3. *Measurements of the* IR *drop by circuit No. 2 figure 5* [a]

Time	*IR* setting [b]	Swings to left			Swings to right			Correction	Correct *IR* drop
	v	*cm*			*cm*			μ*v*	*v*
9:20 a.m.	start								
9:37 a.m.	1.0182103	0.7,	0.6,	1.1	0.3,	0.6,	1.1	−0.3	1.0182100
10:12 a.m.	1.0182103	.3,	.3,	0.2	.2,	.4,	0.2	.0	1.0182103
10:52 a.m.	1.0182103	1.0,	.1,	.7	1.2,	.2,	.4	.0	1.0182103
11:29 a.m.	1.0182103	0.5,	.2,	.6	0.2,	.7,	.4	.0	1.0182103
12:11 p.m.	1.0182103	.2,	.1,	.3	.2,	.1,	.3	.0	1.0182103
12:16 p.m.	1.0182103	.5,	.5,	.2	.3,	.5,	.3	−.1	1.0182102
12:52 p.m.	1.0182102	.7,	.6,	.4	.7,	.6,	.4	.0	1.0182102
1:27 p.m.	1.0182102	.4,	.2,	.5	.4,	.3,	.6	.1	1.0182103
2:07 p.m.	1.0182103	1.3,	.1,	.2	1.3,	.1,	.2	.0	1.0182103
2:20 p.m.	end								
Mean value									1.0182103

[a] On May 22, 1958.
[b] As given by circuit No. 1, figure 5.

compared prior to and after a run with two cells in the National Reference Group (the group of standard cells used to maintain the volt for the United States).

Throughout a run frequent measurements were made of the potential of the silver anode against the reference electrode using the voltmeter, *V*, having a resistance of 25,000 ohms. The average number of coulombs used in these measurements for an entire run was only 0.0005 coulomb; this correction for each run was made, see footnote ([a]) of table 10.

Finally, a check was made on the time delay that might have occurred in the current reaching a steady value when the circuit was closed at the start of a run. This was done by connecting an oscilloscope across the standard resistor in a simulated experiment. When the starting switch was closed the oscilloscope indicated that a steady current was reached immediately.

In some runs, the initial current through the coulometer deviated very slightly from that desired; in these cases adjustments were quickly made and the coulombs were corrected accordingly. These corrections were almost negligible but are incorporated in the values of the coulombs given in tables 10, 15, and 17.

5. Magnitude of the Current

The NBS standard resistors were housed in a well-stirred oil bath and the temperatures of the resistors were measured at intervals throughout a run with calibrated mercurial thermometers placed in the central hole of the resistor coils. From the time-averaged temperature the values of the resistance of the standard resistors were calculated by known equations expressing the resistance of the coils as a function of temperature. These equations are of the form:

$$R_t=(nv+k)[1+\alpha(t-25)+\beta(t-25)^2]\text{ohms},$$

where nv (nominal value of resistor), k, α, and β have the values as given in table 4 for the seven different resistors used in this investigation. The temperature, t, is in degrees Celsius. Various combinations of the resistors were used; these will be

discussed later. The resistance of the standard resistors on the date the measurements were made were interpolated from the data for k given in table 4; the coefficients α and β did not change with time. The values, as calculated from the above equation and the data of table 4, are for conditions under which the heating due to the test current is negligible. Of course, during the coulometric experiments the current through the resistors is larger and part of the heat generated may alter the resistance of the standard resistors. In use, then, the load resistance rather than the nonload resistance of the standard resistors must be employed. These load resistances, as determined by the Resistance and Reactance Section of NBS, for currents of approximately 0.1, 0.2, 0.3, and 0.5 amp which were used in the runs, are given in table 5.

TABLE 4. *Constants of the equation for the resistance of the standard resistors as a function of temperature*

$$R_t=(nv+k)[1+\alpha(t-25°C)+\beta(t-25°C)^2]$$

Resistor No. (NBS)	Nominal value (nv)	k			$\alpha\times10^6$	$\beta\times10^6$
		March 1956	April 1957	April 1958		
	Ohms	*Ohm*	*Ohm*	*Ohm*		
204	10	+0.00002	0	+0.00001	+5.8	−0.53
205	10	+.00002	0	−.00001	+6.0	−.56
12	10	−.00044	−0.00046	−.00047	+3.4	0
17	10	+.00078	+.00078	+.00077	−1.0	−.24
8	1	+.000530	+.000529	+.000528	+9.2	−.50
12	1	0	−.000009	−.000016	−3.8	−.12
13	1	+.000617	+.000617	+.000617	+5.4	−.51

As shown in table 5, the load resistance differed from the nonload resistance only for high currents, i.e., 0.5 amp.

For illustration in the run of May 22, 1958, resistors 12 and 17 were used in parallel. Therefore, the magnitude of the current during the run was as given in table 6. The mean (i.e., time-averaged) current was, therefore, 0.20363887 amp which agrees exactly with the value obtained from the quotient of the mean IR drop and the mean resistance. In all cases the mean current agreed with the quotient of the mean IR drop and the mean resistance to within 0.1 ppm.

TABLE 5. *Load resistances of standard resistors*

Current	Resistor No. (NBS)	Temperature	Total resistance (no load correction)	Total resistance (with load correction)
amp		*°C*	*Ohms*	*Ohms*
0.1	204	25.1	10.000026	10.000026
.2	204	24.8	9.999988	
	205	24.8	9.999998[a]	
			4.999997	4.999997
.3	12	25.2	0.999992	
	13	25.2	1.000620 [b]	
	8	25.2	1.000527	
			3.001139	3.001139
.5	12	25.4	0.999991	
	13	25.3	1.000621[b]	
			2.000612	2.0006104

[a] = in parallel; [b] = in series.

6. Time

The duration of a run was determined with the aid of an NBS chronograph. The second pulses were supplied by NBS standard crystal oscillators which keep mean solar time and the time of day was obtained from broadcasts of WWV. Since the 59th pulse is omitted in the NBS broadcasts from WWV the beginning of each minute could be identified with the time of day. The chronograph had two pencils, one (No. 1) was activated by the second signals (NBS crystal oscillators) by direct wire and indicates the start of each second on the chronograph chart; the 59th second has a characteristic trace. Pencil No. 2 was activated simultaneously with the opening or closing of the coulometer circuit by a double-pole switch (see fig. 5). This switch was closed after the signal from WWV had indicated the beginning of a new minute, and a displacement in the marking on the chronograph chart indicated the start or end of a run, as illustrated for a start in figure 6. A similar procedure was followed just prior to the end of a run. A radio receiver was used for picking up signals from WWV. The chronograph drum was started about 20 to 30 sec before the start and the end of a run.

TABLE 6. *Magnitude of the current in run of May 22, 1958*

Time	IR drop	Temperature resistor 12	Resistance of resistor 12	Temperature resistor 17	Resistance of resistor 17	Total resistance	Current
	v	*°C*	*Ohms*	*°C*	*Ohms*	*Ohms*	*amp*
9:20[a]	1.018210_3	24.5	9.9995130	24.5	10.0007744	5.000072	0.20363913
9:37	1.018210_6	24.6	9.9995164	24.6	10.0007736	5.000073	.20363903
10:12	1.018210_3	25.1	9.9995334	25.1	10.0007690	5.000076	.20363896
10:52	1.018210_3	25.4	9.9995436	25.4	10.0007656	5.000077	.20363892
11:29	1.018210_3	25.6	9.9995504	25.6	10.0007631	5.000078	.20363888
12:11	1.018210_3	25.7	9.9995538	25.7	10.0007618	5.000079	.20363884
12:16	1.018210_2	25.8	9.9995572	25.8	10.0007605	5.000079	.20363882
12:52	1.018210_2	25.9	9.9995606	25.9	10.0007591	5.000080	.20363878
1:27	1.018210_3	26.0	9.9995640	26.0	10.0007576	5.000080	.20363880
2:07	1.018210_3	26.1	9.9995674	26.1	10.0007561	5.000081	.20363876
2:20[b]	1.018210_3	26.1	9.9995674	26.1	10.0007561	5.000081	.20363876
Mean values						5.000078	0.20363887

[a] Start.
[b] End.

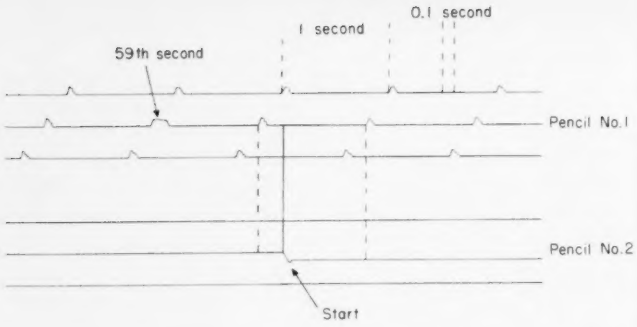

FIGURE 6. *Illustration of recordings on chronograph chart.*

Since the chronograph chart showed a constant distance, 7.48 cm, between the second markings the time could be ascertained to better than 0.01 sec. For a 3-hr run this means that the duration of a run was known to better than 1 ppm; for longer runs it was known, of course, with more accuracy.

To ascertain the delay in activating and deactivating the chronograph pencil when the switch was thrown, an electric timer used in the calibration of watthour meters and activated by a crystal-controlled 60-cps frequency was inserted directly in the coulometer circuit in several simulated starts and stops. Checks were made over 2-min time intervals. The electric timer was calibrated directly against NBS crystal oscillators. The total time indicated by the timer and the chronograph for a 2-min interval differed, on the average, by only 0.009 ± 0.006 sec with the chronograph in all cases giving the lesser time. Thus, the correction used for the duration of a run was $+0.009$ sec. Although this correction is insignificant it was nevertheless applied in all the calculations.

7. Mass

For the runs with mint silver the masses of silver, crucibles, etc., were determined using a semimicrobalance. For those runs with purified silver rods a microbalance was used; its capacity was 20 g. Weighings were made by double transposition, with sensitivity measurements interspersed, in a constant-temperature room maintained at 25 $\pm 1°$ C, and with a relative humidity of always less than 50 percent. The balance was supported on an Alberene slab anchored to a wall of the laboratory. All weighings were repeated until constancy was achieved. Silver sediment (see later) was collected in Pyrex crucibles and weighed using an identical crucible as a tare. The silver sediment was retained in the crucibles from one run to another. The densities of silver (10.50) and the laboratory air and also the densities of the brass (8.4), platinum (21.5), and aluminum (2.7) weights were used in making buoyancy corrections.

In calculating the density of the laboratory air the following data were used:

(a) Smithsonian Meteorological Tables, 6th revised edition, 1951, Smithsonian Institution Publication (specifically table 46). This publication gives data for correcting the barometric pressure at an observed laboratory temperature in degrees Celsius to the barometric pressure at 0° C.

(b) Psychrometric Tables for Obtaining the Vapor Pressure, Relative Humidity, and Temperature of the Dew Point, by C. F. Marvin, Weather Bureau, U.S. Department of Commerce, U.S. Government Printing Office, Washington, D.C., 1941. This publication gives the relation between relative humidity and the temperature difference, in degrees Fahrenheit, as given by a dry- and a wet-bulb thermometer.

(c) Design and Tests of Standards of Mass, NBS Circ. No. 3, 1918. Table 15 in this publication gives the data required for correcting the barometer for the observed relative humidity.

(d) National Bureau of Standards gravity $=980.100$ cm sec^{-2}; standard gravity at 45° latitude and sea level$=980.665$ cm sec^{-2}.

(e) 1.293052 g liter^{-1}=density of dry air containing 0.04-percent carbon dioxide at 0° C and 1 atm, NBS Circ. No. 3, 79 (1918).

(f) 1/1.000028=factor to reduce values of milligrams milliliter^{-1} to milligrams cm^{-3}.

The barometric pressure, temperature, and the humidity of the laboratory air were measured at the time of each weighing.

8. Materials and Purification

8.1. Materials

In the determination of the faraday by anodic dissolution of silver in aqueous solutions of perchloric acid containing a small amount of silver perchlorate four materials were needed. These were: (1) silver, (2) perchloric acid, (3) silver perchlorate, and (4) water. The silver used was high-grade samples received from the U.S. Mint in Philadelphia, Pa. It was stated by the mint that the silver was of high purity, had been purified by one or two electrolyses, was melted in silica, was rolled into sheet form on steel rolls, contained a trace of copper and perhaps lead, contained no occluded hydrogen, and was believed by the mint to be free of occluded and combined oxygen, unless allowed to stand exposed to the atmosphere.

The perchloric acid was reagent grade. The silver perchlorate was prepared from reagent grade silver oxide and perchloric acid solution. Conductivity water was used in diluting the perchloric acid and in the necessary analytical operations [23]. It was produced in a conductivity still and one-third of the condensate was collected; the feed was distilled water treated with alkaline permanganate. The conductivity water had a conductivity of 0.6 to 1.0×10^{-6} (ohm cm)$^{-1}$. The solution of perchloric acid (20 wt %) and silver perchlorate (0.5 wt %) was slowly filtered through a fritted filter containing finely-divided silver prior to use in the coulometer. This precluded the possibility of the solution containing anions which would have precipitated silver ion during a coulometric run.

8.2. Purity of the Silver

Samples of two separate lots of mint silver were leached in concentrated hydrochloric acid solution and then in 10 percent aqueous ammonium hydroxide (extensive etching of the surface of the silver was deliberately avoided) to remove surface impurities. Both the etched and unetched samples [4] were then analyzed spectrochemically. The results for the etched samples are given in table 7 and show that the purity of the two etched silvers was high; the total impurities in samples 1 and 2 were, respectively, 8.4 and 4.6 ppm, with copper being the highest in both cases. Since the copper percentage was relatively high sample No.1 was analyzed photometrically. The silver was first dissolved in nitric acid and was then removed from the solution as the chloride. The copper remaining in the filtrate was determined by the carbamate-photometric method. The results agreed well with those obtained spectrochemically (see table 7). Since the etched samples dissolved completely in dilute nitric acid they were free of halides or sulfides.

TABLE 7. *Spectrochemical analyses of the various silver samples*

Element	Mint sample No. 1	Mint sample No. 2	Anode 1	Anode 2	Anode 4	Anode 5
	ppm	*ppm*	*ppm*	*ppm*	*ppm*	*ppm*
Al	0.5	0.05	0.00_5	0.00_5	0.01	0.02_5
Ca	.5	[b] $.25_5$	.01	$.01_5$	.01	$.00_5$
Cu	[a] 4.0	4.0	$.2_5$	$.2_5$	.10	$.07_5$
Fe	0.5	0.1_5	.1	$.1_5$	.05	.1
Mg	.20	.02	.01	$.01_5$	.01	.01
Mn	.5	----	----	----	----	----
Pb	----	----	----	----	----	----
Si	1.0	.10	----	.10	----	.57
Sn	0.2	----	----	----	0.05	----
Pd	.5	----	----	----	----	----
Au	.5	----	----	----	----	----
Total	8.40	4.57_5	$.37_5$	$.53_5$	.23	$.78_5$

[a] Photometric method gave 3.5 ppm.
[b] Subfigures refer to differences between top and bottom of samples; differences, as seen, are insignificant.

Although the amount of metallic impurities was low in both samples of mint silver and methods were known for correcting for them, it was deemed advisable, nevertheless, to purify a sample of mint silver. Purification of silver posed quite a problem because, whether conventional chemical or electrochemical methods were used in the purification, the resulting material (silver) would be in granular or powder form unsuitable for use as electrodes. Not only would a purification be involved but also a process required wherein the silver could be made into electrodes without serious contamination. The methods by which this was achieved are described in the next section.

[4] Spectrochemical analysis gave different results for etched and unetched mint silver; the unetched silver contained a somewhat higher percentage of impurities. Photometric chemical analysis confirmed this finding and showed that unetched silver contained an appreciable amount of iron (4 ppm) whereas etched silver showed an insignificant amount of iron (the iron apparently came from the steel rolls used in forming the sheets of silver). Undoubtedly the larger amount of impurities found in unetched silver arose from surface impurities. Only the results obtained with etched silver were used in the final evaluation of the faraday.

8.3. Purification of Silver

After considering the various methods described in the literature for the purification of silver it was decided that the electrolytic method was the most suitable for the present purpose. This method requires the preparation of a small quantity of only one pure reagent, viz., silver nitrate solution, and any occlusions of water or of electrolyte in the electrolytically deposited silver is readily expelled by subsequent vacuum fusion (the amount of occlusions is not significant, but complete expulsion is required). The electrolytic method thereby avoids the possibility of contaminating the final silver by occlusions of reagents which are not expelled by vacuum fusion and which are not detected by spectrochemical analysis. It may, of course, be said that the electrolytic method introduces the possibility that the deposited silver may be enriched with one or the other isotope of silver. However, as will be shown later, no measurable separation of the isotopes of silver occurred in this process. Furthermore, the atomic weight of the silver used in this investigation was determined in an associated experiment (see later).

The electrolytic cell used in purifying the silver consisted of two beakers containing silver nitrate solution joined by a siphon with a glass frit sealed halfway between the legs of the siphon. This silver nitrate solution was prepared from a small quantity of recrystallized silver nitrate. A stopcock was sealed to the top of each leg and on each side of the frit so that both legs of the siphon could be readily filled by suction after silver nitrate solution was poured into each beaker. The frit prevented mixing of the anolyte and catholyte and also migration of particles. Both electrodes were bars of mint silver having a cross section of 4.0×0.25 cm and were about 10 cm in height. The bulk of the purified silver came by the mass transport from the anode to the cathode and the initial silver nitrate solution served only for initial conductivity. The silver bars were part of a third sample obtained from the Philadelphia Mint and had a purity less than that of the first two samples; total impurities amounted to about 120 ppm. During the electrolysis a little silver oxide was added at intervals to the anode beaker to keep the anolyte slightly basic thereby precipitating many metallic impurities as the oxides. Also during the electrolysis a little concentrated nitric acid was added at intervals to the cathode beaker to keep the catholyte acidic whereby the deposition of silver was favored over that of metallic impurities. The electrolysis was carried out in a closed cabinet to minimize exposure of the electrolytic cell to dust and fumes.

At intervals the cathode was removed from the cell and the deposited silver was easily scraped from the underlying silver cathode into a Pyrex beaker by a silver spatula. Each portion of silver so removed was kept in a separate beaker containing dilute nitric acid. The beakers were covered and kept in a closed cabinet until the silver was used to

prepare anodes. Most of the silver deposited as clusters of glistening crystals; the remainder was in the form of needles. Spectrochemical analyses showed no significant difference in the purity of the two forms. Typical results of spectrochemical analyses of samples of the finely-divided silver are given below:

Sample No.	Impurities detected
1	<1 ppm Mg
2	<1 ppm Mg
3	<1 ppm Mg and <1 ppm Cu 1—10 ppm Si
4	none
5	0.01 ppm Mg and 0.01 ppm Ca
6	0.01 ppm Mg and 0.01 ppm Ca 0.05 ppm Al

8.4. Preparation of Pure Silver Anodes

When a portion of the electrolytic silver was needed to prepare an anode, the dilute nitric acid was decanted and the silver transferred to a polyethylene container which had been soaked in hydrofluoric acid solution. The silver was then covered with fresh hydrofluoric acid solution and allowed to stand for at least 2 weeks to remove any silica that may have been attached to or embedded in the surface of the silver during its purification. The hydrofluoric acid was then decanted and the silver washed with conductivity water. The silver was allowed to stand under conductivity water for a period of at least 2 weeks with frequent changes of the water and then transferred to a perforated silver dish and dried at 110° C for several hours in an oven.

The dried and glistening silver was then transferred to a transparent fused silica tube which had been inserted and sealed into a cylindrical opening in the detached flange of the head of a high-temperature furnace. Before sealing the silica tube to the detached flange the tube was closed at one end and dented and then leached in hot concentrated nitric acid, well rinsed with conductivity water, and dried in an oven. "O" rings and a suitable wax were used in sealing the tube into the flange. With the tube sealed in the flange and in a vertical position the space between the bottom of the tube and the dent was filled with the finely-divided silver. The flange was then attached to the furnace head with the tube in a horizontal position. The dent in the tube served to restrict the flow of the silver when it melted.

When the furnace was operating the head was cooled by circulating water thereby keeping the wax seal and the "O" rings cool. The furnace was of the resistive type and was provided with automatic programing equipment, temperature recorder, a mechanical pump, a diffusion pump, a pressure gauge, and a cold trap. After the silver was melted the furnace was allowed to cool and the silver to solidify. When the temperature was well below the melting point of silver the heating elements were pulled back and the tube was allowed to cool more rapidly. This procedure caused the tube to crack where it was in contact with the solidified silver and finally the silver fell from the tube and was caught with a towel. The cross section of the silver rods, thus produced, was approximately elliptical. Some pieces of the silica tube adhered to the silver when it fell from the tube. No attempt was made to remove any adhering silica mechanically; this was removed by soaking the silver in hydrofluoric acid solution and its complete removal was judged by the constancy of the weight of the silver with repeated treatment with fresh hydrofluoric acid. The same furnace was used in the heat treatment of the sheet (mint) silver. The heat treatment of the sheet silver and the melting of the purified silver is described below.

Samples were then cut from the silver for spectrochemical analysis and two small holes were then drilled in one end (upper) of the silver and silver wire was entwined through these holes (see fig. 4). This wire served to suspend the silver in the analytical balance and also for an electrical connection. The constancy of the weight of the anode after prolonged soaking in hydrofluoric acid was again checked; this check was followed by soaking the anode first in 10-percent aqueous ammonium hydroxide and then in the perchloric acid-silver perchlorate solution. Since silver is remarkably stable in the latter solution etching ensued only in the ammonium hydroxide solution (appreciable etching was purposely avoided, as before for mint silver).

In all, five different anodes were made according to the above general procedure; in each case, the anode was prepared with some modification in the general procedure and these will be outlined in the next subsection. Spectrochemical analyses of the anodes, anode No. 3 excepted, are given in table 7. As will be seen, the anodes were of very high purity and the extremely small amounts of impurities are inconsequential in a faraday determination (correction for these impurities was 1 ppm, see later). As will be discussed in appendix 2, anode 3 was prepared by melting silver in an atmosphere of hydrogen in a silica tube. This procedure caused the silver to blister and to absorb relatively large amounts of impurities from the silica tube. Accordingly, anode 3 was not used in determining the value of the faraday.

8.5. Treatment of the Silver

It is well known that silver has an affinity for oxygen. Steacie and Johnson [26] in a comprehensive study of the silver-oxygen system found that the solubility of oxygen in silver is proportional to the square root of the oxygen pressure and exhibits a minimum solubility at about 400° C at each pressure. They concluded that oxygen existed as the element in silver above 400° C and combined with silver as the lower oxide, Ag_2O, below 400° C. Since Ag_2O is readily soluble in perchloric acid its existence in metallic silver would lead to appreciable errors in a faraday determination since the dissolved

Ag_2O would bear no relation to the quantity of electricity passed through the coulometer.

Fortunately, Ag_2O readily decomposes on heating, and as early as 1888 Carnelly and Walker [27] showed the decomposition of Ag_2O is complete between 300° and 430° C. Lewis [28], Keyes and Hara [29], and Benton and Drake [30] measured the decomposition of Ag_2O over a temperature range of 173° to 500° C with the results given in table 8. By an extrapolation of his data Lewis calculated the decomposition pressure of silver oxide to be 5×10^{-4} atm at 25° C. In a recent electrochemical study of the Ag,Ag_2O electrode Hamer and Craig [31] obtained 2,723 cal for the free energy of decomposition of Ag_2O at 25° C; this value corresponds to 0.988×10^{-4} atm for the decomposition pressure of Ag_2O at 25° C.

TABLE 8. *Decomposition pressure of silver oxide,* Ag_2O

Temperature	Pressure of oxygen	Reference	Temperature	Pressure of oxygen	Reference
°C	atm		°C	atm	
173	0.555	[30]	374	74.3	[29]
178	.670	[30]	403	114.5	[29]
183	.796	[30]	445	207.0	[28]
188	.943	[30]	452	213.5	[29]
191	1.039	[30]	467	257.8	[29]
302	20.5	[28]	484	323.5	[29]
325	32.0	[28]	500	388.3	[29]

Since oxygen exists at a partial pressure of about 0.21 atm in air (air contains about 21% oxygen) at NTP it is apparent by extrapolation of the data in table 8 that silver must be heated above 150° C in an open system to effect the decomposition of any Ag_2O it may contain. However, heating to temperatures above 150° C in an open system will not insure the removal of all silver oxide (or oxygen) since some oxygen will remain or redissolve in the silver to maintain the solubility relations given by Steacie and Johnson (see appendix 1). Therefore, the oxygen, as it is formed in the decomposition of the silver oxide, must be removed from the system. If oxygen remains in the silver it will, of course, affect the apparent value of the faraday because it would be included in the weight of the silver dissolved.

The oxygen formed in the decomposition of Ag_2O may be removed either by evacuation or by heating the silver in hydrogen. In the latter case the gaseous water formed in the reaction:

$$H_2\ (gas)+(\tfrac{1}{2})\ O_2\ (gas)\rightarrow H_2O\ (gas)$$

and all hydrogen remaining must be removed either by evacuation or by complete displacement with an inert gas. Hydrogen should be removed for it may reduce silver ions formed in the electrolytic dissolution of silver back to metallic silver causing errors in the faraday. Water must be removed since its presence will cause errors in determining the weight of the silver dissolved.

In view of the above considerations the silver, whether it was mint silver No. 1, mint silver No. 2, or electrolytically purified silver, was given special treatments designed to completely decompose the silver oxide and remove all of the oxygen from the starting silver. These treatments were as follows.

a. Mint Silver No. 1

Experiments 1, 2, and 3: Silver used in these experiments was from one sheet. The sheet was treated with hydrogen in a clear silica tube at 862° C (98° C below the melting point of silver) for 2 hr. The hydrogen was then displaced slowly by helium over a period of 118 hr with the temperature maintained at 862° C. The tube containing the silver and helium was then cooled to 540° C in 3 hr and finally to room temperature in an additional hour. The silver was then removed from the tube, etched in 10-percent aqueous ammonium hydroxide, washed with conductivity water, and dried at 110° C in an oven.

Experiments 4, 5, and 6: Silver used in these experiments was from one sheet. The sheet was treated with hydrogen in a silica tube at 860° C (100° C below the melting point of silver) for 96 hr or considerably longer than samples used in experiments 1, 2, and 3. The hydrogen was then displaced slowly by helium over a period of 250 hr with the temperature maintained at 860° C. The tube containing the silver and helium was then cooled slowly to room temperature. The silver was then removed from the tube and treated in the same manner as the samples used in the preceding experiments.

b. Mint Silver No. 2

Experiment 7: The silver used in this experiment was heated in *vacuo*, 5μ, in a silica tube at 500° C for 1 hr and then cooled in *vacuo* to room temperature in a little over an hour. The silver was then removed from the tube and treated in the same manner as that used in the preceding experiments.

Experiments 8, 9, and 10: Silver used in these experiments was from one sheet. The sheet was heated in *vacuo*, 2μ, in a silica tube at 500° C for 5 hr and then cooled in *vacuo* to room temperature in a little over an hour. The silver was then removed from the tube and treated in the same manner as the samples used in the preceding experiments.

Experiments 11, 12, and 13: Silver used in these experiments was from one sheet. The sheet was heated in *vacuo*, 3μ, in a silica tube at 500° C for 10 hr and then cooled in *vacuo* to room temperature in a little over an hour. The silver was then removed from the tube and treated in the same manner as the samples used in the preceding experiments.

Experiments 14 and 15: Silver used in these experiments was from one sheet. The sheet was placed in a silica tube which was then evacuated to 50μ in 1 hr. Helium was then introduced for 30 min and then the tube evacuated. Hydrogen was then introduced into the tube which was then heated to 860° C over a 15-hr period. The tube containing the silver and the hydrogen was then kept at 860° C (100° C below the melting point of silver) for 96 hr and then cooled to room temperature in 1 hr. The silver was then removed from the tube and

treated in the same manner as the samples used in the preceding experiments.

Experiments 16 and 17: The silver used in these experiments was of one sheet. The sheet was placed in a silica tube which was then evacuated to 200μ in ½ hr. Helium was then introduced and the temperature raised to 860° C in 3 hr and then flushed with hydrogen. The tube containing silver and hydrogen was kept at 860° C for 101 hr and then cooled to room temperature in 1 hr. The silver was then removed from the tube and treated in the same manner as samples used in the preceding experiments.

c. Purified Silver

Experiments 18, 19, and 20 (anode No. 1): One rod or anode of silver was used in these three separate experiments. The finely-divided silver was heated in *vacuo* in a silica tube to 975° C (15° C above the melting point of silver); the rate of heating from room temperature was 100° C/hr. The silver was held in the molten state at 975° C for ½ hr in *vacuo*, 0.7 μ, and then cooled in *vacuo*, 0.7 μ, until the tube cracked. The silver was then removed from the tube and placed in a solution of hydrofluoric acid to remove any attached quartz as discussed in section 8.4. The anode was then etched slightly in 10-percent aqueous ammonium hydroxide, soaked for a short time in perchloric acid-silver perchlorate solution, washed with conductivity water, and dried at 110° C in a confined space. The anode was then ready for use.

Experiments 21, 22, 23, 24, and 25 (anode No. 2): One rod or anode was used in these five separate experiments. The finely-divided silver was heated in a silica tube to 975° C for 1 hr in *vacuo*, 0.5 μ, and then cooled in *vacuo* until the tube cracked. The silver was then removed from the tube and treated in the same fashion as the preceding anode.

Experiment 26 (anodes 1 and 2 combined): Portions of anodes 1 and 2 which were left after the above experiments (18 to 25, inclusive) were combined for this experiment.

Experiments 27 and 28 (anode 4): One rod or anode was used in these two separate experiments. The finely-divided silver was placed in a silica tube which was then evacuated at room temperature over a 2-hr period to 1 μ. Hydrogen was then introduced and the tube heated to 500° C in 5 hr, and kept at this temperature overnight. The hydrogen was then displaced by helium in 1 hr and the tube evacuated to 1 μ. The evacuated tube containing the silver was then heated to 975° C for 1 hr at 0.7 μ and then cooled in *vacuo* until the tube cracked. The silver was then removed from the tube and treated in the same manner as the preceding anodes.

Experiments 29, 30, and 31 (anode 5): One rod or anode was used in these three separate experiments. The finely-divided silver was placed in a silica tube which was then evacuated at room temperature over a 4-day period to 50 μ. Hydrogen was then introduced into the evacuated tube which was then heated at 500° C in 5 hr and held at 500° C for an additional 3 hr. The tube was then evacuated to 70 μ overnight, further evacuated to 0.9 μ in 2 hr and finally heated to 975° C. The tube with the molten silver was held at 975° C for 1 hr at 0.9 to 0.7 μ and then cooled to 895° C (65° C below melting point of silver) over a 20-min period (i.e., through the solidification period) and finally cooled in *vacuo* until the tube cracked. The silver was then removed from the tube and treated in the same manner as the preceding anodes. X-ray measurements showed this anode had a single crystal orientation.

The treatments discussed above may be summarized as follows: (1) All mint silver was heated *below* the melting point of silver while all anode silver was heated to 15° C *above* the melting point; (2) mint silver was heated in hydrogen, hydrogen and helium, or *vacuo* for various periods of time; and (3) anode silver was heated in *vacuo*, in hydrogen, or in hydrogen and helium for various periods of time. The effect of these various treatments are discussed in section 11.

9. Procedure

9.1. General Procedure

In the foregoing sections some of the procedures, particularly those dealing with the maintenance and constancy of the electric current and measurements of mass and time, were outlined. In this section, manipulative procedures involved in actual determinations of the electrochemical equivalent of silver will be described. Mint silver in sheet form, or purified silver in rod form, after being accurately weighed was suspended in a filtered aqueous solution of perchloric acid (20-wt %)-silver perchlorate (0.5-wt %) contained in a Pyrex beaker by the arrangement shown in figure 3. The coulometer and chronograph circuits were then closed simultaneously and a controlled electric current was passed through the coulometer for several hours. At the end of the run, the silver sheet or rod was removed, washed with conductivity water, dried at 110° C, and weighed.

As the silver goes into solution some particles (sediment) fall to the bottom of the anode beaker. This sediment was collected in a weighed Pyrex crucible with a fritted bottom, repeatedly washed with conductivity water, dried at 110° C, and weighed. This weight of the sediment was then subtracted from the difference between the initial and final weights of the sheet or rod to give the weight of the silver which was electrolytically dissolved (see later). Since the coulometer was open so that the silver sheet or rod could be lowered as it dissolved the possibility existed that the solution might be contaminated with dust, even though the entire coulometer was housed under a plastic cabinet. Accordingly, another Pyrex beaker containing the coulometer solution in an amount equal to that used in the anode beaker was placed uncovered beside the anode beaker. This solution was not a part of the coulometer but served as a blank. At the end of a coulometer run this beaker was covered with an inverted beaker. A day later this solution was filtered through the same fritted crucible used to collect the

silver sediment. The change in weight of the fritted crucible for the blank solution was always small, nearly negligible, but nevertheless was used as a blank correction for the weight of silver sediment. In the early runs with mint silver an average blank correction was used; for the later runs with purified silver anodes the blank correction was obtained for each individual run.

9.2. Variation in Conditions

In all, 31 quantitative and 22 informative measurements were made. The latter are discussed in the appendices. The conditions of the experiments were varied as follows:

a. *The current density, i.e., amperes per square centimeter of anode surface, was varied.* This was accomplished either by using different areas of exposed silver in the coulometer solution or by passing currents of different magnitudes through the coulometer. The different magnitudes of current are listed in table 9. The current density for both the mint silver anodes and the purified silver anodes was varied from 0.025 to 0.150 amp/cm² and no trend in the value of the faraday was found. The resistors used, their assembly, and a code for the assembly (for use in tables 10, 15, and 17) are also given in table 9.

TABLE 9. *Magnitudes (nominal) of current and resistance used in the faraday determinations*

Measurements	Nominal current	Nominal resistance	Resistors[a]	Resistor code
	amp	*Ohms*		
1	0.09	11	13(1Ω), 12(10Ω), *S*	A
2	.10	10	204(10Ω)	B
2	.15	6⅔	204(10Ω), 17(10Ω) *S*, 12(10Ω) *P*	C
1	.17	6	12(10Ω), 17(10Ω) *P*, 13(1Ω) *S*	D
2	.20	5	204(10Ω), 205(10Ω), *P*	E
12	.20	5	12(10Ω), 17(10Ω), *P*	F
26	.33	3	8(1Ω), 12(1Ω), 13(1Ω) *S*	G
7	.50	2	12(1Ω), 13(1Ω) *S*	H

[a] *S*=series, *P*=parallel.

b. *The potential of the silver anode during the electrolysis was varied.* This change resulted from the changes outlined in (a) above. When the electrode areas were decreased or the current increased the potential of the corroding anode, relative to the reference electrode, became higher. The average values of the silver anode potentials, E_r, during each run are given in table 10. These values ranged from 0.088 to 0.201 v for the mint silver anodes and from 0.089 to 0.149 v for the purified silver anodes.

c. *The duration of the coulometric runs and the amount of silver dissolved were varied.* The shortest time was 2 hr, the longest 6½ hr. The least amount of silver dissolved in any one run was 2.4 g, the most 5.0 g.

d. As stated in preceding sections *different samples of silver were used.*

e. As stated in preceding sections the *samples of silver were treated in various ways.*

10. Electrophoresis of Silver

During a run the possibility existed that some of the silver sediment may have been so finely divided that it might have electrophoretically migrated toward the cathode, and thereby be removed from the anode beaker. To check if such were the case after the siphons were drained the solution in the beaker adjacent to the anode beaker (see fig. 1) was carefully filtered through the Pyrex crucible after many runs. No significant difference was found in any experiment between the weight of the sediment contained in this beaker and the weight of the sediment in the blank beaker. Thus, no silver sediment was transferred from the anode beaker by electrophoresis, or any other mechanism.

11. Results

11.1. Electrochemical Equivalent of Silver

The experimental quantity obtained directly from the coulometric measurements is the electrochemical (or coulometric) equivalent of silver. In table 10 the results of the 31 quantitative experiments are given. The headings of each column are in general self-explanatory. Column 10 gives the quantity of silver anodically dissolved by the coulombs given in column 8. Column 11 gives the amount of sediment produced in each run; it was used to obtain the values given in column 10. It will be noted that the amount of sediment produced varied widely and was extremely small in the last 5 runs made with purified anodes; the last and perhaps all anodes had a single crystal orientation. In some cases lumps of silver fell from the anode during the electrolysis; for these see runs No. 3, 7, 14, 15, 16, 17, and 20. Even though the amount of sediment differed widely between the various runs this variation did not affect the final results as is apparent from the concordance obtained (this fact also shows that the sediment could not have consisted predominantly of one or other of the two isotopes of silver, see page 382). Column 9 gives the average potential of the silver anode during the electrolysis. A high value means either that the anode surface immersed in the solution was smaller or the magnitude of the current higher than in those runs in which the potential was lower. Inspection of the values in column 13 show that they are independent of the values of the anode potentials, E_r.

The values of the electrochemical equivalent of silver in the next to last column of table 10 are based on the simple relation:

$$Ag^{bulk}_{initial} - Ag^{bulk}_{final} - sediment = Ag_{measured\,(or\ dissolved)} = Ag_m \qquad (1)$$

and are, therefore, uncorrected for the minute amounts of metallic impurities in the silver. Actually, in these calculations the quantity $Ag^{pure}_{electrolytic}$ should be used rather than Ag_m in determining the

TABLE 10. *Final results of the electrochemical equivalent of silver*

Experiment No.	Date	Time	*IR* drop	Resistor code	Resistance	Current	Coulombs [a]	E_r	Silver corroded, Ag_m	Sediment	Electrochemical equivalent	
											Uncorrected	Corrected
Mint silver No. 1—Hydrogen, 2 hr, 862° C, Helium (118 hr), not melted, *o*[c]												
		sec	*v*		*Ohms*	*amp*	*amp-sec*	*v*	*g*	*g*	*mg coulomb*$^{-1}$	*mg coulomb*$^{-1}$
1	11-28-56	7,199.959	1.0182138	H	2.000609	0.5089519	3,664.4323	0.125	4.096763	0.020678	1.117980	[d] 1.117971 (17)
2	12-13-56	18,000.013	1.0182133	E	5.000001	.2036426	3,665.5690	.091	4.097912	.051298	1.117947	1.117938 (17)
3	12-18-56	10,800.053	1.0182139	G	3.001136	.3392761	3,664.1979	.201	4.096574	.767097	1.118000	1.117991 (17)
Mint silver No. 1—Hydrogen, 96 hr, 860° C, Helium (250 hr), not melted, *e*[c]												
4	4-11-57	10,802.313	1.0182129	G	3.001130	0.3392765	3,664.9702	0.122	4.097160	0.032410	1.117925	1.117949 (16)
5	4-16-57	10,200.067	1.0182102	G	3.001126	.3392761	3,460.6383	.124	3.868779	.058122	1.117938	1.117962 (16)
6	4-18-57	9,900.074	1.0182118	G	3.001125	.3392767	3,358.8637	.117	3.754894	.056315	1.117906	1.117930 (16)
Mint silver No. 2—Vacuum, 1 hr, 550° C, not melted, *o*												
7	3- 6-57	13,199.981	1.0182131	G	3.001133	0.3392762	4,478.4388	0.111	5.006858	0.471592	1.117992	1.117986 (12)
Mint silver No. 2—Vacuum, 5 hr, 550° C, not melted, *o*												
8	3-11-57	9,900.062	1.0182101	G	3.001130	0.3392756	3,358.8491	0.098	3.755131	0.102182	1.117982	1.117975 (12)
9	3-14-57	10,500.078	1.0182125	G	3.001139	.3392754	3,562.4159	.159	3.982688	.104516	1.117974	1.117968 (12)
10	4- 8-57	10,800.037	1.0182131	G	3.001137	.3392758	3,664.1903	.112	4.096469	.118233	1.117974	1.117968 (12)
Mint silver No. 2—Vacuum, 10 hr, 550° C, not melted, (*e'*)[c]												
11	4-30-57	10,800.040	1.0182131	G	3.001143	0.3392751	3,664.1842	0.100	4.096415	0.075844	1.117961	1.117970 (4)
12	5- 2-57	10,799.967	1.0182133	G	3.001141	.3392754	3,664.1627	.088	4.096383	.090773	1.117959	1.117968 (4)
13	5- 8-57	10,800.117	1.0182139	G	3.001143	.3392754	3,664.2125	.144	4.096498	.065560	1.117975	1.117984 (4)
Mint silver No. 2—Hydrogen, 96 hr, 860° C, not melted, *e*												
14	5-28-57	10,500.032	1.0182132	G	3.001141	0.3392754	3,562.4021	0.104	3.982489	0.228977	1.117922	1.117936 (8)
15	6- 3-57	10,800.083	1.0182129	G	3.001137	.3392757	3,664.2051	.106	4.096410	.244528	1.117953	1.117967 (8)
Mint silver No. 2—Hydrogen, 101 hr, 860° C, not melted, *e*												
16	6-26-57	10,200.407	1.0182123	G	3.001139	0.3392753	3,460.7454	0.110	3.869000	0.208168	1.117967	1.117980 (7)
17	7- 2-57	10,500.086	1.0182129	G	3.001137	.3392757	3,562.4233	.105	3.982423	.269498	1.117897	1.117910 (8)
Anode 1—Vacuum, 0.5 hr, 975° C, melted, *e*												
18	1-21-58	18,000.021	1.0182119	F	5.000071	0.2036395	3,665.5447	0.106	4.098127	0.016516	1.118013	1.118014 (1)
19	1-28-58	21,600.031	1.0182112	C	6.666528	.1527349	3,299.0730	.104	3.688228	.020922	1.117959	1.117960 (1)
20	2-12-58	23,400.024	1.0182101	A	11.000122	.0925635	2,165.9930	.106	2.421491	.392851	1.117959	1.117960 (1)
Anode 2—Vacuum, 1 hr, 975° C, melted, *e*												
21	2-26-58	18,000.048	[b] 1.0181863	F	5.000072	0.2036343	3,665.4270	0.089	4.097824	0.017288	1.117966	1.117968 (1)
22	3- 4-58	18,000.036	1.0182090	F	5.000075	.2036388	3,665.5053	.100	4.097795	.007993	1.117934	1.117936 (1)
23	3-11-58	18,000.075	1.0182098	F	5.000073	.2036390	3,665.5169	.105	4.097900	.005706	1.117960	1.117961 (1)
24	3-18-58	21,600.055	1.0182098	D	6.000684	.1696823	3,665.1505	.107	4.097576	.002229	1.117983	1.117984 (1)
25	5-28-58	18,000.018	1.0182104	F	5.000075	.2036390	3,665.5048	.149	4.097921	.066674	1.117969	1.117970 (1)
Anodes 1 and 2 combined—0.75 hr, 965° C, melted, *e*												
26	7- 9-58	15,300.060	1.0182111	C	6.666547	0.1527344	2,336.8449	0.120	2.612583	0.002269	1.117996	1.117997 (1)
Anode 4—Hydrogen, 21 hr, vacuum, 975° C, melted, *e*												
27	5-20-58	18,000.015	1.0182100	F	5.000075	0.2036390	3,665.4555	0.127	4.097800	0.000613	1.117951	1.117951 (0)
28	5-22-58	18,000.016	1.0182103	F	5.000078	.2036389	3,665.5027	.134	4.097844	.000631	1.117949	1.117949 (0)
Anode 5—Hydrogen, 7.75 hr, vacuum, 975° C, melted, *e*												
29	6-18-58	17,999.998	1.0182105	F	5.000077	0.2036390	3,665.4962	0.109	4.097935	0.000940	1.117976	1.117976 (1)
30	6-24-58	17,999.945	1.0182105	F	5.000076	.2036390	3,665.4904	.115	4.097861	.000796	1.117957	1.117958 (1)
31	7- 2-58	17,999.955	1.0182110	F	5.000079	.2036390	3,665.4922	.132	4.097897	.000636	1.117966	1.117967 (1)

[a] Includes corrections for any initial off-balance and coulombs utilized in side-circuit measurements of reference silver electrode.
[b] NBS cell No. 1063 used instead of NBS cell No. 1064.
[c] *o*-impurities are metallic oxides, *e*-impurities are metallic, *e'*-impurities are metallic oxides except Fe and Cu which are metallic.
[d] Uncertainties in purity corrections, given in parentheses.

electrochemical equivalent of silver and is obtained from values of Ag_m by the relation:

$$Ag^{pure}_{electrolytic} = Ag_m + Ag_{precipitated} - \Sigma' i = Ag_m(1+X-Y). \quad (2)$$

In this relation $Ag_{precipitated}$ and $\Sigma' i$ are given, respectively, by $X\,Ag_m$ and $Y\,Ag_m$ where X is the summation of the percentage of each metal impurity multiplied by the respective metal-ion valence and Y is the summation of the percentage of each metal impurity other than silicon which must exist as SiO_2.[5]

The derivation of eq (2) follows: The metal impurities in the silver when released during the dissolution of silver will reduce Ag^+ ions formed during the electrolysis to metallic silver according to the general reaction:

$$Metal + \gamma Ag^+ \rightarrow \gamma Ag_{precipitated} + M^{\gamma+}$$

where γ is the valence of the metal-ion impurity, and thus the electrochemical equivalent of each metal is used. This silver will become part of the sediment. If, however, the metallic impurities are directly oxidized electrochemically, no error arises in these calculations assuming the above mechanism. The SiO_2 released from the silver during the electrolysis will become part of the sediment. Also any other inert material, Σi_{inert} (Pd or Au, for example in mint silver No. 1) released as the silver is electrolytically dissolved will also become part of the sediment. Accordingly, then, the sediment is given by:

$$Sediment = Ag^{bulk}_{sediment} + Ag_{precipitated} + SiO_2 + \Sigma i_{inert}. \quad (3)$$

Substitution of (3) in (1) gives:

$$Ag^{bulk}_{initial} - Ag^{bulk}_{final} - Ag^{bulk}_{sediment} - Ag_{precipitated} - SiO_2 - \Sigma i_{inert} = Ag_m \quad (4)$$

or

$$Ag^{bulk}_{electrolytic} - Ag_{precipitated} - SiO_2 - \Sigma i_{inert} = Ag_m. \quad (5)$$

Now,

$$Ag^{bulk}_{electrolytic} = Ag^{pure}_{electrolytic} + SiO_2 + \Sigma' i + \Sigma i_{inert} \quad (6)$$

since the bulk silver that goes into solution during the electrolysis is equal to the sum of the pure silver electrolyzed, the SiO_2 released, and the impurities other than SiO_2 released. Substitution of (6) in (5) leads to eq (2) since SiO_2 and Σi_{inert} cancel. In making corrections for the impurities they were taken as metallic except when the solid silver was only superficially heated in hydrogen or in *vacuo* for a very short time in which case they were taken as the oxide.

Final values of the electrochemical equivalent of silver, after corrections were made for the presence of trace metallic impurities, are given in the last column of table 10. Corrections for impurities are very small, in fact for the purified silver anodes the corrections amount to only 1 ppm or less. For mint silver No. 1 the average correction is 16.5 ppm while for mint silver No. 2 the average correction is 9.6 ppm.

The average value for all the mint samples is 1.117962 ($s_{\bar{x}} = 5.1 \times 10^{-6}$) whereas the average value for all the purified silver anodes is 1.117968 ($s_{\bar{x}} = 5.7 \times 10^{-6}$). The average of all values is 1.117965 ($s_{\bar{x}} = 3.8 \times 10^{-6}$). $s_{\bar{x}}$ designates the estimated standard deviation of the mean.[6] The agreement between the mint and purified samples is good. These averages, however, do not give a complete picture of the results. If instead, the average of the hydrogen values (silver treated with hydrogen) and the average of the vacuum values (silver heated or melted in *vacuo*) are tabulated, the following comparison is obtained:

	Hydrogen	$s_{\bar{x}} \times 10^6$	Vacuum	$s_{\bar{x}} \times 10^6$	Difference
Mint silver	1.117953 (10)[a]	6.7	1.117974 (7)	8.0	0.000021
Purified silver	1.117960 (5)	9.5	1.117972 (9)	7.0	.000012
All values	1.117956 (15)	5.5	1.117973 (16)	5.3	.000017

[a] Numbers in parentheses equal number of runs.

The hydrogen value is lower than the vacuum value for both mint and purified silvers. The difference is statistically significant at the 0.05-probability level,[7] and furthermore, this is most important, the hydrogen values are lower. This agrees with the fact that the electrochemical equivalent of hydrogen is considerably less than that of silver and, therefore, its presence could result in a lowering of the experimental value of the electrochemical equivalent of silver.

In view of the above comparison a more detailed comparison of the individual treatments given the silver was made and is outlined in table 11. Of the five distinct groups of values given in table 11 (3 for hydrogen and 2 for vacuum), the value of group 5, the last vacuum group, is 1.117972 mg coulomb^{-1}. For this group, the silver had been purified, *melted* in *vacuo*, the impurity corrections were almost neg-

[5] $Ag_{precipitated}$ and Σ' are actually given by,

$$Ag_{precipitated} = X(Ag_m + Ag_{precipitated} + SiO_2 + \Sigma i_{inert})$$

and

$$\Sigma' i = Y(Ag_m + Ag_{precipitated} + SiO_2 + \Sigma i_{inert}),$$

wherein a series of successive approximations are required to obtain $Ag_{precipitated}$ and $\Sigma' i$. However, the amounts of impurities were so small that Ag_m may be used for the quantities in parentheses in calculating the faraday. Differences in the faraday obtained by using Ag_m for the quantities in parentheses are less than 1 ppm.

[6] Computed in each case from $s_{\bar{x}} = s/\sqrt{n}$ where n is the number of values entering into the mean and s is the estimate of the standard deviation of a single value obtained by pooling the dispersions within the 12 groups given in table 10, and is based on 19 degrees of freedom.

[7] The value of | difference of means |/(standard deviation of difference) = 2.37 exceeds 2.093, the critical value (0.05 probability point) of Student's t for 19 degrees of freedom.

TABLE 11. *Distinct groups of values for the electrochemical equivalent of silver*

Group No.	Silver	Number of runs	Treatment	Hours of treatment	Electrochemical equivalent of silver (average)	Group average for electrochemical equivalent of silver	$s_{\bar{z}} \times 10^6$
					mg coulomb^{-1}	*mg coulomb*$^{-1}$	
1	Mint No. 1	3	Hydrogen	2	1.117967	1.117957	8.6
	Mint No. 1	3	Hydrogen	96	1.117947		
2	Mint No. 2	2	Hydrogen	96	1.117952	1.117948	10.6
	Mint No. 2	2	Hydrogen	101	1.117945		
3	Purified	3	Hydrogen	73¼	1.117967	1.117960	9.5
	Purified	2	Hydrogen	21	1.117950		
	Average	15	Hydrogen		1.117956	1.117956	5.5
4	Mint No. 2	1	Vacuum	1	1.117986	1.117974	8.0
	Mint No. 2	3	Vacuum	5	1.117970		
	Mint No. 2	3	Vacuum	10	1.117974		
5	Purified	3	Vacuum	½	1.117978	1.117972	7.0
	Purified	1	Vacuum	¾	1.117997		
	Purified	5	Vacuum	1	1.117960		
	Average	16	Vacuum		1.117973	1.117973	5.3
	Total average	31			1.117965	1.117965	3.8

ligible (1 ppm or less), and no foreign substance, viz, hydrogen or helium had been used in heat treatment. The data for the hydrogen groups show that the longer the silver was treated with hydrogen the lower was the measured value of the electrochemical equivalent of silver even though attempts had been made to remove the hydrogen (group 2, excluded); no exception was noted in the three cases. On the other hand, no definite trend with time was found in the vacuum values for either mint or purified silver (the purified samples were melted in silica tubes but were not kept in the molten state for extended periods of time because of the danger of contaminating the samples. Previous to melting only a relatively small portion of the silver was in contact with the silica tube). Because of the trend in the hydrogen values they were all extrapolated linearly to zero time of hydrogen treatment. Since for mint silver No. 2 the times of treatment were so nearly identical, the correction for 96 hr obtained for mint silver No. 1 was used to correct mint silver No. 2 for both 96 and 101 hr. The average values obtained after these corrections are as follows:

Silver	Number of runs	Extrapolated value	
			$s_{\bar{z}} \times 10^6$
Mint No. 1	6	1.117968	12.5
Mint No. 2	4	1.117969	20.8
Purified	5	1.117977	10.0
Average	15	1.117971	10.7

The average value 1.117971 agrees very well with the value, 1.117972, for the last vacuum group, group 5 in table 11. The average of all the vacuum and all the hydrogen corrected values is 1.117972 ($s_{\bar{z}}=5.9\times10^{-6}$). For completeness the final individual values of the electrochemical equivalent of silver corrected for metallic impurities and residual hydrogen are given in table 12. The electrochemical equivalent of silver is, therefore, **1.117972 mg coulomb^{-1}** with an overall uncertainty of 0.000019 which includes 0.000012 as the limit to the effect of random errors (see bottom of table 12) and 0.000007 for the effects of known sources of possible systematic error.

TABLE 12. *Final values for the electrochemical equivalent of silver*

Sample No.	Mint silver	Δ	Sample No.	Purified silver	Δ
		ppm			*ppm*
1	1.117972	0	18	1.118014	+4.2
2	1.117939	−3.3	19	1.117960	−1.2
3	1.117992	+2.0	20	1.117960	−1.2
4	1.117970	−0.2	21	1.117968	−0.4
5	1.117983	+1.1			
			22	1.117936	−3.6
6	1.117951	−2.1	23	1.117961	−1.1
7	1.117986	+1.4	24	1.117984	+1.2
8	1.117975	+0.3	25	1.117970	−0.2
9	1.117968	−0.4	26	1.117997	+2.5
10	1.117968	−.4			
			27	1.117978	+0.6
11	1.117970	−.2	28	1.117976	+.4
12	1.117968	−.4	29	1.117986	+1.4
13	1.117984	+1.2	30	1.117968	−0.4
14	1.117957	−1.5	31	1.117977	−.5
15	1.117988	+1.6			
16	1.118001	+2.9			
17	1.117931	−4.1			
Average					1.117972
$s_{\bar{z}}$					5.9×10^{-6}

Uncertainty (95% confidence limit for the mean) = 2.093 $s_{\bar{z}} = \pm 0.000012$

11.2. Atomic Weight of Silver

Since the faraday is given by the ratio of the atomic weight to the electrochemical equivalent of silver it is necessary to know, or determine, the atomic weight of the silver used in the faraday determinations. The international value for the chemical atomic weight is 107.880 [32]. There is abundant evidence that the isotopic composition of natural occurring silver is nearly constant [12 and 13, also

33]. Using this value for the atomic weight of silver and 1.117972 mg coulomb^{-1} for the electrochemical equivalent of silver one obtains 96496.16 coulombs g-equivalent^{-1} and 96522.70 coulombs g-equivalent^{-1} for the faraday on the chemical and physical scales, respectively; the factor 1.000275 being used in the conversion [32].

The chemical value 107.880 is based primarily on the experimental ratio $AgNO_3/Ag$ using the chemical atomic weights of oxygen and nitrogen (14.008). If the value of the atomic weight for nitrogen (14.00733) as calculated from nuclidic masses and abundances, measured by mass spectrometry [34], is used, an average value for the atomic weight (chemical scale) of 107.8771 is obtained. If the atomic weight of silver is calculated from the most recent work on the I/Ag ratio, assigning the mass spectrometer value to iodine (126.9101), the atomic weight of silver is 107.8770.

Ratio	Ratio value	Atomic weight of silver chemical scale	Reference
$AgNO_3/Ag$	1 574801	107. 8762	[12]
$AgNO_3/Ag$	1. 574791	107. 8781	[13]
I/Ag	1. 176433	107. 8770	[35]
Average		107. 8771	

This average value then leads to 96493.56 coulombs g-equivalent^{-1} and 96520.10 coulombs g-equivalent^{-1} for the faraday on the chemical and physical scales, respectively.

Since it is the value of the faraday on the physical scale that is of most concern to those interested in atomic constants a direct determination of the physical atomic weight of silver was deemed most important. Accordingly, the physical atomic weight of silver was determined by mass spectrometry in an associated experiment by W. R. Shields and V. H. Dibeler of the Mass Spectrometry Section of the National Bureau of Standards. Their results are described in detail in reference [33]. They also measured the isotope ratio, Ag^{107}/Ag^{109}, in the mint and electrolytically purified silver anodes used in the present investigation and obtained 1.08148 uncorrected for instrumental bias. This ratio agreed with the ratio obtained for the silver in certified reagent grade silver nitrate and, within the experimental uncertainty, with the ratio obtained for native silver from various sources [33]. The agreement obtained between mint silver and the electrolytically purified silver is conclusive evidence that no measureable isotopic separation had occurred in the electrolytic process used to purify the silver for the anodes. Incidentally, these measurements also show that no separation of isotopes was likely during silver deposition in the earlier experiments of Rosa, Vinal, and McDaniel [21] or of Vinal and Bates [8,9].

In order to measure the bias, isotopically enriched silvers from the Oak Ridge National Laboratory at Oak Ridge, Tenn., were used. The silvers as obtained were stated to have the isotopic composition as outlined in table 13. The samples were also

TABLE 13. *Isotopic composition of isotopically enriched silvers*

	Ag^{107}	Ag^{109}	Notes
Silver "107"	98. 81	1. 19	Oak Ridge.
	98. 804	1. 196	NBS.
	98. 79$_8$	1. 20$_2$	NBS, bias corrected.
Silver "109"	0. 94	99. 06	Oak Ridge.
	.915	99. 085	NBS.
	.91$_0$	99. 09$_0$	NBS, bias corrected.

measured by Shields and Dibeler at the National Bureau of Standards and their results agreed closely with those of the Oak Ridge National Laboratory.

Synthetic blends of weighed quantities of the isotopically enriched silvers were prepared and their isotope ratios were calculated using the calculated atomic weights of each enriched silver. The nuclidic masses used for Ag^{107} and Ag^{109} were, respectively, 106.93899 $\pm$0.00010 and 108.93928 $\pm$0.00010 [36]. Finally, the isotope ratios were measured with the mass spectrometer [33] and the results are given in table 14. In the last two experiments the synthetic blends were made with Ag^{107} and Ag^{109} which were purified electrolytically by the same procedure used to prepare the pure silver anodes used in the coulometer experiments with a few minor modifications needed because of the small samples of isotopically enriched silvers that were available. Small silver rods of the enriched silvers were made as in section 8.4 and used as cathodes on which to deposit the purified samples.

Silver nitrate solution prepared from each isotopically enriched silver was used as the electrolyzing solution in each case. After deposition the purified silver was easily removed from the cathode and was leached in hydrofluoric acid solution and then in conductivity water. After it was dried at 110 °C, the silver was put in a small well-cleaned quartz tube and melted in *vacuo*. The resulting buttons were again leached in hydrofluoric acid solution and in conductivity water. Portions of each button were used to prepare synthetic mixtures, and other portions were analyzed spectrochemically. These analyses gave the following:

Impurity	Ag "107"	Ag "109"
	ppm	*ppm*
Copper	0. 05	0. 05
Iron	. 20	. 20
Magnesium	. 02	. 05
Tin	. 10	. 5
Total	. 37	. 80

The total impurities in each case were less than 1 ppm; the two silvers were, therefore, of almost identical purity and the small difference would be

without significant effect on the calculated or measured isotope ratios.

Originally, each of the two silvers contained about 125 ppm of total impurities. The results shown in table 14 for the measured isotope ratios show quite clearly that the impurities in the silver, providing they are of about the same amount in both silvers, do not affect the mass spectrometer determinations.

The weighted average of the bias ratio between the calculated and the measured isotope ratios (Ag^{107}/Ag^{109}) was 0.99467. Therefore, the mass spectrometer is biased in favor of the light isotope. However, this bias must also be taken into account in the values obtained for the analysis of silver "107" and "109". When this is done for four successive calculations, the analyses of the original enriched materials are as shown in table 13. Using these analyses of silvers "107" and "109" the isotope ratios were recalculated. These are given in the second portion of table 14; the weighted average bias between the calculated and measured ratios is now 0.99444. Hence the true isotope ratio for the "faraday silver" is 1.07547. This value is equivalent to

$$107.9028 \pm 0.0013 = \text{at. wt. of silver (physical scale)}$$

and

$$107.8731 \pm 0.0013 = \text{at. wt. of silver (chemical scale)}.$$

The uncertainty of 0.0013 comes from the assigned uncertainty in the nuclidic masses of Ag^{107} and Ag^{109} and the statistical uncertainty (95% confidence level) in the mass spectrometer measurements. No additional uncertainty is assigned in conversion to the chemical scale since the adopted conversion factor is taken as 1.000275 exactly.

TABLE 14. *Isotope ratios in synthetic blends of silvers*

Experiment No.	Weight of silver "107"	Weight of silver "109"	Isotope ratio		Bias ratio (calculated/measured)
			Calculated	Measured	
	g	*g*			
1	0.107004	0.100151	1.07998	[b] 1.08628 (8)	0.99417
2	.107135	.101350	1.06873	1.07462 (8)	.99452
3	.108413	.101766	1.07688	1.08118 (8)	.99602
4 [a]	.107736	.101732	1.07065	1.07599 (6)	.99504
5 [a]	.110689	.103758	1.07835	1.08555 (6)	.99337
Weighted average					0.99467

	Isotope ratio	Bias ratio	Bias× 1.08148	Atomic weight	
				Physical	Chemical
1	1.07970	0.993942	1.07493	107.9030	107.8734
2	1.06848	.994283	1.07530	107.9028	107.8732
3	1.07663	.995790	1.07693	107.9021	107.8724
4 [a]	1.07040	.994803	1.07586	107.9026	107.8729
5 [a]	1.07810	.993136	1.07406	107.9034	107.8738
Weighted average		.99444	1.07547	107.9028	107.8731

[a] Electrolytically purified.
[b] Numbers in parentheses equals number of analyses.

11.3. The Faraday

From the above determinations of the electrochemical equivalent of silver and the atomic weight of silver measured with the mass spectrometer, the faraday is

$$F = 96{,}516.5 \pm 2.4 \text{ coulombs } g\text{-equivalent}^{-1} \text{ (physical scale)}.[8]$$

Using the conversion factor, the faraday on the chemical scale is

$$F = 96{,}490.0 \pm 2.4 \text{ coulombs } g\text{-equivalent}^{-1} \text{ (chemical scale)}$$

where the uncertainties include both the uncertainties in the electrochemical equivalent and atomic weight of silver.[9]

The authors wish to express their appreciation to the following for their assistance or advice in the various areas of the work:

Electrical measurements—to Miss Anna Skapars for assistance in controlling the current in some of the measurements; to W. H. Wood for measurements of the load resistance of the standard resistors.

Mass measurements—to L. B. Macurdy for assembling and testing the microbalance used in the work with the silver anodes.

Time measurements—to A. W. Spinks and R. W. Balcom for installing the lines from the NBS crystal oscillators and the receiver for picking up standard time signals, and to F. D. Weaver for checking the accuracy of the time measurements.

Purity of silver—to Mrs M. M. Darr for her painstaking spectrochemical analyses of the silver and to Bruce Bendigo for his photometric analyses of copper and iron.

State of silver—to G. A. Moore for his invaluable help in treating the finely divided silver and melting it into anodes and to T. H. Orem for his X-ray analyses of anode No. 5.

Atomic weight of silver—to V. H. Dibeler and W. R. Shields for their mass spectrometric determination of the physical atomic weight of silver used in this investigation.

Statistical analyses—to J. M. Cameron and Churchill Eisenhart for their advice on the statistical analysis of the results.

The authors are also indebted to F. B. Silsbee, Edward Wichers, F. L. Mohler, A. G. McNish, and to B. F. Scribner for many fruitful discussions during the course of this work.

---

[8] This uncertainty includes allowances of 0.0007 in the atomic weight of silver and 0.000007 in the electrochemical equivalent as the possible effect of systematic errors and 2.1 times the standard deviation in the ratio of the atomic weight to the electrochemical equivalent of silver as the limit to the effect of random errors.

[9] These values are based on the electrical standards as presently maintained at the National Bureau of Standards. Recently, Driscoll [37] by means of an electrodynamometer of the Pellat type found that 1 NBS amp=1.000013±0.000008 abs amp. In the same year Driscoll and Cutkosky [38] by using a current balance found that 1 NBS amp=1.000008±0.000006 abs amp. Since the acceleration of gravity is a common factor in these two determinations, it was taken out before averaging, and then reentered after averaging. On doing this Driscoll and Cutkosky [38] obtained 1 NBS amp= 1.000010 ±0.000005 abs amp. On this basis the values of the faraday given above would be 10 ppm higher. However, since the electrical standards as maintained are used in the dissemination of the units and in international comparisons, the values of the faraday based on the electrical standards as maintained are the ones given.

12. Appendix 1. Effect of Oxygen

In this paper, it was stressed that efforts were made to remove oxygen and silver oxide from the starting silver. To show specifically the effect of oxygen three runs were made in which no attempt was made to remove the oxygen as it may normally exist in silver, and eight runs were made with silver in which only a superficial attempt was made to remove the oxygen, i.e., it was simply heated to dull redness in a Bunsen flame.

All measurements, electrical and chemical, were made with the same care and precision as in the best measurements. The treatments given to the silver were as follows:

Experiments A1–1 and A1–2: Mint silver No. 2 as received from the U.S. Mint at Philadelphia, Pa., was given no treatment whatsoever.

Experiment A1–3: Mint silver No. 2 was slightly etched in 10-percent aqueous ammonium hydroxide; given no other treatment.

Experiments A1–4 and A1–5: Mint silver No. 2 was heated to dull redness.

Experiments A1–6 and A1–7: Mint silver No. 2 was heated to dull redness and etched slightly in 10-percent aqueous ammonium hydroxide.

Experiments A1–8, A1–9, A1–10, and A1–11: Mint silver No. 1 was treated in the same manner as samples A1–6 and A1–7.

The results obtained with these experiments are given in table 15. Inspection of table 15 shows that the values for the electrochemical equivalent are high, especially for those samples not heated to dull redness. Mere heating to dull redness decomposes at least part of the silver oxide and removes part but not all of the dissolved oxygen. That these high results are a consequence of dissolved oxygen may be shown by the following calculations. The data of Steacie and Johnson [26] on the solubility of oxygen in silver at various temperatures and pressures are reproduced in table 16.

The solubility of oxygen in silver passes through a minimum at about 400° C. Steacie and Johnson concluded that oxygen exists as the element in silver above 400° C and as the lower oxide, Ag_2O, below 400° C. Since normal atmospheric air contains about 21 percent of oxygen the partial pressure of oxygen in air at normal temperature and pressure

TABLE 16. *Solubility of oxygen in silver*

t° C	Pressure (mm)					
	50	100	(160)	200	400	800
	Volume O_2 (NTP) per volume Ag					
200	0.030	0.050	(0.064)	0.071	0.100	0.142
300	.021	.032	(.040)	.045	.070	.097
400	.020	.031	(.039)	.044	.061	.087
500	.022	.034	(.043)	.048	.067	.095
600	.033	.047	(.059)	.066	.093	.132
700	.048	.068	(.087)	.096	.134	.193
800	.088	.124	(.157)	.175	.247	.354

TABLE 15. *Results with silver containing oxygen*

Experiment No.	Date	Time	IR drop	Resistor code	Resistance	Current	Coulombs [a]	E_r	Silver corroded, Ag_m	Sediment	Electrochemical equivalent		
											Uncorrected	Corrected [b]	Corrected [c]
Mint silver No. 2—no treatment, *o* [d]													
		sec	*v*		*Ohms*	*amp*	*amp-sec*	*v*	*g*	*g*	*mg coulomb*$^{-1}$	*mg coulomb*$^{-1}$	*mg coulomb*$^{-1}$
A1–1	1–3–57	10,799.982	1.0182141	G	3.001127	0.3392772	3,664.1873	0.094	4.100657	0.043981	1.119118	1.119111	1.118776
A1–2	1–8–57	10,799.945	1.0182132	G	3.001129	.3392767	3,664.1693	.099	4.100600	.059223	1.119108	1.119101	1.118766
Mint silver No. 2—etched only, *o* [d]													
A1–3	2–28–57	10,800.040	1.0182132	G	3.001135	0.3392760	3,664.1940	0.091	4.100969	0.033223	1.119201	1.119195	1.118859
Mint silver No. 2—annealed only, *o* [d]													
A1–4	1–17–57	9,000.244	1.0182127	G	3.001127	0.3392768	3,053.5735	0.117	3.414747	0.106558	1.118279	1.118272	1.118110
A1–5	1–23–57	9,600.043	1.0182119	G	3.001133	.3392758	3,257.0620	.097	3.642077	.101450	1.118209	1.118202	1.118040
Mint silver No. 2—annealed and etched, *o* [d]													
A1–6	2–11–57	8,999.949	1.0182127	G	3.001131	0.3392763	3,053.4690	0.105	3.414218	0.121079	1.118144	1.118138	*1.117975
A1–7	2–18–57	9,600.009	1.0182125	G	3.001133	.3392760	3,257.0522	.099	3.641862	.162788	1.118147	1.118140	*1.117977
Mint silver No. 1—annealed and etched, *o* [d]													
A1–8	7–17–56	10,800.140	1.0182203	H	2.000612	0.5089544	5,496.7786	0.082	6.146287	0.697158	1.118162	1.118152	*1.117988
A1–9	8–3–56	7,200.042	1.0182135	H	2.000612	.5089510	3,664.4684	.081	4.097390	.508128	1.118140	1.118131	*1.117968
A1–10	8–9–56	7,200.107	1.0182119	H	2.000612	.5089502	3,664.4956	.093	4.097430	.296137	1.118143	1.118133	*1.117971
A1–11	8–15–56	11,999.980	1.0182153	G	3.001145	.3392756	4,071.3004	.087	4.552775	.484088	1.118261	1.118251	*1.118088

[a] Includes corrections for any initial off-balance and coulombs utilized in side-circuit measurements of reference silver electrode.
[b] With corrections for metallic impurities.
[c] With corrections for metallic impurities and estimated corrections for oxygen solubility.
[d] Impurities are metallic oxides.

Average (total) 1.118020
Average (*) 1.117995
Average (* omitting A1–11) 1.117976

is 160 mm. The solubility of oxygen in silver at this pressure was obtained by interpolation of the data of table 16 and the interpolated values are given in parentheses in column 4 of table 16. Unfortunately, Steacie and Johnson did not extend their measurements below 200° C. They stated, however, that "it appears probable that the solubility is considerably greater at room temperature than at 200° C". To obtain an *estimate* of the solubility at 25° C the data at 160 mm pressure were fitted to the distorted parabolic equation:

$$-\log S = -\log S_m + a(t-m)^2 + ct^2$$

where S_m is the minimum solubility (S); m, the temperature (400° C) for the minimum solubility; t, deg Celsius; and a, b, and c are empirical constants. Values of log S_m, a, b, and c were determined by the method of least squares; then the equation with numerical values is:

$$-\log S = 1.4089 - 4.0\times10^{-6}\,(t-400)^2 + 2.4\times10^{-8}\,t^2.$$

For 25° C this equation gives 0.15 for the volume of oxygen dissolved in a unit volume of silver at 25° C and 160 mm of oxygen pressure. Now taking the density of silver as 10.50 the volume of oxygen associated with 1 g of silver is 0.0143 ml. At 25° C, this oxygen exists combined with silver in the form of the lower oxide, Ag_2O. Thus, 0.0003 g of Ag_2O is associated with 1 g of silver or silver contains 0.03 percent of Ag_2O. This Ag_2O will be chemically soluble in perchloric acid, and thus if corrections are not made for its presence high values (as seen in column 13 of table 15) for the electrochemical equivalent of silver will result. Values obtained when the above estimated corrections are made are given in the last column of table 15 (first 3 values).

When the silver is heated to dull redness in air the situation is quite different. According to Bone and Wheeler [39] the temperature of silver at dull redness is about 650° C. From table 16 the volume of oxygen associated with 1 volume of silver at 650° C and 160-mm pressure is 0.074; this is equivalent to 0.00001006 g oxygen/g of silver. Now when the silver is cooled to room temperature (25° C) this oxygen will exist combined with silver as Ag_2O or 0.0001457 g of Ag_2O is associated with 1 g of silver. Since this Ag_2O will be chemically soluble in perchloric acid, high values (see column 13 of table 15) of the electrochemical equivalent of silver will result if corrections are not made for the presence of Ag_2O. Values obtained when these estimated corrections are made for experiments A1–4 to A1–11, inclusive, are given in the last column of table 15. In this case, corrections can be made without an extrapolation, or use of an empirical equation, since the amount of Ag_2O can be calculated from the amount of oxygen dissolved in silver at 650° C and for which data are available (table 16).

The average value for the electrochemical equivalent of unannealed silver is 1.118800 mg coulomb^{-1}; if only the annealed and etched samples are used the average is 1.117995 (omitting the last value the average is 1.117976). These average values for the annealed samples agree remarkably well with the final value given in the text; the agreement is remarkable in view of the rough estimates that were made of the oxygen content. For the unannealed samples the values are still high indicating that underestimates of the amount of Ag_2O in silver result from the use of the above parabolic equation to calculate oxygen content and from that the Ag_2O content. One would not pretend to use this procedure to arrive at an accurate and precise value of the faraday; this appendix was included here to show the need for the removal of oxygen or silver oxide from the starting silver.

13. Appendix 2. Effect of Hydrogen

It was stressed earlier that all hydrogen must be removed from the silver. During the course of these investigations two specific effects of hydrogen were noted. Mint silver No. 1 was used in a series of nine experiments in which the silver was treated in a silica tube with hydrogen for 72 hr at 875.5° C and then cooled abruptly in helium to room temperature within 2 hr. Nine coulometric measurements were then made with this treated silver with the same care and precision, as were made with the best measurements, and the results are given in table 17. These results became puzzling in view of later experiments in that the values for the electrochemical equivalent of silver were quite low. The presence of hydrogen would lower the electrochemical equivalent but when mint silver No. 2 was treated in like manner the final results were quite different and agreed closely with the vacuum values. The reason for this difference was not at once apparent until it was found that mint silver No. 1 contained traces of palladium and gold which were not detected in mint silver No. 2. Palladium could catalyze the reaction $Ag^+ + (\frac{1}{2})H_2 \rightarrow Ag + H^+$ in a manner similar to that at a hydrogen electrode.

Steacie and Johnson [40] in a comprehensive study of the solubility of hydrogen obtained the results given in table 18. Since the silver in the present experiments was abruptly cooled from 875.5° C to room temperature in 2 hrs and with only superficial replacement of hydrogen by helium it is assumed that the dissolved hydrogen was not completely displaced or removed. Furthermore, it is known that metal-hydrogen systems show marked hysteresis in their isotherms [41]. Thus, 0.046 volume of hydrogen per volume of silver was used since the silver was heated at 875.5° C at a pressure slightly exceeding atmospheric. Thus 0.000000394 g hydrogen is associated with 1 g of silver and this amount of hydrogen will produce 0.0000425 g of silver by reduction of Ag^+ ion. When corrections are made for the Ag^+ ions which are reduced the values given in the last column of table 17 are obtained. The average value, after these corrections, for the electrochemical equivalent of silver is 1.117878 mg coulomb^{-1}. This value differs by 8 parts in 100,000 from the value given in the main part of this paper and is in the direction expected for silver containing hydrogen in excess of

TABLE 17. *Results of specific effects of hydrogen on silver*

Experiment No.	Date	Time	*IR* drop	Resistor code	Resistance	Current	Coulombs [a]	E_r	Silver corroded, Ag_m	Sediment	Electrochemical equivalent		
											Uncorrected	Corrected [b]	Corrected [c]
Mint silver No. 1—excess hydrogen, not melted, [d]													
		sec	*v*		*Ohms*	*amp*	*amp-sec*	*v*	*g*	*g*	*mg coulomb*$^{-1}$	*mg coulomb*$^{-1}$	*mg coulomb*$^{-1}$
A2-1	8-28-56	14,400.096	1.0182142	G	3.001143	0.3392755	4,885.5993	0.092	5.461195	0.065717	1.117815	1.117839	1.117888
A2-2	8-30-56	10,800.455	1.0182125	H	2.000613	.5089503	5,496.8942	.126	6.144322	.114476	1.117781	1.117805	1.117854
A2-3	9-17-56	8,400.100	1.0182130	H	2.000613	.5089505	4,275.2345	.119	4.778785	.078265	1.117783	1.117808	1.117857
A2-4	9-19-56	10,800.311	1.0182140	G	3.001142	.3392755	3,664.2805	.097	4.095865	.035293	1.117782	1.117806	1.117855
A2-5	9-24-56	22,500.065	1.0182133	B	10.000017	.10182115	2,290.9822	.067	2.560846	.036912	1.117794	1.117818	1.117868
A2-6	9-27-56	22,500.075	1.0182139	B	9.999983	.10182156	2,290.9923	.073	2.560977	.068333	1.117846	1.117871	1.117920
A2-7	10-16-56	7,203.775	1.0182142	H	2.000612	.5089513	3,666.3703	.110	4.098252	.052391	1.117795	1.117820	1.117869
A2-8	10-18-56	10,799.954	1.0182138	G	3.001142	.3392754	3,664,1583	.098	4.095960	.074096	1.117845	1.117869	1.117918
A2-9	10-23-56	18,000.038	1.0182138	E	5.000001	.2036427	3,665.5759	.092	4.097376	.056630	1.117799	1.117823	1.117872
												Average	1.117878
Anode 3—melted in hydrogen													
A2-10	4-8-58	18,000.019	1.0182100	E	5.000085	0.2036385	3,665.4965	0.101	4.098482	0.003117	1.118125		
A2-11	4-28-58	17,999.998	1,0182097	E	5.000087	.2036384	3,665.4903	.126	4.098288	.000875	1.118074		

[a] Includes corrections for any initial off-balance and coulombs utilized in side-circuit measurements of reference silver electrode.
[b] With corrections for metallic impurities.
[c] With corrections for metallic impurities and estimate corrections for hydrogen solubility.
[d] Impurities are metallic.

TABLE 18. *Solubility of hydrogen in silver*

t° C	Pressure (mm)				
	50	100	200	400	800
	Volume H_2 (NTP) per volume silver				
200	0	0	0	0	0
300	Trace	Trace	Trace	Trace	Trace
400	Trace	0.002	0.003	0.004	0.006
500	0.003	.004	.006	.008	.012
600	.005	.007	.010	.014	.019
700	.006	.009	.013	.018	.025
800	.009	.013	.018	.025	.036
900	.012	.016	.023	.033	.046

that given by the solubility data of Steacie and Johnson.

Steacie and Johnson worked with silver foil and stated that there was no adsorption of hydrogen and that only absorption or solution of hydrogen occurred in silver. Bone and Wheeler [39], however, found that silver gauze which had been repeatedly used, i.e., had a roughened surface retained as much as 1.3 volumes of hydrogen per unit volume of silver. Also it is known that Pd-Ag alloys absorb more hydrogen than pure silver [42]. Accordingly, the data in table 18 may be considered as minimum solubility values and that a small additional amount of hydrogen was probably adsorbed on the surface of the silver, which would lead to a further but small rise in the corrected values of the electrochemical equivalent of silver given in table 17.

Another experiment involved the melting of purified silver (anode No. 3) in an atmosphere of hydrogen. The anode was first heated in *vacuo* from room temperature to 530° C in 17 hr, hydrogen was then introduced and the temperature raised to 975° C in 4 hr. The silver in the molten state was kept under hydrogen for 15 min. The hydrogen was then replaced over a 45-min period with helium. The tube was then evacuated, cooled slowly to 900° C (60° C below melting point), and then cooled abruptly to room temperature. Melting the silver in hydrogen caused blistering of the silver and when the anode was electrolytically corroded in the first experiment it was seen that the anode contained cavities. These cavities could have caused not only small uncertainties in the vacuum corrections but also could have prevented the complete removal of electrolyte from the anode when it was washed with conductivity water in the usual manner. Furthermore, the spectrochemical analyses of the silver (anode No. 3) given in table 19 indicate that the silver extracted considerable amounts of impurities from the silica tube. This observation is similar to that found by Baxter and Lundstedt [35] who observed that when silver is melted on pure lime in dry hydrogen that the silver became contaminated with calcium. Owing to the relatively large contamination and the cavities in the silver meaningful corrections for impurities could not be made in these experiments; only the uncorrected values for the electrochemical equivalent are given in the last two rows of table 17.

This appendix shows the effects of hydrogen on determining the electrochemical equivalent of silver and emphasizes the need for the complete removal of hydrogen from the silver.

TABLE 19. *Spectrochemical analyses of anode No. 3*

Element	Top [a]	Bottom
	ppm	*ppm*
Al	<1.0	<1.0
Cd	0.01	0.01
Cu	0.1-0.2	0.1-5.0
Fe	0.05-1.0	0.2-5.0
Mg	0.1-0.5	0.01-2.0
Ni		<10
Pb		<50
Si	<1	0.1-0.5
Sn		<5

[a] Top of anode near supporting wires.

14. References

[1] International Conference on Electrical Units and Standards, 1908: Minutes and Verbatim Report of the Meeting of the Delegates: together with Final Report: Printed for His Majesty's Stationery Office by Darling and Sons, London, p. 73 (1909).
[2] E. B. Rosa and G. W. Vinal, BS Sci. Pap. **285,** 479 (1916).
[3] E. W. Washburn and S. J. Bates, J. Am. Chem. Soc. **34,** 1341, 1515 (1912).
[4] F. F. Herroun, Phil. Mag. 5, **40,** 91 (1895).
[5] H. Danneel, Z. Electrochem. **4,** 154 (1897).
[6] D. A. Kreider, Am. J. Sci. 4, **20,** 1 (1905).
[7] G. Gallo, Gazg. Chim. Ital. **36,** II, 116 (1906).
[8] G. W. Vinal and S. J. Bates, BS Sci. Pap. **218,** 425 (1914).
[9] S. J. Bates and G. W. Vinal, J. Am. Chem. Soc. **36,** 916 (1914).
[10] H. Sommer and J. A. Hipple, Electrochemical Constants, NBS Circ. **524,** 21 (1953).
[11] D. N. Craig and J. I. Hoffman, Electrochemical Constants, NBS Circ. **524,** 13 (1953).
[12] T. W. Richards and G. S. Forbes, Publication of the Carnegie Institution (1906).
[13] O. Hönigschmid, E. Zintle, and P. Thilo, Z. Anorg. Chem. **163,** 65 (1927).
[14] G. W. Vinal and W. M. Bovard, Bul. BS **13,** 147 (1916) S271.
[15] J. S. Laird and G. A. Hulett, Trans. Am. Electrochem. Soc. **22,** 345 (1912).
[16] W. M. Bovard and G. A. Hulett, J. Am. Chem. Soc. **39,** 1077 (1917).
[17] T. W. Richards and F. O. Anderegg, J. Am. Chem. Soc. **37,** 7 (1915).
[18] A. F. Scott, Electrochemical Constants, NBS Circ. **524,** 1 (1953).
[19] E. Mascart, J. de Phys. Series II **1,** 109 (1882).
[20] T. Gray, Phil. Mag. **22,** 389 (1886).
[21] E. B. Rosa, G. W. Vinal, and A. S. McDaniel, Bul. BS **9,** 209 (1912) reprint No. 195.
[22] D. N. Craig and J. I. Hoffman, Phys. Rev. **80,** 487 (1950) and abstract, XIIth Congress of Pure and Applied Chemistry, New York, N.Y. (Sept. 10–13, 1951).
[23] D. N. Craig, C. A. Law, and W. J. Hamer, J. Research NBS **64A,** 127 (1960) Paper 64A1–34.
[24] W. M. Latimer, Oxidation Potentials; 2d Ed., p. 340–345 (Prentice-Hall, Inc., N.Y., N.Y., 1952).
[25] H. B. Brooks, J. Research NBS **11,** 223 (1933) RP586.
[26] E. W. R. Steacie and F. M. G. Johnson, Proc. Roy. Soc. (London) **A112,** 542 (1926).
[27] T. Carnelly and J. W. Walker, Trans. Chem. Soc., **53,** 79 (1888).
[28] G. N. Lewis, J. Am. Chem. Soc. **28,** 139 (1906).
[29] F. G. Keyes and H. Hara, J. Am. Chem. Soc. **44,** 479 (1922).
[30] A. F. Benton and L. C. Drake, J. Am. Chem. Soc. **54,** 2186 (1932).
[31] W. J. Hamer and D. N. Craig, J. Electrochem. Soc. **104,** 206 (1957).
[32] E. Wichers, J. Am. Chem. Soc. **80,** 4121 (1958), **78,** 3235, (1956).
[33] W. R. Shields, D. N. Craig, and V. H. Dibeler, J. Am. Chem. Soc. (September 1960).
[34] A. O. Nier, Science **121,** 737 (1955).
[35] G. P. Baxter and O. W. Lundstedt, J. Am. Chem. Soc. **62,** 1829 (1940).
[36] W. H. Johnson, Jr. and A. O. Nier, private communications to V. H. Dibeler and W. R. Shields (see ref. [33]).
[37] R. L. Driscoll, J. Research NBS **60,** 287 (1958) RP 2845.
[38] R. L. Driscoll and R. D. Cutkosky, J. Research NBS **60,** 297 (1958) RP2846.
[39] W. A. Bone and R. V. Wheeler, Phil. Trans. Roy. Soc. (London) **A206,** 1 (1906).
[40] E. W. R. Steacie and F. M. G. Johnson, Proc. Roy. Soc. (London) **A117,** 662 (1928).
[41] D. P. Smith, Hydrogen in metals, pp. 87–100, 116, 161, 166, 167 (The University of Chicago Press, Chicago, Ill., 1948).
[42] A. Sieverts, E. Jurisch, and A. Metz, Z. Anorg. Allgem. Chem. **92,** 329 (1915).

(Paper 64A5–63)

JOURNAL OF RESEARCH of the National Bureau of Standards—A. Physics and Chemistry
Vol. 64A, No. 5, September–October 1960

Systems Silver Iodide-Sodium Iodide and Silver Iodide-Potassium Iodide[1]

G. Burley and H. E. Kissinger

(May 12, 1960)

The phase relations for the systems AgI-NaI and AgI-KI have been determined for the temperature range from room temperature to 685° C, using differential thermal analysis techniques. The AgI-NaI system has a eutectic at 50 mole percent NaI and 384° C. The AgI-KI system has eutectics at 20.8 and 28.5 mole percent KI and 254° C and 244° C, respectively. A compound of formula KAg_3I_4 is formed with a congruent melting point of 268° C.

1. Introduction

During the last decade, silver iodide has been used extensively in weather modification attempts. Because of the crystallographic similarity, silver iodide can serve as an epitaxial nucleation site for the growth of ice crystals. This greatly decreases the supercooling tendency of water vapor in the atmosphere.

One technique of generating a smoke of this substance consists of dissolving a mixture of AgI and an alkali iodide in acetone and feeding the resulting solution into the nozzle of a burner [1].[2] Under normal operating conditions this gives particles ranging from 10^{-2} to 10^{-3} μ in diameter, and produces about 10^{12} nuclei per second.

Since both AgI and either NaI or KI are in the original solution and the solvent is presumably evaporated in the burner, the solid state relations of these constituent compounds are of interest. Mason [2] has reported that the product resulting from the combination of AgI and KI had little relation to either of the original compounds. This investigation of the phase relationships in the systems AgI-NaI and AgI-KI was undertaken in order to obtain information on equilibrium conditions in these systems.

2. Apparatus

A differential thermal analysis (DTA) unit was used to obtain most of the data. The apparatus has been described previously [3]. Specimen holders made of 5 mil platinum sheet in the form of tubular cups 4 cm in depth and 1 cm in diameter were used. The bottom of each container included a closed reentrant central tube, extending one-half the length of the cup, which fitted over the thermocouple junction. This arrangement served to contain the molten sample and to protect the thermocouples. Thermocouples were made of 15 mil Pt-Pt 10 percent Rh wire. The reference material was aluminum oxide.

The heating rate of the furnace was generally 5° C/min. The rate was reduced to 2° C/min to resolve complex peak shapes. The thermocouples were calibrated by using the quartz inversion at 573° C as an external standard. In addition, AgI has a reversible transformation at 146° C. This transformation produces a well defined thermal arrest which was used as an internal standard.

Near the eutectics and near the end member compositions, melting was accompanied by the characteristic endothermic DTA deflection. For intermediate compositions, the beginning and end of melting was indicated by a change in the slope of the base line.

A high-temperature powder X-ray goniometer [4] was used to give an approximate indication of melting points. Since the pattern decreases in intensity as the temperature is increased, the exact temperature of disappearance is difficult to determine by this method. For this reason all results reported here are those obtained with the DTA apparatus. The X-ray method was useful, however, in checking for possible phase changes having negligible heat effects.

3. Materials

The materials used were reagent grade chemicals. No special purification procedures were used. Chemical analysis supplied by the manufacturer showed a maximum of 0.01 percent Cl^- and 0.0003 percent IO_3^- for the KI and 0.02 percent Cl^- and 0.001 percent IO_3^- for the NaI. In order to minimize absorption of moisture from the atmosphere all transfers from reagent to weighing bottles were done in a drybox through which a stream of dry air was passed. The components were thoroughly mixed and then immediately used as starting materials for the DTA. In a number of cases, the thoroughly mixed reactants were melted, ground, mixed, and remelted before using them for the DTA. The results appeared to be identical with those obtained

[1] This research was supported by the National Science Foundation Grant NSF-G5242.
[2] Figures in brackets indicate the literature references at the end of this paper.

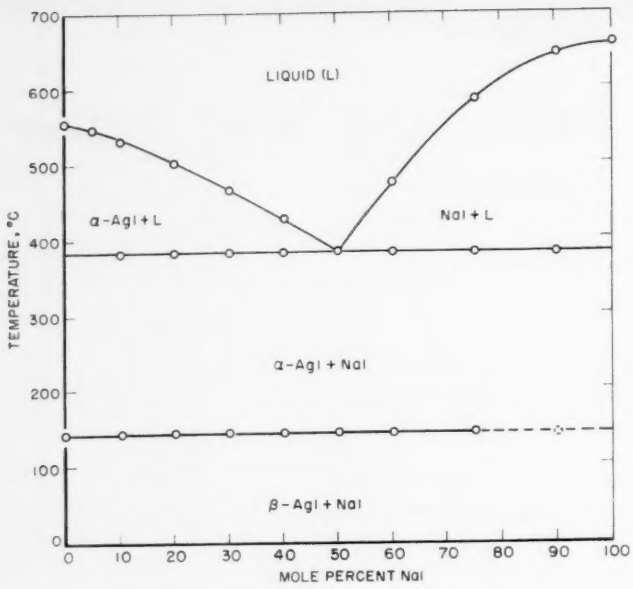

FIGURE 1. *Phase diagram of the system AgI-NaI.*

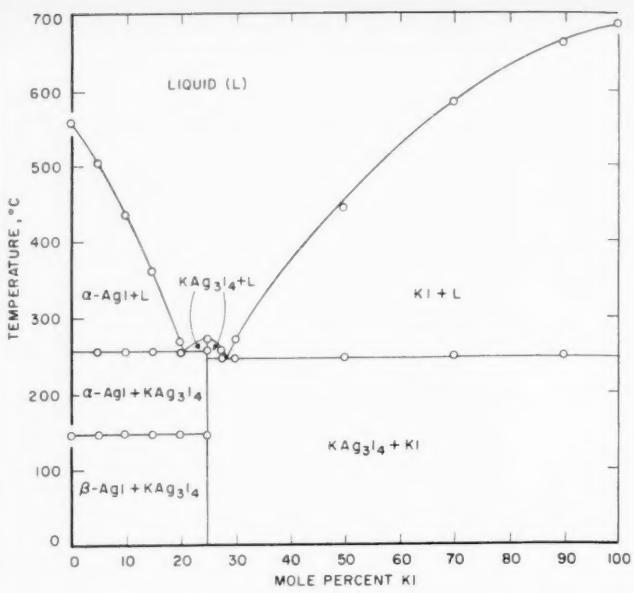

FIGURE 2. *Phase diagram of the system AgI-KI.*

using mechanical mixtures, and it must be assumed that diffusion rates are high enough to assure rapid mixing and equilibrium.

4. Results

The phase diagram of the system AgI-NaI is given in figure 1 and that of the system AgI-KI in figure 2.

Silver iodide has two low-temperature modifications [5]. These are a face-centered cubic sphalerite type (γ) structure and a hexagonal wurtzite type (β) structure. Only the latter appears to be stable [6]. At 146° C these change reversibly to a body-centered cubic type (α) structure which persists to the melting point at 555° C [7].

Sodium iodide has the face-centered cubic sodium chloride type structure. No phase changes occur to the melting point at 662° C [7]. Potassium iodide has the same structure type as sodium iodide and no phase changes. Its melting point is 685° [7].

The AgI-NaI system has a eutectic at 50 mole percent NaI and a temperature of 384° C. No solid solution region was observed. No compound formation occurs. The AgI transformation at 146° C apparently persists across the entire field, although it is difficult to observe at low AgI concentration.

The AgI-KI binary phase diagram shows two eutectics and formation of a compound. The eutectics are at 20.8 mole percent KI and 254° C and at 28.5 mole percent KI and 244° C. A 3AgI·KI compound is formed with a congruent melting point at 268° C.

5. Accuracy

The reproducibility and accuracy of the composition of the starting materials is estimated at ± 0.5 mole percent because of the hygroscopicity of the alkali iodides. The temperature of a transformation appears to be reproducible to $\pm 1°$ C in the DTA apparatus. In many cases solidification involved some supercooling, so that the melting temperatures were judged more reliable. The temperature of a eutectic, when far from the eutectic composition, is subject to a somewhat greater error. In general, the cumulative errors of composition, temperature measurement, and possible loss of iodine are estimated to amount to no more than ± 1 mole percent for each measured composition and $\pm 2°$ C for each measured temperature. Interpolated values are subject to the additional errors inherent in this procedure.

6. References

[1] B. Vonnegut, J. Colloid Sci. **5,** 37 (1950).
[2] B. J. Mason and J. Hallett, Nature **177,** 681 (1956).
[3] H. E. Kissinger, J. Research NBS **57,** 217 (1956) RP 2712.
[4] F. A. Mauer and L. H. Bolz, Wright Air Develop. Center TR 55–473 (1957).
[5] N. H. Kolkmeijer and J. W. A. van Hengel, Z. Kristallog. **88,** 317 (1934).
[6] G. Burley and H. F. McMurdie, Abstract-Am. Cryst. Assoc. Meeting, Wash., D.C. (Jan. 24–27, 1960).
[7] F. D. Rossini, D. D. Wagman, W. H. Evans, S. Levine, and I. Jaffe, Selected values of chemical thermodynamic properties, NBS Cir. 500 (1952).

(Paper 64A5–64)

JOURNAL OF RESEARCH of the National Bureau of Standards—A. Physics and Chemistry
Vol. 64A No. 5, September–October 1960

Conformations of the Pyranoid Sugars. III. Infrared Absorption Spectra of Some Acetylated Aldopyranosides

R. Stuart Tipson and Horace S. Isbell

(May 5, 1960)

The infrared absorption spectra of twenty-four acetylated aldopyranosides in the range of 5,000 to 250 cm^{-1} are reported. The conformation adopted by each of seventeen of the corresponding *unacetylated* glycosides had previously been assigned by us from a study of their infrared spectra. Analysis of the spectra revealed, for the acetylated glycosides (as for the parent glycosides), groups of absorption bands which showed a concerted shift on change of anomeric disposition. Assignment of conformation by the methods developed earlier led to the conclusion that each acetylated glycoside has the same conformation as its parent glycoside.

Intercomparison of the spectra of four of the remaining acetates with those of related acetates, especially in regard to the characteristic groups of absorption bands, afforded evidence that the anomeric methoxyl group is axial in methyl hepta-*O*-acetyl-4-*O*-β-D-glucopyranosyl-α-D-mannopyranoside, and equatorial in methyl tetra-*O*-acetyl-β-D-mannopyranoside, methyl penta-*O*-acetyl-D-*glycero*-β-L-*manno*-heptopyranoside, and methyl hepta-*O*-acetyl-4-*O*-β-D-glucopyranosyl-β-D-mannopyranoside. For lack of spectra of related acetylated aldopyranosides, assignments cannot yet be made for methyl hepta-*O*-acetyl-6-*O*-β-D-glucopyranosyl-β-D-glucopyranoside, methyl penta-*O*-acetyl-D-*glycero*-β-D-*ido*-heptopyranoside, and methyl hepta-*O*-acetyl-4-*O*-β-D-galactopyranosyl-β-D-altropyranoside.

1. Scope and Purpose of the Project

The purpose of the present project was twofold. The first objective was to record the infrared absorption spectra of a variety of acetylated aldopyranosides for use in the identification of supposedly identical samples. The spectra of three of the compounds included in the present study were recorded by Kuhn [1][1] for a limited range (1,250 to 667 cm^{-1}). In the following year, the spectra of 13 of the compounds were given (for the range of 5,000 to 667 cm^{-1}) by Isbell and coworkers in a privately circulated report [2] which was subsequently published [3]. Twelve of the spectra obtained by these investigators were later discussed by Whistler and House [4], who noted certain bands in the range of 1,205 to 855 cm^{-1}. Next, Barker and coworkers [5] examined the spectra of two of Kuhn's compounds and of four others that are included in the present study, but have not published them in sufficient detail to permit comparison over a wide spectral range; some of the bands in the range of 960 to 730 cm^{-1} were discussed. In the present article, the infrared absorption spectra of 24 acetylated aldopyranosides, in the range of 5,000 to 250 cm^{-1}, are given; all of the bands of all of these compounds have been measured and have received consideration.

The second objective was the discovery of correlations that might be of value in structural analysis, both as regards (a) the presence of certain functional groups and (b) the particular conformation assumed by each compound. Isbell and coworkers [3] recorded the infrared spectra of 13 of the compounds dissolved in suitable solvents, and were able to reach certain conclusions regarding correlations of the kind mentioned. However, at the low concentrations they employed, minor bands were absent or difficult to detect. The spectrograms have now been recorded for the solid phase, as pellets consisting of crystalline material suspended in an alkali-metal halide. [Such spectra show more bands than those for the same compounds dissolved in a solvent. This is because, for the solid, the following factors are operative: (1) A removal of degeneracies by perturbations from lattice forces; (2) occurrence of combination vibrations between molecular and lattice modes in the solid; and (3) an intensification of overtones and combination vibrations.]

In part II of this series of articles [6], a method was described for gaining information regarding the conformations of unsubstituted aldopyranosides from analysis of their infrared spectra. The analysis revealed groups of absorption bands, characteristic for each group-configuration, which displayed a concerted shift on change of anomeric disposition. This empirical observation was employed, in conjunction with a consideration of instability factors (arrived at on theoretical grounds), in making conformational assignments and in deciding the arrangement of groups (e.g., axial or equatorial) at the anomeric carbon atom of these and related compounds. The results were essentially in agreement with those obtained experimentally by Reeves [7] from a study of the behavior of these unsubstituted aldopyranosides on forming complexes with the cuprammonium reagent. The present article describes the results obtained on applying the same kind of analysis to the infrared spectra of the fully acetylated derivatives

[1] Figures in brackets indicate the literature references at the end of this paper. The references for table 1 are given at the end of the table.

of 17 of the aldopyranosides studied in part II and of 7 acetylated aldopyranosides whose unacetylated parents were not included therein.

2. Compounds Investigated

Table 1 gives a list of the compounds, their code numbers [8], and an index to the spectrograms; the serial number of a compound is the same as the number of its spectrogram. Also included in table 1 are (a) the conformation (where known) of the corresponding unacetylated glycoside, as determined in the preceding paper in this series [6], and (b) assignments of conformations to the acetylated glycosides. The conformations are indicated by the system devised by Isbell and Tipson [9, 10].

The spectra were measured in the region of 5,000 to 667 cm^{-1} (sodium chloride optics) and in the region of 667 to 250 cm^{-1} (cesium bromide optics). The spectrograms are given together with a discussion of (a) the structure of the compounds and (b) some of the outstanding features of their spectra.

All of the compounds listed in table 1 are fully acetylated glycosides of aldoses, and all have the pyranoid ring. As a common structural feature, all but one of the glycosides have a glycosidic methoxyl group; one has a glycosidic cyclohexyloxy group. The acetylated glycosides differ in regard to one or more of the following structural features: (a) The α or β anomeric configuration at carbon atom 1; (b) the configurations of the other carbon atoms of the pyranoid ring (including C5 in the hexosides and heptosides); (c) the nature of the substituent, if any, at C5 (including the configuration at C6 of the heptosides); and (d) the nature of the substituent at the C–4 and C–6 hydroxyl groups.

TABLE 1. *Compounds measured, stable conformations, and index to spectrograms*

Code [a]	Compound	Reference	Stable conformation [b]			Spectrogram
			Assignment for unacetylated glycoside [c]	Present assignment [d]	Anomeric disposition [d]	
12.11111(2,3,4)21	Methyl α-D-xylopyranoside, triacetate	1	CA	CA	*a*	1
12.11211(2,3,4)21	Methyl β-D-xylopyranoside, triacetate	2,3	CA	CA	*e*	2
12.21111(2,3,4,6)21	Methyl α-D-glucopyranoside, tetraacetate	4 to 6	CA	CA	*a*	3
12.21211(2,3,4,6)21	Methyl β-D-glucopyranoside, tetraacetate	4, 6	CA	CA	*e*	4
22.21?(2,3,4,6)21*(1–6).21?11(2,3,4)21	Methyl β-D-glucopyranosyl-(1→6)-β-D-glucopyranoside, heptaacetate.[e]	7				5
12.35?11(2,3,4,6,7)21	Methyl D-*glycero*-β(?)-D-*ido*-heptopyranoside, pentaacetate	8				6
12.12511(2,3,4)21	Methyl α-D-lyxopyranoside, triacetate	9, 10	CA+CE; non-chair.	CA+CE; non-chair.	*a*+*e*; *a*,*e*, or *q*.	7
12.12511(2,3,4)21	Methyl β-D-lyxopyranoside, triacetate	11	CA+CE; non-chair.	CA+CE; non-chair.	*a*+*e*; *a*,*e*, or *q*.	8
12.22111(2,3,4)21(6)80	Methyl 6-deoxy-α-L-mannopyranoside, triacetate	12, 13	CA	CA	*a*	9
12.22211(2,3,4)21(6)80	Methyl 6-deoxy-β-L-mannopyranoside, triacetate	12	CA	CA	*e*	10
12.22111(2,3,4,6)21	Methyl α-D-mannopyranoside, tetraacetate	14, 15	CA	CA	*a*	11
12.22211(2,3,4,6)21	Methyl β-D-mannopyranoside, tetraacetate	14, 15		CA	*e*	12
12.42211(2,3,4,6,7)21	Methyl D-*glycero*-β-L-*manno*-heptopyranoside, pentaacetate.	11		CA	*e*	13
22.21?(2,3,4,6)21*(1–4).22111(2,3,6)21	Methyl β-D-glucopyranosyl-(1→4)-α-D-mannopyranoside, heptaacetate.	16, 17		CA	*a*	14
22.21?(2,3,4,6)21*(1–4).22211(2,3,6)21	Methyl β-D-glucopyranosyl-(1→4)-β-D-mannopyranoside, heptaacetate.	16		CA	*e*	15
12.26511(2,3,4,6)21	Methyl α-D-gulopyranoside, tetraacetate	18	CA+CE; non-chair.	CA+CE; non-chair.	*a*+*e*; *a*,*e*, or *q*.	16
12.36111(2,3,4,6,7)21	Methyl D-*glycero*-α-D-*gulo*-heptopyranoside, pentaacetate	11	CA	CA	*a*	17
12.36211(2,3,4,6,7)21	Methyl D-*glycero*-β-D-*gulo*-heptopyranoside, pentaacetate	19	CA	CA	*e*	18
12.36213(2,3,4,6,7)21	Cyclohexyl D-*glycero*-β-D-*gulo*-heptopyranoside, pentaacetate.	20	CA	CA	*e*	19
12.13311(2,3,4)21	Methyl β-L-arabinopyranoside, triacetate	21	CE	CE	*a*	20
12.23111(2,3,4)21(6)80	Methyl 6-deoxy-α-L-galactopyranoside, triacetate	22	CA	CA	*a*	21
12.23111(2,3,4,6)21	Methyl α-D-galactopyranoside, tetraacetate	23, 24	CA	CA	*a*	22
12.23211(2,3,4,6)21	Methyl β-D-galactopyranoside, tetraacetate	6, 24	CA	CA	*e*	23
22.23?(2,3,4,6)21*(1–4).27?11(2,3,6)21	Methyl β-D-galactopyranosyl-(1→4)-β-D-altropyranoside, heptaacetate.	25				24

[a] The third figure after the point was inserted after the present conclusions as to conformation had been reached.
[b] Named by the system of H. S. Isbell and R. S. Tipson, Science **130,** 793 (1959); J. Research NBS **64A,** 171 (1960).
[c] Assignment made by R. S. Tipson and H. S. Isbell, J. Research NBS **64A,** 239 (1960).
[d] After accepting several of the assignments for the unacetylated glycosides (see text).
[e] A sample of the original material, prepared by J. M. Johnson in November 1916, was kindly presented by N. K. Richtmyer.

References for table 1

1. C. S. Hudson and J. K. Dale, J. Am. Chem. Soc. **40,** 997 (1918).
2. C. S. Hudson and J. M. Johnson, J. Am. Chem. Soc. **37,** 2748 (1915).
3. J. K. Dale, J. Am. Chem. Soc. **37,** 2746 (1915).
4. C. S. Hudson and J. K. Dale, J. Am. Chem. Soc. **37,** 1264 (1915).
5. E. Fischer and E. F. Armstrong, Ber. deut. chem. Ges. **34,** 2890 (1901).
6. W. Koenigs and E. Knorr, Ber. deut. chem. Ges. **34,** 957 (1901).
7. C. S. Hudson and J. M. Johnson, J. Am. Chem. Soc. **39,** 1272 (1917).
8. H. L. Frush and H. S. Isbell, J. Research NBS **35,** 111 (1945) RP1663.
9. P. A. Levene and M. L. Wolfrom, J. Biol. Chem. **78,** 525 (1928); **79,** 471 (1928).
10. F. P. Phelps and C. S. Hudson, J. Am. Chem. Soc. **50,** 2049 (1928).
11. H. S. Isbell and H. L. Frush, J. Research NBS **24,** 125 (1940) RP1274.
12. E. Fischer, M. Bergmann, and A. Rabe, Ber. deut. chem. Ges. **53,** 2362 (1920).
13. M. Bergmann and H. Schotte, Ber. deut. chem. Ges. **54,** 1569 (1921).
14. J. K. Dale, J. Am. Chem. Soc. **46,** 1048 (1924).
15. T. L. Harris, E. L. Hirst, and C. E. Wood, J. Chem. Soc. **1932,** 2108.
16. H. S. Isbell, BS J. Research **7,** 1115 (1931) RP392.
17. W. N. Haworth, E. L. Hirst, H. R. L. Streight, H. A. Thomas, and J. I. Webb, J. Chem. Soc. **1930,** 2636.
18. H. S. Isbell, BS J. Research **8,** 1 (1932) RP396.
19. W. N. Haworth, E. L. Hirst, and M. Stacey, J. Chem. Soc. **1931,** 2864.
20. E. Glaser and N. Zuckermann, Z. physiol. Chem. **166,** 103 (1927).
21. C. S. Hudson and J. K. Dale, J. Am. Chem. Soc. **40,** 992 (1918).
22. J. Minsaas, Rec. trav. chim. **56,** 623 (1937).
23. F. Micheel and O. Littmann, Liebigs Ann. Chem. **466,** 115 (1928).
24. J. K. Dale and C. S. Hudson, J. Am. Chem. Soc. **52,** 2534 (1930).
25. H. L. Frush and H. S. Isbell, J. Research NBS **27,** 413 (1941) RP1429.

3. Reference Aldopyranosides (of Known Conformation) and Their Acetates

In part II of this series, the stable conformation of each of 21 aldopyranosides was deduced from an analysis of the respective infrared absorption spectrum, and was found to be in agreement with the assignment reached from a consideration of instability factors.

In the present study, the crystalline, fully acetylated derivatives of 17 of these aldopyranosides were available (group A). In addition, 7 acetylated aldopyranosides (group B) whose unacetylated relatives had not been available (in the crystalline form) were examined. The spectra of the compounds comprising group A were analyzed, in order to determine if they were explicable on the basis that the acetate of a glycoside has the same conformation as its parent, unacetylated glycoside. The conclusions drawn from this study were then applied to deducing the stable conformation of members of group B.

4. Classification of the Acetylated Glycosides Into Configurationally Related Groups

The 24 compounds were classified into three groups; the members of each group have like configurational features.

4.1. Acetylated Aldopyranosides of the *xylo* Configuration

The members of this group of acetylated methyl aldopyranosides have the following general formula (I) for the CA conformation.

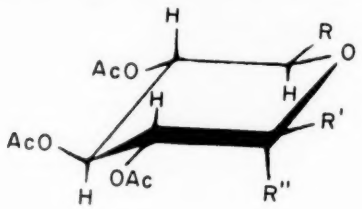

I

Compounds 1 to 5, in this conformation, have the above general structure, with the following substituents.

1. Methyl α-D-xylopyranoside triacetate, R=H; R′=H; and R″=OCH_3.
2. Methyl β-D-xylopyranoside triacetate, R=H; R′=OCH_3; and R″=H.
3. Methyl α-D-glucopyranoside tetraacetate, R=CH_2OAc; R′=H; and R″=OCH_3.
4. Methyl β-D-glucopyranoside tetraacetate, R=CH_2OAc; R′=OCH_3; and R″=H.
5. Methyl β-D-glucopyranosyl-(1→6)-β-D-glucopyranoside heptaacetate, R=tetra-*O*-acetyl-β-D-glucopyranosyl-OH_2C; R′=OCH_3; and R″=H.

Compound 6, if it is the β anomer, has the following formulas (II) for the two chair-conformations.

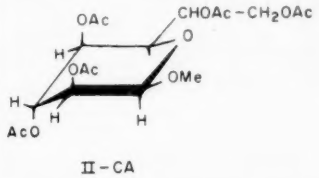

II-CA

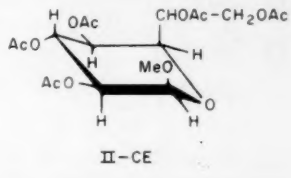

II-CE

6. Methyl D-*glycero*-β-D-*ido*-heptopyranoside pentaacetate

4.2. Acetylated Aldopyranosides of the *lyxo* Configuration

Six of the members of this group of configurationally related compounds have the D-*lyxo* or D-*manno* configuration and the following general formula (III) for the CA conformation.

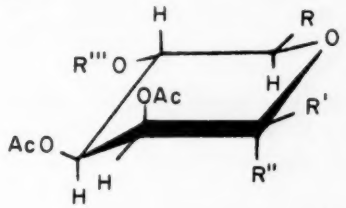

III

Compounds 7, 8, 11, 12, 14, and 15, in this conformation, have the above general structure, with the following substituents.

7. Methyl α-D-lyxopyranoside triacetate, R=H; R′=H; R″=OCH_3; and R‴=Ac.
8. Methyl β-D-lyxopyranoside triacetate, R=H; R′=OCH_3; R″=H; and R‴=Ac.
11. Methyl α-D-mannopyranoside tetraacetate, R=CH_2OAc; R′=H; R″=OCH_3; and R‴=Ac.
12. Methyl β-D-mannopyranoside tetraacetate, R=CH_2OAc; R′=OCH_3; R″=H; and R‴=Ac.
14. Methyl β-D-glucopyranosyl-(1→4)-α-D-mannopyranoside heptaacetate, R=CH_2OAc; R′=H; R″=OCH_3; and R‴=tetra-*O*-acetyl-β-D-glucopyranosyl.
15. Methyl β-D-glucopyranosyl-(1→4)-β-D-mannopyranoside heptaacetate, R=CH_2OAc; R′=OCH_3; R″=H; and R‴=tetra-*O*-acetyl-β-D-glucopyranosyl.

Compounds 9, 10, and 13 have the L-*manno* configuration and the following general formula (IV) for the CA conformation.

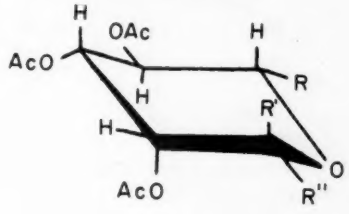

IV

9. Methyl 6-deoxy-α-L-mannopyranoside triacetate, R=CH_3; R′=OCH_3; and R″=H.

10. Methyl 6-deoxy-β-L-mannopyranoside triacetate, R=CH_3; R′=H; and R″=OCH_3.

13. Methyl D-*glycero*-β-L-*manno*-heptopyranoside, pentaacetate,

HCOAc

R is CH_2OAc; R′=H; and R″=OCH_3.

Compounds 16 to 19 have the D-*gulo* configuration and the following general formula (V) for the CA conformation.

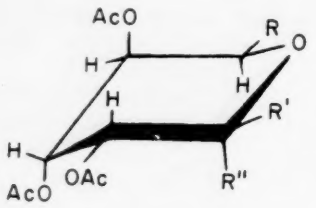

V

16. Methyl α-D-gulopyranoside tetraacetate, R=CH_2OAc; R′=H; and R″=OCH_3.

17. Methyl D-*glycero*-α-D-*gulo*-heptopyranoside pentaacetate,

HCOAc

R is CH_2OAc; R′=H; and R″=OCH_3.

18. Methyl D-*glycero*-β-D-*gulo*-heptopyranoside pentaacetate,

HCOAc

R is CH_2OAc; R′=OCH_3; and R″=H.

19. Cyclohexyl D-*glycero*-β-D-*gulo*-heptopyranoside pentaacetate,

HCOAc

R is CH_2OAc; R′=OC_6H_{11}; and R″=H.

4.3. Acetylated Aldopyranosides of the *arabino* Configuration

The CE conformation of compound 20 and the CA conformation of compounds 22 and 23 are depicted in general formula VI.

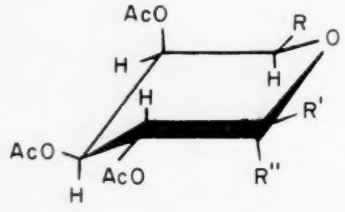

VI

20. Methyl β-L-arabinopyranoside triacetate, R=H; R′=H; and R″=OCH_3.

22. Methyl α-D-galactopyranoside tetraacetate, R=CH_2OAc; R′=H; and R″=OCH_3.

23. Methyl β-D-galactopyranoside tetraacetate, R=CH_2OAc; R′=OCH_3; and R″=H.

The CA conformation of compound 21 and the CE conformation of compound 24 are depicted in general formula VII.

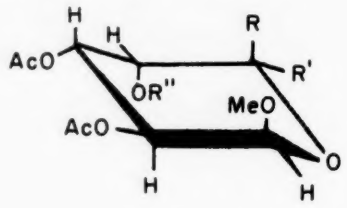

VII

21. Methyl 6-deoxy-α-L-galactopyranoside triacetate, R=H; R′=CH_3; and R″=Ac.

24. Methyl β-D-galactopyranosyl-(1→4)-β-D-altropyranoside heptaacetate, R=CH_2OAc; R′=H; and R″=tetra-*O*-acetyl-β-D-galactopyranosyl.

5. Discussion of the Spectra

In the present study, the positions of the various absorption bands for each of 24 acetylated aldopyranosides have been determined; the relative intensities of absorption were not examined in detail. The bands were compiled, and were studied by statistical and comparative methods, as previously described [11].

The conformations of 17 of the corresponding *unacetylated* glycosides had previously been assigned by us [6] from a study of their infrared absorption spectra (see table 1). Assignment was made on the basis of the empirical observation that, for the aldopentopyranosides and for members of any one group-configuration of the 5-*C*-substituted aldopentopyranosides, a change of anomeric disposition was accompanied by a concerted shift of certain groups of absorption bands.

The same kind of examination has now been applied to the spectra of the fully acetylated derivatives of these 17 aldopyranosides. A similar effect was observed, namely, that certain groups of absorption bands show a concerted shift on change of anomeric disposition. Assignments were then made, on the basis of this empirical observation, for 15 of the acetylated derivatives, and were found to be in agreement with those previously made for the unacetylated relatives. Consequently, compounds 3 and 4 were assigned the CA conformation, which had previously been inferred for their parent glycosides [6].

The remaining seven spectra were those of acetylated glycosides whose parent glycosides had received no conformational assignment. Intercomparison of the spectra of four of these acetates (compounds 12 to 15, table 1) with those of related acetates (especially in regard to the characteristic, anomer-differentiating absorption bands) was then under-

taken. For lack of spectra of related acetates, assignments could not be made for the remaining three compounds (see table 1; compounds 5, 6, and 24).

5.1. Absorption Bands Possibly Indicative of the Disposition of Groups at the Anomeric Carbon Atom of the Methyl Tri-*O*-acetyl-aldopentopyranosides

As the starting point in these analyses, we selected methyl tri-*O*-acetyl-β-D-xylopyranoside (compound 2) because, if this compound adopts a chair conformation, the reference groups will either be all axial (CE) or all equatorial (CA). Its spectrum was compared with that of its α anomer (compound 1), in order to determine the effect, on the spectrum, of changing the anomeric group from equatorial to axial, or vice versa. A comparison was then made with the spectrum of methyl tri-*O*-acetyl-β-L-arabinopyranoside (compound 20).

Bands that are essentially the same for these three compounds are given [2] in table 2. It seemed reasonable to assume tentatively that bands shown by *all* of these acetylated glycosides might be independent of total configuration, whereas those shown by one pair of anomers (*e.g.*, compounds 1 and 2) having the same group-configuration might be a reflection, *via* shifting of bands, of an effect of the configuration of that pair.

[2] For comparison, bands (in about the same positions) shown by either or both anomers of methyl tri-*O*-acetyl-D-lyxopyranoside are also given in table 2.

In table 3 are given the bands shown by *one* anomer (but not by the other) of the methyl tri-*O*-acetyl-D-xylopyranosides and by methyl tri-*O*-acetyl-β-L-arabinopyranoside. If the "anomer-differentiating" bands have any relationship to the axial or equatorial disposition of the respective glycosidic

TABLE 3. *Bands shown by only one anomer of the methyl tri-O-acetyl-D-xylopyranosides (compounds 1 and 2) and by methyl tri-O-acetyl-β-L-arabinopyranoside (20), compared with bands for both anomers of methyl tri-O-acetyl-D-lyxopyranoside (7 and 8)*

1	20	2	7	8
2933	2941	.....	2941	.....
2841	2849	.....	2849	.....
[a] 1205	[a] 1202	.....	.....	1209
949	951	.....	.....	949
921	926	.....	.....	.....
738	757	.....	771	755
659	660	.....	668	665
607	612	.....	606	608
366	365(?)	.....	.....	.....
358	359	.....	.....	.....
350	350	.....	.....	351(?)
263	284(?)	.....	.....	.....
.....	.....	3012	.....	.....
.....	.....	2967	.....	2967
.....	.....	2890	2899	.....
.....	.....	2874	.....	2865
.....	.....	1754	.....	1745
.....	.....	1403	1399	.....
.....	.....	1256	.....	.....
.....	.....	.....	1233	.....
.....	.....	1155	.....	1148
.....	.....	992	.....	.....

[a] See footnote b of table 2.

TABLE 2. *Bands (cm^{-1}) shown by both anomers of methyl tri-O-acetyl-D-xylopyranoside (compounds 1 and 2) and by methyl tri-O-acetyl-β-L-arabinopyranoside (20), and positionally corresponding bands of the methyl tri-O-acetyl-D-lyxopyranosides (7 and 8)*

Methyl tri-*O*-acetyl-D-xylopyranosides		Methyl tri-*O*-acetyl-β-L-arabinopyranoside	Methyl tri-*O*-acetyl-D-lyxopyranosides		Methyl tri-*O*-acetyl-D-xylopyranosides		Methyl tri-*O*-acetyl-β-L-arabinopyranoside	Methyl tri-*O*-acetyl-D-lyxopyranosides	
1	2	20	7	8	1	2	20	7	8
Possibly non-configurational bands					Bands possibly affected by configuration and conformation				
1745	1742	1739	1736	1733	1473	1477	1468	.....	.....
1456	1462	1453	1462	1456	1368	1370	.....	1370	1370
1441	1443	1445, 1437	1437	1439	1321	1316	.....	1318	1311
1383	1376	1377	1377	1385	1161	1167	.....	.....	.....
1339	1332	1333	1348	1333	[b] 1138	1129	[b] 1136	[b] 1140	.....
1294	1287	1299	1290	1272	1124	1119	.....	.....	.....
1247	1244	1247	1250	1247	[a] 1055	[b] 1058	.....	1060	1064, 1057
1225	1221	1224	1224	1222	1044	1040	[a] 1048	.....	1045
1185	1175	1172	1179	1190	1031	1024	.....	1027	1024
1105	1100	1107	1104	1099	1013	1003	1006	1014	.....
[a] 1075	[a] 1075	[a] 1068	1085	1074	984	980	.....	980	977
885	899	895	899	889	.....	.....	.....	963	962
674	689	695	690	710	[a] 936	936	938	936	.....
586	585	578	590	596	.....	.....	913	917	917
491	499	506	498, 491	491	904	906	902	.....	901
459	458	459, 447	453	453	877	880	877	882	.....
401	399	407	408(?)	399	.....	.....	848	856	851
385	392	387	382	383	648	647	.....	638	642
376	375	378(?)	376	376	619	621	626	.....	625
344	346	345(?)	332	336(?), 332(?)	600	601	601	.....	.....
292	291(?)	291(?)	291(?)	291(?)	551	550	.....	.....	.....
					528	527	.....	538	517
					479	475, 470	482	.....	466
					.....	.....	418	421	413
					371	370	371(?)	.....	.....
					317	313	.....	310	.....

[a] These bands were mentioned by R. L. Whistler and L. R. House [4].
[b] These bands were mentioned by H. S. Isbell and coworkers [3].

methoxyl group, the results in table 3 clearly indicate that compounds 1 and 20 have the same anomeric disposition (that is, both have an equatorial, or both have an axial, methoxyl group), and that the anomeric disposition for compound 2 is different. If the assignment previously made [6] for the unacetylated relative of *any one of these three* acetylated glycosides is extended to its acetate, the conformations of the other two may be deduced from the results in table 3. For example, if the anomeric group of methyl tri-*O*-acetyl-β-D-xylopyranoside is equatorial and that of its α anomer is axial, the results indicate that the anomeric group of methyl tri-*O*-acetyl-β-L-arabinopyranoside is axial. These conclusions are in complete agreement with the assignments previously made [6] for the related unacetylated glycosides.

The corresponding bands of the methyl tri-*O*-acetyl-D-lyxopyranosides (compounds 7 and 8) are also given in table 3. The results suggest that, for each anomer thereof, either (a) a conformation is adopted that is not a chair form and has a quasi, or a different kind of axial or equatorial, anomeric group, or (b) the crystalline material is a mixture of the CA and CE conformations. These conclusions agree with the previous findings for the unacetylated D-lyxopyranosides [6].

5.2. Analysis of the Spectra of Groups of Configurationally Related, Acetylated Aldopyranosides, Excluding the Acetylated Aldopentopyranosides

As a test of the method of analysis, an examination was made of the spectra of methyl tetra-*O*-acetyl-α-D-gulopyranoside (compound 16), the anomers of methyl penta-*O*-acetyl D-*glycero*-D-*gulo*-heptopyranoside (17 and 18), and cyclohexyl penta-*O*-acetyl-D-*glycero*-β-D-*gulo*-heptopyranoside (19), because assignments of anomeric disposition had previously been made [6] for the corresponding unacetylated glycosides. The results are given in table 4,[3] in which the anomer-differentiating bands shown by compounds 17 and 18 are compared with corresponding bands of compound 16 on the one hand and compound 19 on the other. Such bands, shown by two of the compounds (but not by the other two) are listed as follows: Column A, compounds 16 and 17, B, 16 and 18; C, 17 and 19; D, 18 and 19. It may be seen that compound 16 shows about equal similarity to either compound 17 or 18. In contrast, compound 17 has only one such band in common with compound 19, but compounds 18 and 19 have twelve such bands in common. If the assignment previously made for the unacetylated parent is extended to the acetate, for any one of the acetates 17, 18, or 19, the results are in accordance with the assignments previously made for all four parent glycosides. These are, for the anomeric group, as follows: Compound 17, axial; compounds 18 and 19, equatorial; and compound 16, quasi, or a different kind of axial or equatorial disposition, or a mixture of axial and equatorial forms.

As a further check on the results accruing from our method of analysis, a second group of acetylated glycosides (for whose parent glycosides assignments had previously been made [6]) was studied. The results are given in table 5: column A lists three bands shown by methyl tetra-*O*-acetyl-β-D-galactopyranoside (compound 23) but not by compounds 21 and 22; column B lists eleven bands shown by methyl tri-*O*-acetyl-6-deoxy-α-L-galactopyranoside (compound 21) and by the α anomer, compound 22. Compounds 21 and 23 showed no anomer-differentiating bands in common. Consequently, if the assignment previously made for the unacetylated parent of *any one of these three compounds* is extended to the corresponding acetate, the assignments for the acetates are in harmony with those for the three parent glycosides. For the disposition of the ano-

TABLE 4. *Comparison* [a] *of absorption bands* (cm^{-1}) *shown by methyl tetra*-O-*acetyl*-α-D-*gulopyranoside* (*compound 16*), *the anomers of methyl penta*-O-*acetyl*-D-glycero-D-gulo-*heptopyranoside* (*17 and 18*), *and cyclohexyl penta*-O-*acetyl*-D-glycero-β-D-gulo-*heptopyranoside* (*19*)

A		B		C		D	
16(α)	17(α)	16(α)	18(β)	17(α)	19(β)	18(β)	19(β)
2841	2849	1736	1745	831	825	2882	2865
1414	1385	943	943			1745	1739
1110	1110	650	649			1282	1274
818	831					1241	1242
						943	942
						858	864
						649	645
						508	506
						472	473
						459	459
						445	443
						341	341

[a] Key: A. Bands shown by compounds 16 and 17, but not by 18. B. Bands shown by compounds 16 and 18, but not by 17. C. Bands shown by compounds 17 and 19, but not by 18. D. Bands shown by compounds 18 and 19, but not by 17.

[3] To conserve space, bands which do not differentiate between anomers have been omitted from tables 4 to 9.

TABLE 5. *Comparison* [a] *of absorption bands* (cm^{-1}) *shown by the anomers of methyl tetra*-O-*acetyl*-D-*galactopyranoside* (*compounds 22 and 23*) *and by methyl tri*-O-*acetyl*-6-*deoxy*-α-L-*galactopyranoside* (*21*)

A	B	
23(β)	21(α)	22(α)
1014	2933	2941
[b] 880	1215	1217
611	1200	[c] 1190
	1133	[c] 1134
	1049	1041
	941	[b] 949
	928	[b] 936
	817	[b] 821
	759	[b] 758
	696	712
	487	490

[a] Key: A. Bands shown by compound 23, but not by compounds 21 and 22. B. Bands shown by compounds 21 and 22, but not by 23.
[b] These bands were mentioned by S. A. Barker and coworkers [5].
[c] See footnotes a and b to table 2.

meric group, these are as follows: Compounds 21 and 22, axial; and compound 23, equatorial.

All of the foregoing deductions are compatible with the concept that an acetylated glycoside adopts the same conformation as its parent (unacetylated) glycoside. Consequently, because of the agreement between the assignments previously made for the parent glycosides [6] and now made for the acetylated glycosides, the utility of our empirical method for analyzing the spectra (and the validity of the deductions) was apparently established. The spectra of the remaining 12 glycosides were, therefore, examined. No assignment had previously been made as to the stable conformation of compounds 5, 6, 12, 13, 14, 15, and 24.

No assignment could be made for compound 5 (in comparison with compounds 3 and 4) because of the lack of the α anomer (with respect to the glycosidic methyl group) of compound 5. However, the anomer-differentiating bands for the anomers of methyl tetra-*O*-acetyl-D-glucopyranoside (compounds 3 and 4) are presented in table 6 for future use.

No assignment could be made for compound 6, because no other acetylated methyl aldopyranosides having the *ido* configuration were available for comparison. Similarly, no assignment could be made for compound 24, because of a lack of acetylated methyl aldopyranosides having the *altro* configuration.

Finally, assignments were sought for compounds 12 to 15; their spectra were compared with those of compounds 9 to 11 (for which we had previously made assignments for the unacetylated glycosides). First of all, the spectra of the anomers of methyl tri-*O*-acetyl-6-deoxy-L-mannopyranoside (compounds 9 and 10) were compared with those of the anomers of methyl tetra-*O*-acetyl-D-mannopyranoside (compounds 11 and 12). The results are given in table 7; column A gives bands shown by compounds 9 and 11 (α anomers) but not by compounds 10 and 12 (β anomers), and column B records bands shown by the two β anomers but not by the α anomers. (Only one discrepancy was noted, namely, that compounds 10 and 11 show a band at 1,168–1,167 cm^{-1} that is absent from the spectra of compounds 9 and 12.) It may be concluded that, assuming the validity of the correlations, if the anomeric group of the α anomers is axial, that of the β anomers is equatorial, or *vice versa*. If the conformation assigned to the unacetylated parent of any one of three of these four compounds (9, 10, and 11) is accepted for its acetate, the deduced conformations for the other two are in agreement with those for the unacetylated compounds. Furthermore, the results indicate that methyl tetra-*O*-acetyl-β-D-mannopyranoside (compound 12) has an equatorial anomeric group.

The anomeric disposition of methyl penta-*O*-acetyl-D-*glycero*-β-L-*manno*-heptopyranoside (13) was now studied by a double comparison—against (a) the anomers of methyl tri-*O*-acetyl-6-deoxy-L-mannopyranoside, and (b) the anomers of methyl tetra-*O*-acetyl-D-mannopyranoside. The results are given in table 8. Column A of table 8 records bands shown by compounds 9 and 13 but not by 10; column B gives bands shown by compound 9 but not by 10 and 13; column C gives bands shown by 10 and 13 but not by 9; column D gives bands shown by 11 and 13 but not by 12; column E gives bands shown by compound 11 but not by 12 and 13; and column F gives bands shown by 12 and 13 but not by 11. It is seen that, whereas the 16 bands in columns B and C indicate similarity between compounds 10 and 13, only two bands in column A suggest similarity of compounds 9 and 13. Similarly, whereas the 18 bands in columns E and F indicate similarity between compounds 12 and 13, only four bands in column D suggest similarity between compounds 11 and 13. Thus, a total of 34 bands indicate relationship of compound 13 to compounds 10 and 12 (as against a total of six bands indicating a relationship of compound 13 to compounds 9 and 11). These results suggest that the anomeric group of compound 13 is equatorial.

To obtain information regarding the disposition of the methoxyl group in the anomers of methyl hepta-*O*-acetyl-4-*O*-β-D-glucopyranosyl-D-mannopyranoside (compounds 14 and 15), the spectra of these compounds were compared with those of the anomers of methyl tetra-*O*-acetyl-D-mannopyranoside (compounds 11 and 12). The results are given in table 9; column A records bands shown by compounds 11

TABLE 6. *Bands (cm^{-1}) differentiating between the anomers of methyl tetra-O-acetyl-D-glucopyranoside (compounds 3 and 4)*

3(α)	4(β)
2865	----------
1241	----------
1078	----------
933	----------
888	----------
761	----------
663	----------
516	----------
321	----------
----------	2915
----------	1318
----------	[a] 918
----------	[a] 873
----------	537(?)
----------	529

[a] See footnote b to table 5.

TABLE 7. *Comparison [a] of absorption bands (cm^{-1}) shown by the methyl tri-O-acetyl-6-deoxy-L-mannopyranosides (compounds 9 and 10) and by the methyl tetra-O-acetyl-D-mannopyranosides (11 and 12)*

A		B	
9(α)	11(α)	10(β)	12(β)
1443	1443	1410	1404
[b] 884	[b] 886	1076	1074
[b] 837	[b] 832	867	[b] 867
[b] 797, [b] 791	[b] 792	752	[b] 752
685	690	724	723
614	616	412, 406	408
514	510		

[a] Key: A. Bands shown by compounds 9 and 11, but not by compounds 10 and 12. B. Bands shown by compounds 10 and 12, but not by compounds 9 and 11.
[b] See footnote b to table 5.

TABLE 8. *Comparison* [a] *of absorption bands* (cm^{-1}) *shown by the methyl tri-*O*-acetyl-6-deoxy-*L*-mannopyranosides (compounds 9 and 10), the methyl tetra-*O*-acetyl-*D*-mannopyranosides (11 and 12), and methyl penta-*O*-acetyl-*D*-glycero-β-*L*-manno-heptopyranoside (13)*

A		B	C		D		E	F	
9(α)	13(β)	9(α)	10(β)	13(β)	11(α)	13(β)	11(α)	12(β)	13(β)
[b] 837	829	1443	1410	1410(?)	1227	1232	1443	1404	1410(?)
495	499	[b] 884	1168	1167	1167	1167	1086	1151	1147
		[b] 797, [b] 791	1076	1073	[b] 832	829	1040	1074	1073
		685	894	894	465(?)	462	[b] 886	[b] 952	947
		614	867	867			[b] 792	[b] 867	867
		514	752	768			690	[b] 752	768
			724	725, 713			510	723	725, 713
			487	489				595	596
			447	447				484	476
			412, 406	409				408	409
								342(?)	341

[a] Key: A. Bands shown by compounds 9 and 13, but not by 10. B. Bands shown by compound 9, but not by 10 and 13. C. Bands shown by compounds 10 and 13, but not by 9. D. Bands shown by compounds 11 and 13, but not by 12. E. Bands shown by compound 11, but not by 12 and 13. F. Bands shown by compounds 12 and 13, but not by 11.
[b] See footnote b to table 5.

TABLE 9. *Comparison*[a] *of absorption bands* (cm^{-1}) *shown by the methyl tetra-*O*-acetyl-*D*-mannopyranosides (compounds 11 and 12) and by the methyl hepta-*O*-acetyl-4-*O*-β-*D*-glucopyranosyl-*D*-mannopyranosides (14 and 15)*

A		B	
11(α)	14(α)	12(β)	15(β)
1086	1083	1010	1003
978	976	[b] 952	952
[b] 792	803	[b] 904	904
690	693	[b] 752	750
616	614	723	731
559	557	570	567

[a] Key: A. Bands shown by compounds 11 and 14, but not b 12 and 15. B. Bands shown by compounds 12 and 15, but not by 11 and 14.
[b] See footnote b to table 5.

and 14 (but not by compounds 12 and 15); column B gives the bands shown by compounds 12 and 15 (but not by compounds 11 and 14). If the assignments previously made for compounds 11 and 12 are accepted, these results indicate that the methoxyl group is axial in compound 14 and equatorial in compound 15.

For molecules as complex as those of the acetylated aldopyranosides, many of the observed bands cannot yet be assigned to particular vibrational modes. Thus, in sections 5.1 and 5.2, we have not been concerned with (a) which bands, arising from vibrations localized in a functional group, are relatively independent of the remainder of the molecule, or (b) which bands involve other parts of the molecule. However, in section 5.3, bands possibly attributable to specific functional groups are considered.

5.3. Other Absorption Bands

All of the compounds in this study are acetates, and their spectra all show at least one band (C=O stretching frequency) at 1,764 to 1,736 cm^{-1} (except for compound 5, with a band at 1,773 cm^{-1}); at 1,264 to 1,241 cm^{-1} (or at 1,259 to 1,239 cm^{-1}); at 1,235 to 1,215 cm^{-1}; at 667 to 632 cm^{-1}; and at 614 to 585 cm^{-1}. All of the spectra show at least one band at 2,994 to 2,941 cm^{-1} (C—H stretching); and at 1,462 to 1,445 cm^{-1} and 1,335 to 1,318 cm^{-1} (C—H bending). All of the spectra show an absorption band at 1,445 to 1,431 cm^{-1} and at 1,379 to 1,368 cm^{-1}, presumably caused by deformation of the CH_3 groups.

Figure 1 gives the percentage of the 24 compounds in this study that show absorption bands in the various regions of the infrared spectrum; the cross-hatched areas in the region of 333 to 250 cm^{-1} correspond to the region marked, on certain spectra, with dashes. For the range of 5,000 to 2,000 cm^{-1}, decrements of 20 cm^{-1} in wavenumber were used; and, for the range of 2,000 to 250 cm^{-1}, decrements of 10 cm^{-1}. Figure 2 depicts the corresponding "profile" for 21 unacetylated glycosides, compiled from the spectra given in part II of this series [6].

Compound 19, having a cyclohexyloxy group, showed bands at 2,941 and 2,865 cm^{-1}, possibly characteristic of $—CH_2—$ (C—H stretching). It also showed bands at 1,451 and 1,435 cm^{-1}, possibly attributable to $—CH_2—$ (C—H deformation).

All of the acetylated methyl aldopyranosides show a band in the range of 2,882 to 2,833 cm^{-1}, excepting compound 4 (band at 2,915 cm^{-1}). This band may possibly be attributable to the glycosidic methoxyl group, since Henbest and coworkers [12] have observed that methoxyl groups absorb in the range of 2,832 to 2,819 cm^{-1}. All of the acetylated methyl glycopyranosides also show bands at 1,374 to 1,325 cm^{-1}, 1,259 to 1,241 cm^{-1}, 1,148 to 1,114 cm^{-1}, and 1,110 to 1,074 cm^{-1}. A band near 1,100 cm^{-1} is characteristic [13] of the methoxyl groups in methoxysteroids.

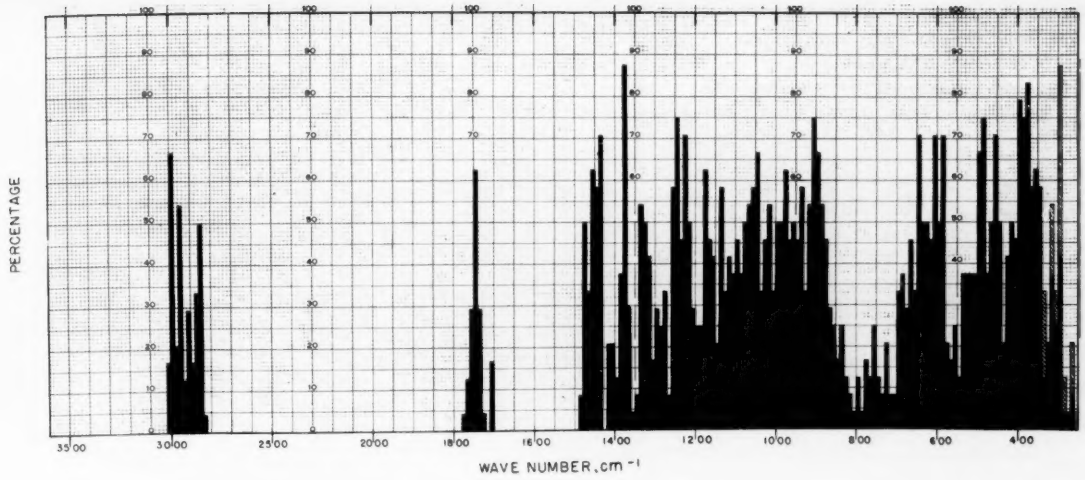

FIGURE 1. *Percentage (of the 24 acetylated glycosides) which showed infrared absorption at the various regions of the infrared spectrum (5,000 to 250 cm^{-1}).*

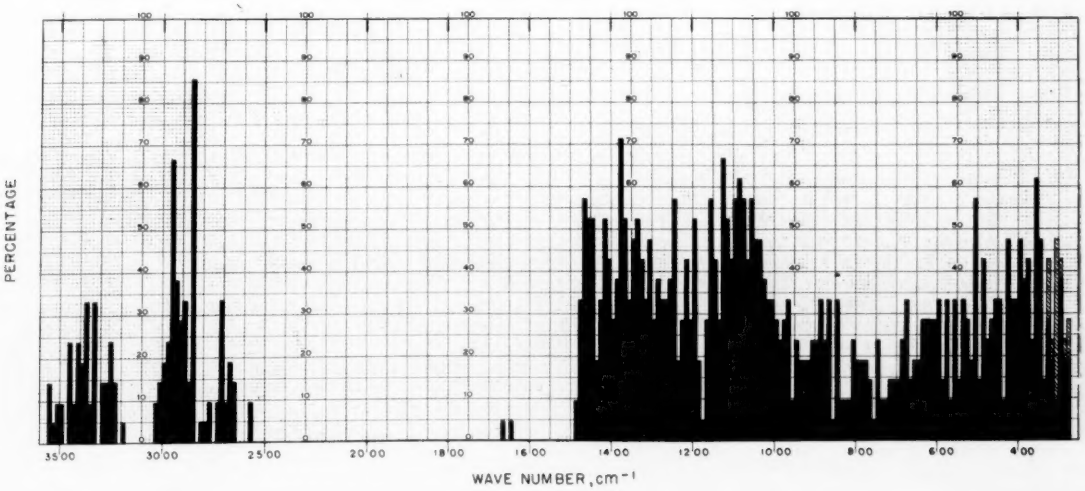

FIGURE 2. *Percentage (of the 21 unacetylated glycosides) which showed infrared absorption at the various regions of the infrared spectrum (5,000 to 250 cm^{-1}).*

6. Experimental Procedures

6.1. Preparation and Purification of the Compounds

The compounds listed in table 1 were prepared by the methods given in the references cited. Most of the compounds were prepared in the course of an earlier study [14] on the structural and configurational relationships of the anomers of the methyl pentopyranosides, hexopyranosides, and heptopyranosides. Each acetate was recrystallized from an appropriate solvent until further recrystallization caused no change in its melting point or optical rotation.

6.2. Preparation of the Pellets

Samples for spectrophotometric study were prepared in the solid phase, as pellets consisting of the crystalline acetate suspended in an alkali-metal halide, exactly as previously described [11]. For the range of 5,000 to 667 cm^{-1}, a concentration of 0.4 mg of acetate per 100 mg of potassium chloride was used, except for compounds 5 (4 mg/100 mg) and 15 (0.8 mg/100 mg). For the range of 667 to 250 cm^{-1}, a concentration of 2 mg of acetate per 100 mg of potassium iodide was used, except for compounds 5 (6 mg/100 mg) and 15 (3 mg/100 mg). Comparisons of intensity of absorption, from one compound to another, can only be true and quantitative where the molar concentration is the same.

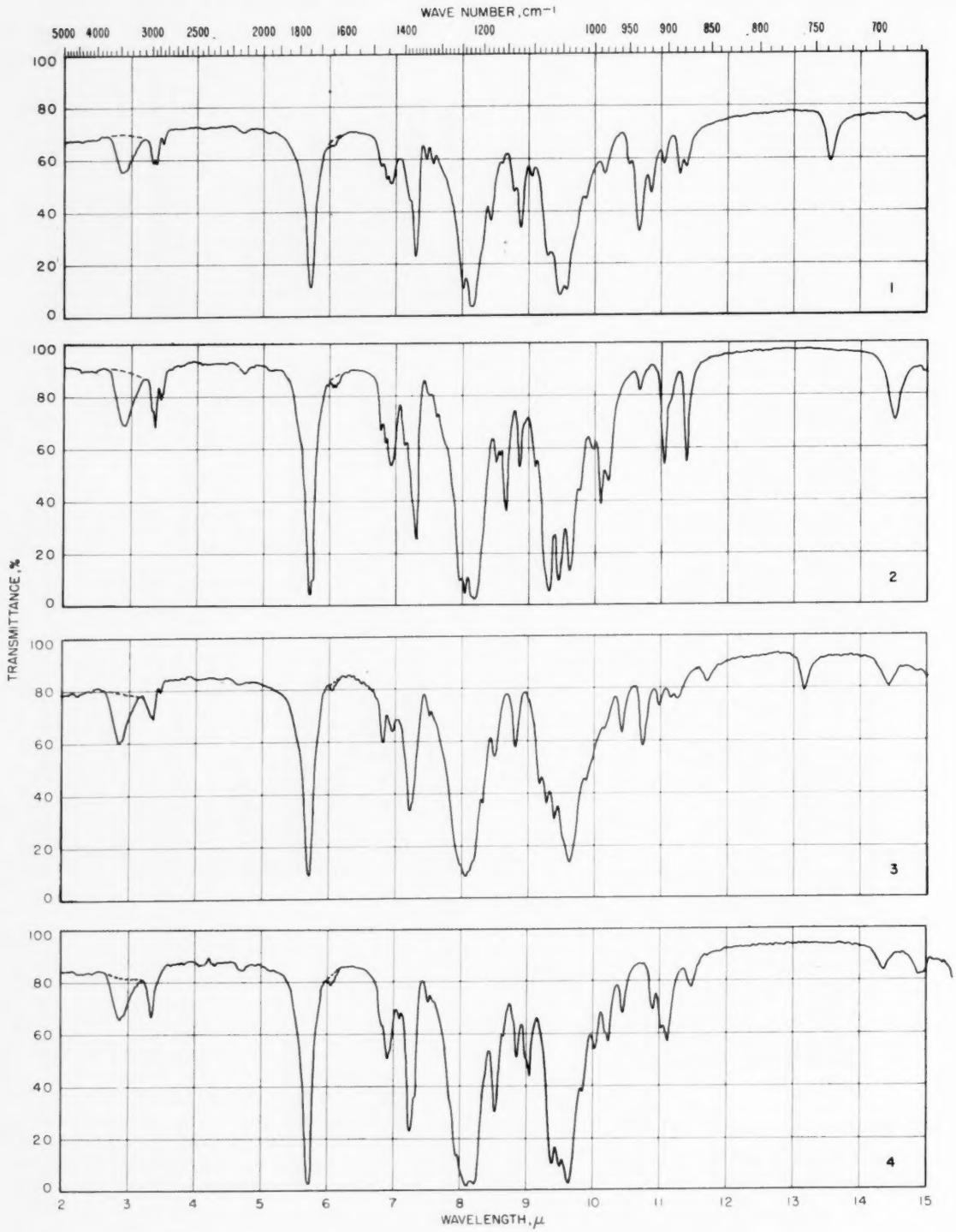

FIGURE 3. *Spectrograms of materials in potassium chloride pellets.*

1, Methyl α-D-xylopyranoside triacetate; **2**, methyl β-D-xylopyranoside triacetate; **3**, methyl α-D-glucopyranoside tetraacetate; **4**, methyl β-D-glucopyranoside tetraacetate.

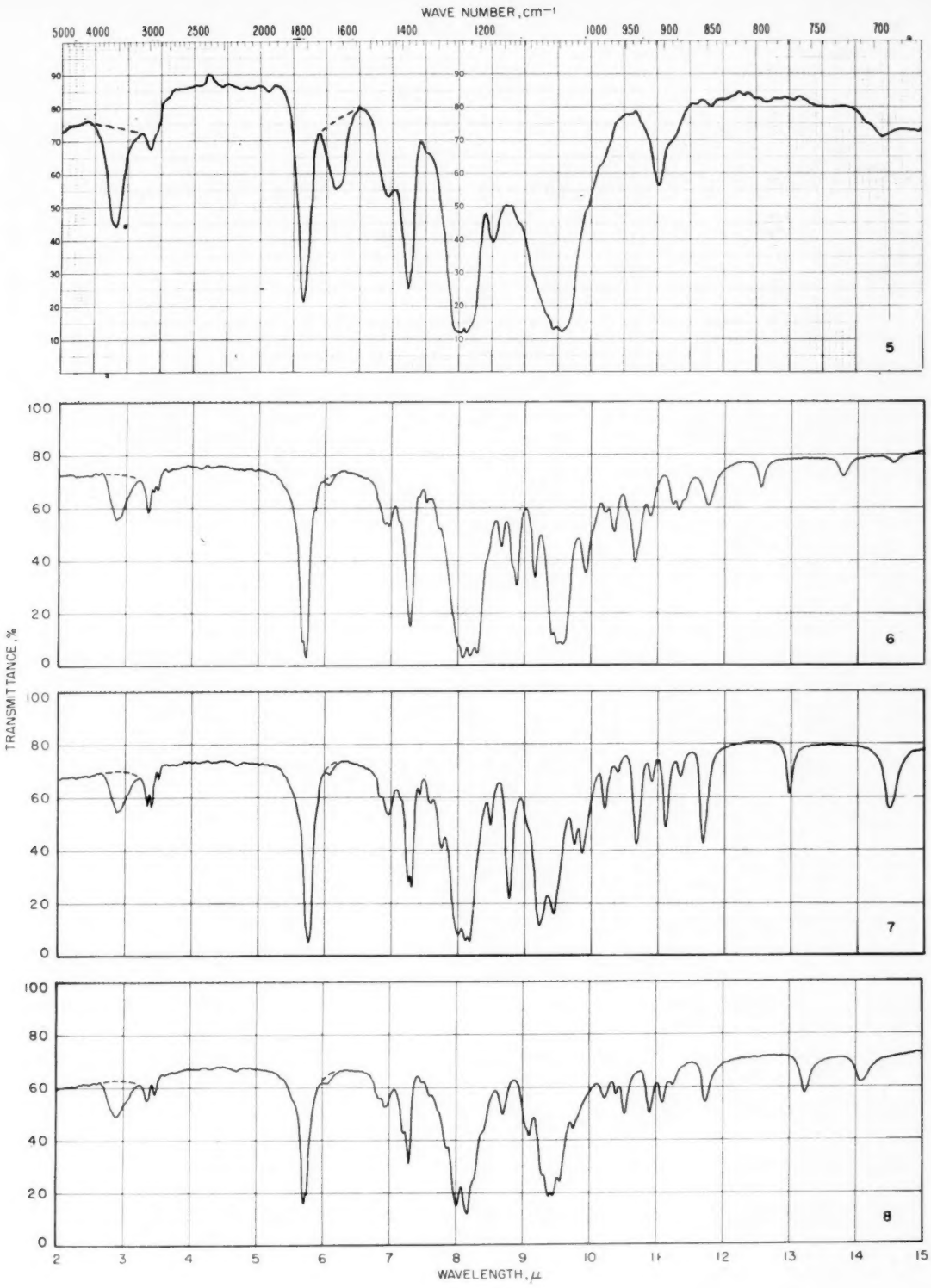

FIGURE 3. *Spectrograms of materials in potassium chloride pellets.*—Continued

5, methyl β-D-glucopyranosyl-(1→6)-β-D-glucopyranoside heptaacetate; 6, methyl D-*glycero*-β(?)-D-*ido*-heptopyranoside pentaacetate; 7, methyl α-D-lyxopyranoside triacetate; 8, methyl β-D-lyxopyranoside triacetate.

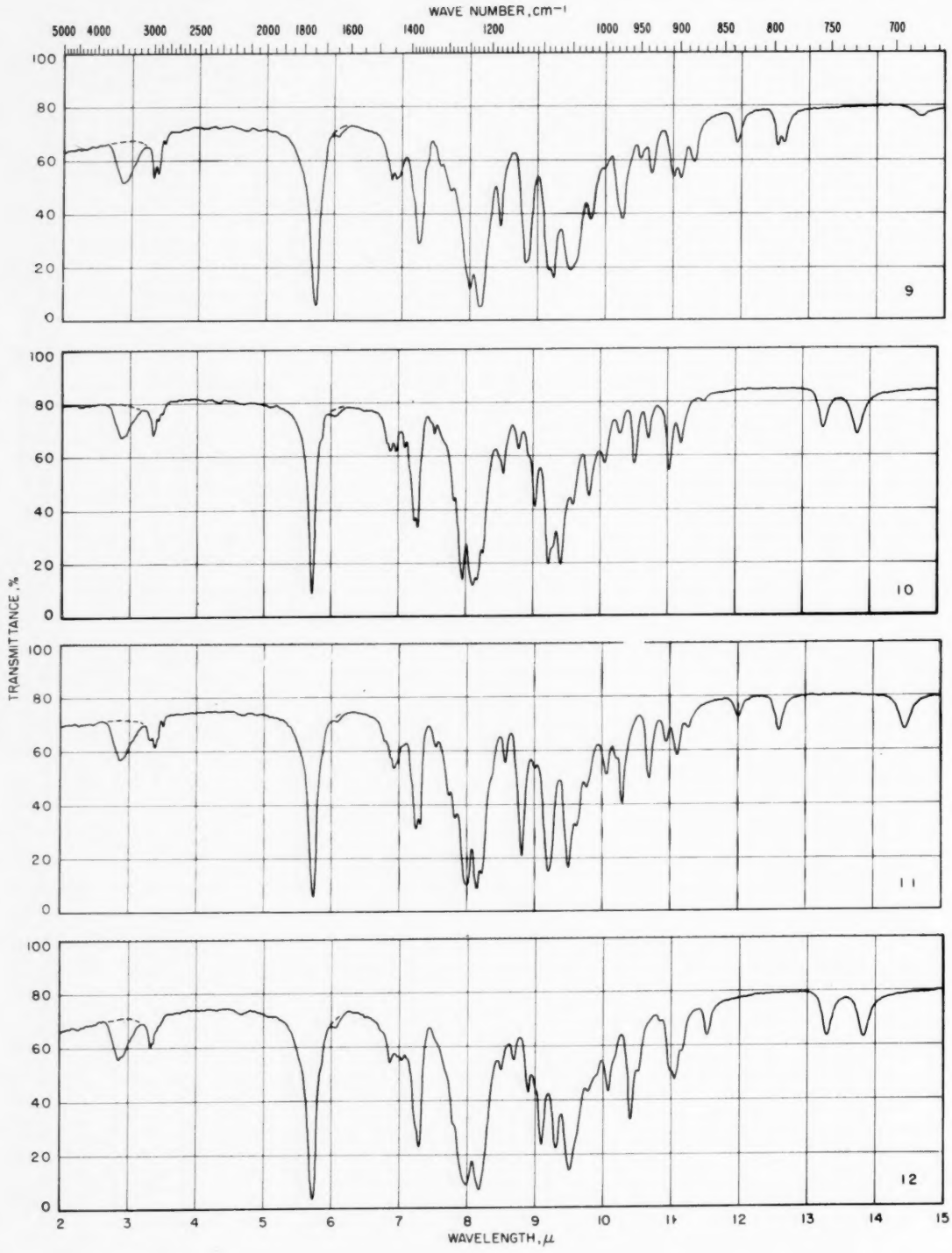

FIGURE 3. *Spectrograms of materials in potassium chloride pellets.*—Continued

9, methyl 6-deoxy-α-L-mannopyranoside triacetate; **10,** methyl 6-deoxy-β-L-mannopyranoside triacetate **11,** methyl α-D-mannopyranoside tetraacetate; **12,** methyl β-D-mannopyranoside tetraacetate.

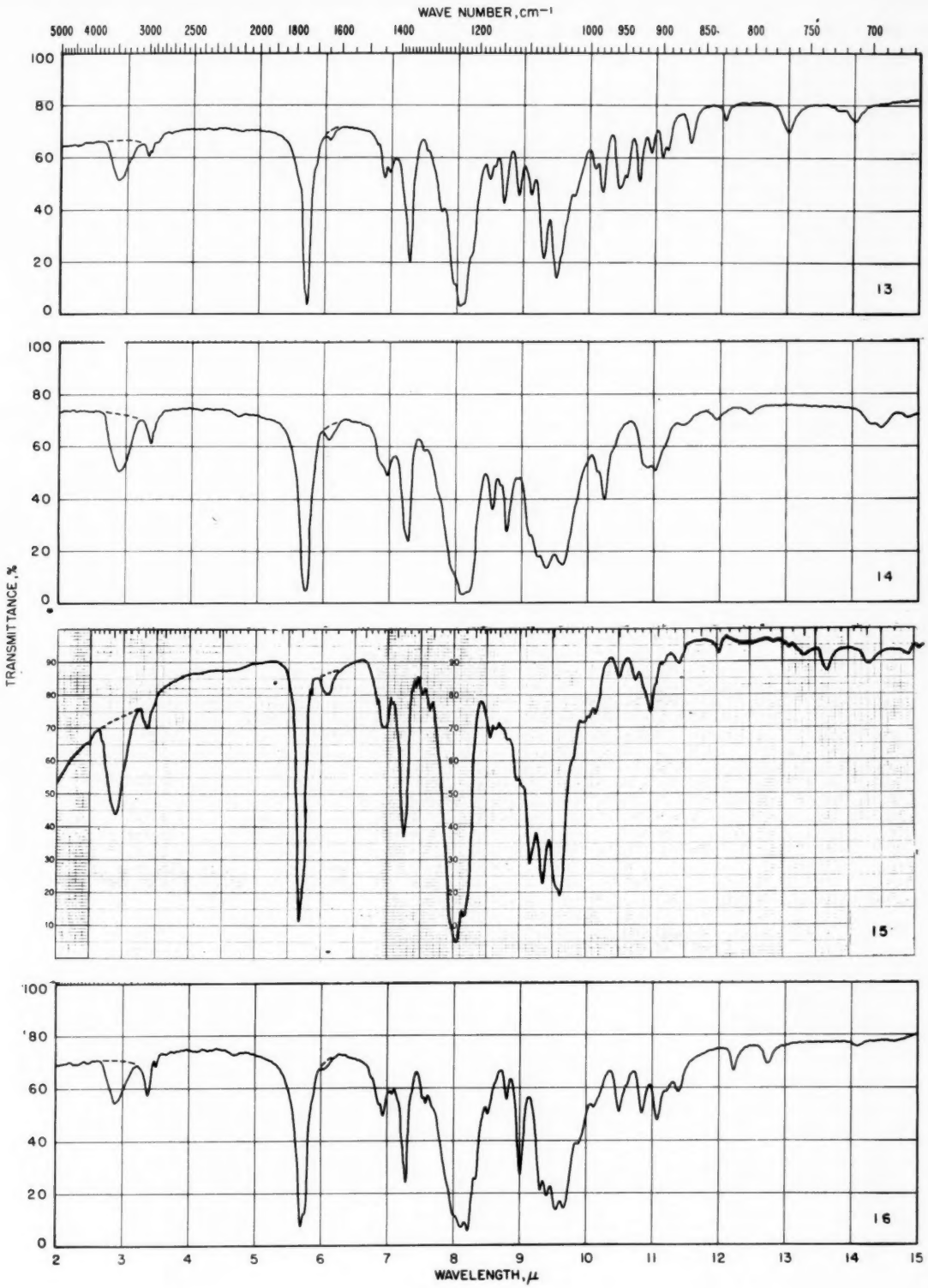

FIGURE 3. *Spectrograms of materials in potassium chloride pellets.*—Continued

13, methyl D-*glycero*-β-L-*manno*-heptopyranoside pentaacetate; **14,** methyl β-D-glucopyranosyl-(1→4)-α-D-mannopyranoside heptaacetate; **15,** methyl β-D-glucopyranosyl-(1→4)-β-D-mannopyranoside heptaacetate; **16,** methyl α-D-gulopyranoside tetraacetate.

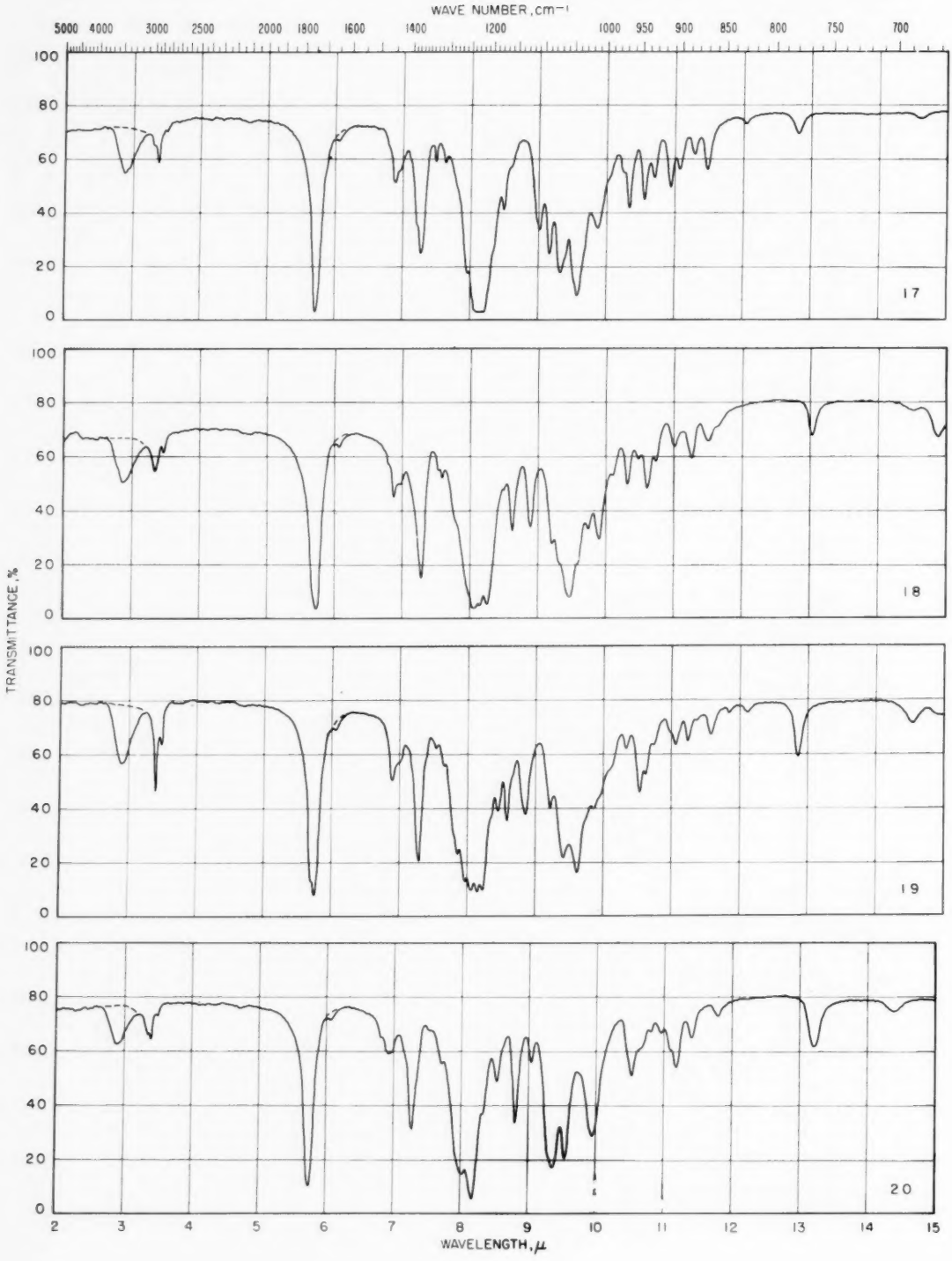

FIGURE 3. *Spectrograms of materials in potassium chloride pellets.*—Continued

17, methyl D-*glycero*-α-D-*gulo*-heptopyranoside pentaacetate; **18,** methyl D-*glycero*-β-D-*gulo*-heptopyranoside pentaacetate; **19,** cyclohexyl D-*glycero*-β-D-*gulo*-heptopyranoside pentaacetate; **20,** methyl β-L-arabinopyranoside triacetate.

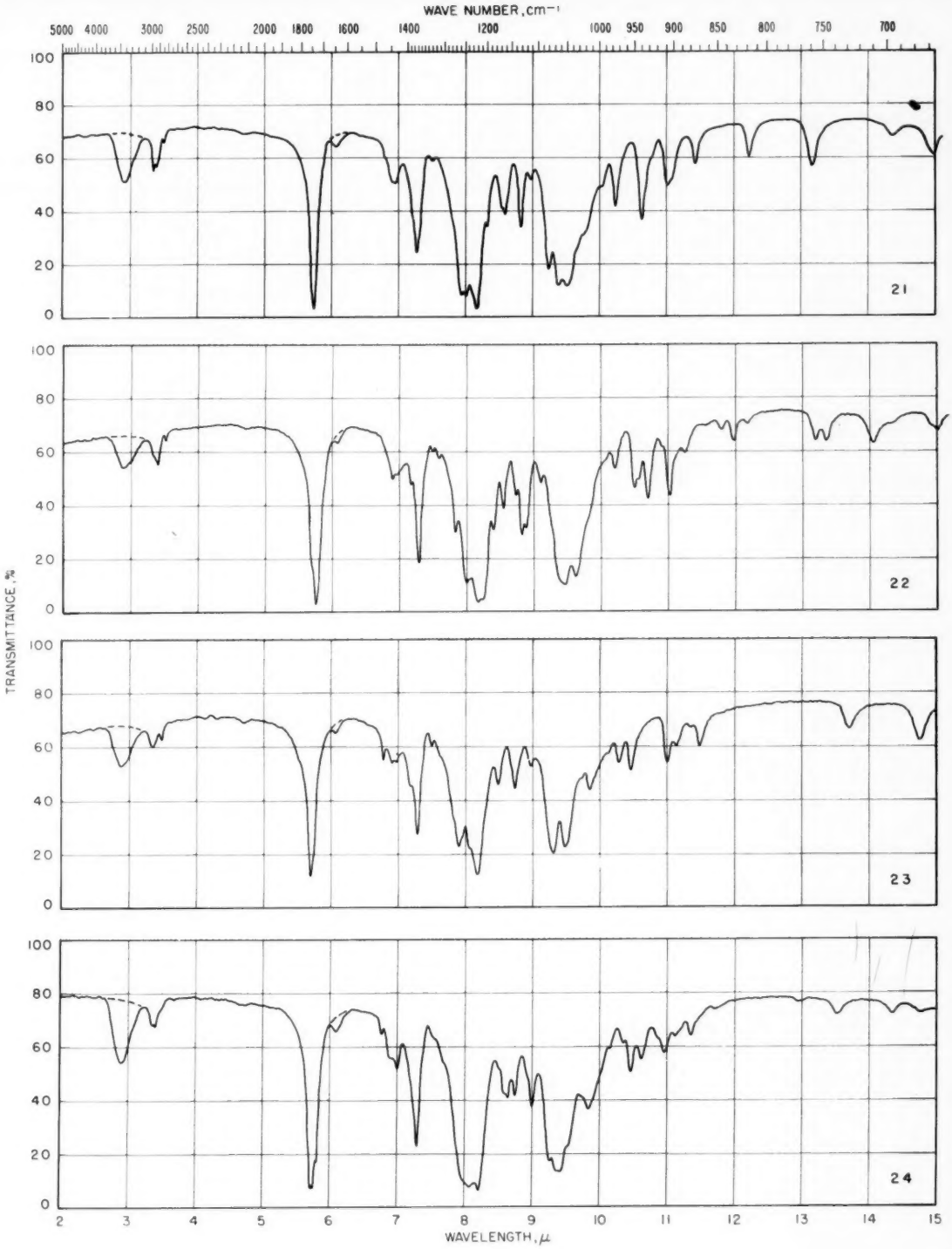

FIGURE 3. *Spectrograms of materials in potassium chloride pellets.*—Continued

21, methyl 6-deoxy-α-L-galactopyranoside triacetate; **22,** methyl α-D-galactopyranoside tetraacetate; **23,** methyl β-D-galactopyranoside tetraacetate; **24,** methyl β-D-galactopyranosyl-(1→4)-β-D-altropyranoside heptaacetate.

555462—60——5

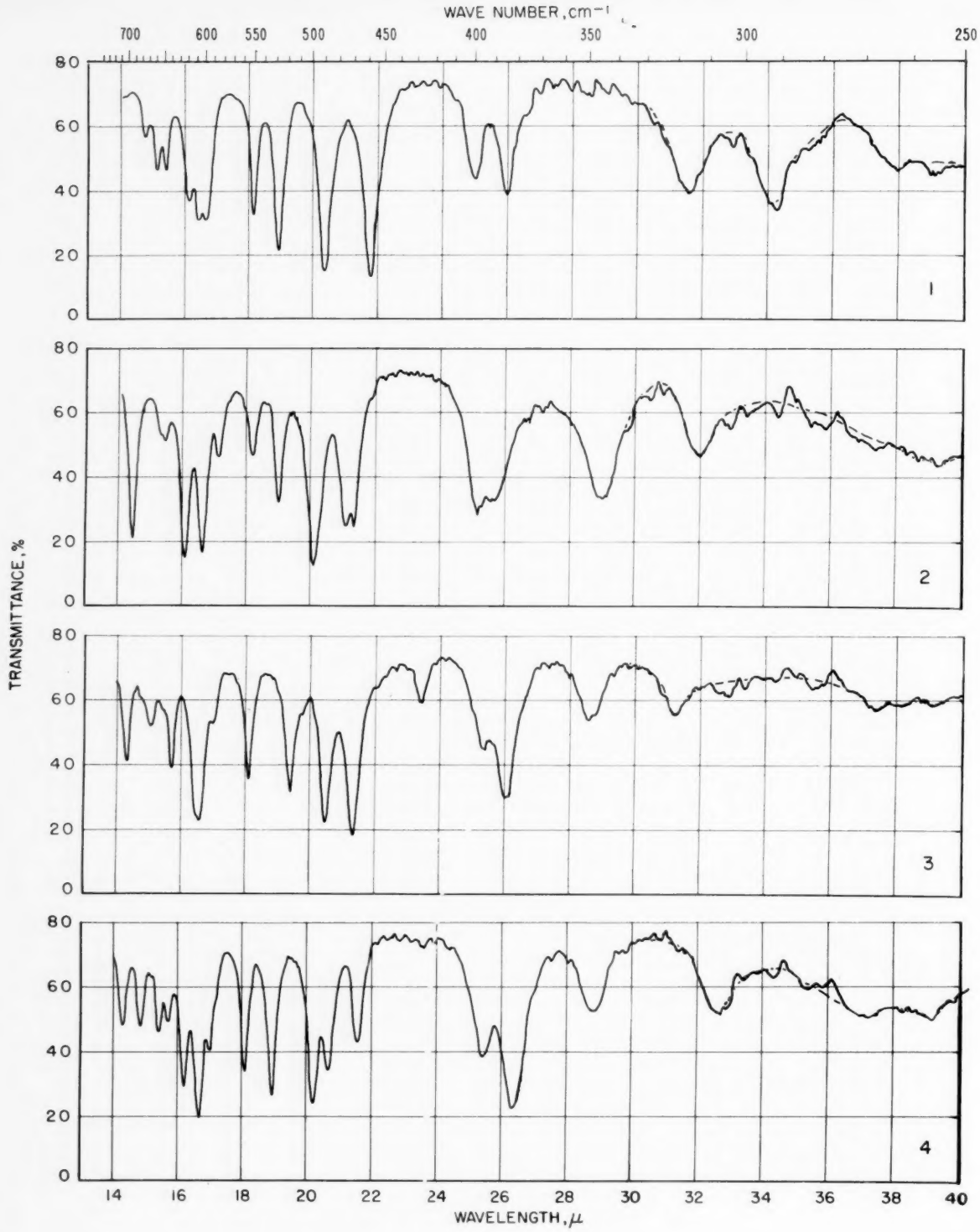

FIGURE 4. *Spectrograms of materials in potassium iodide pellets.*

1, Methyl α-D-xylopyranoside triacetate; **2,** methyl β-D-xylopyranoside triacetate; **3,** methyl α-D-glucopyranoside tetraacetate; **4,** methyl β-D-glucopyranoside tetraacetate.

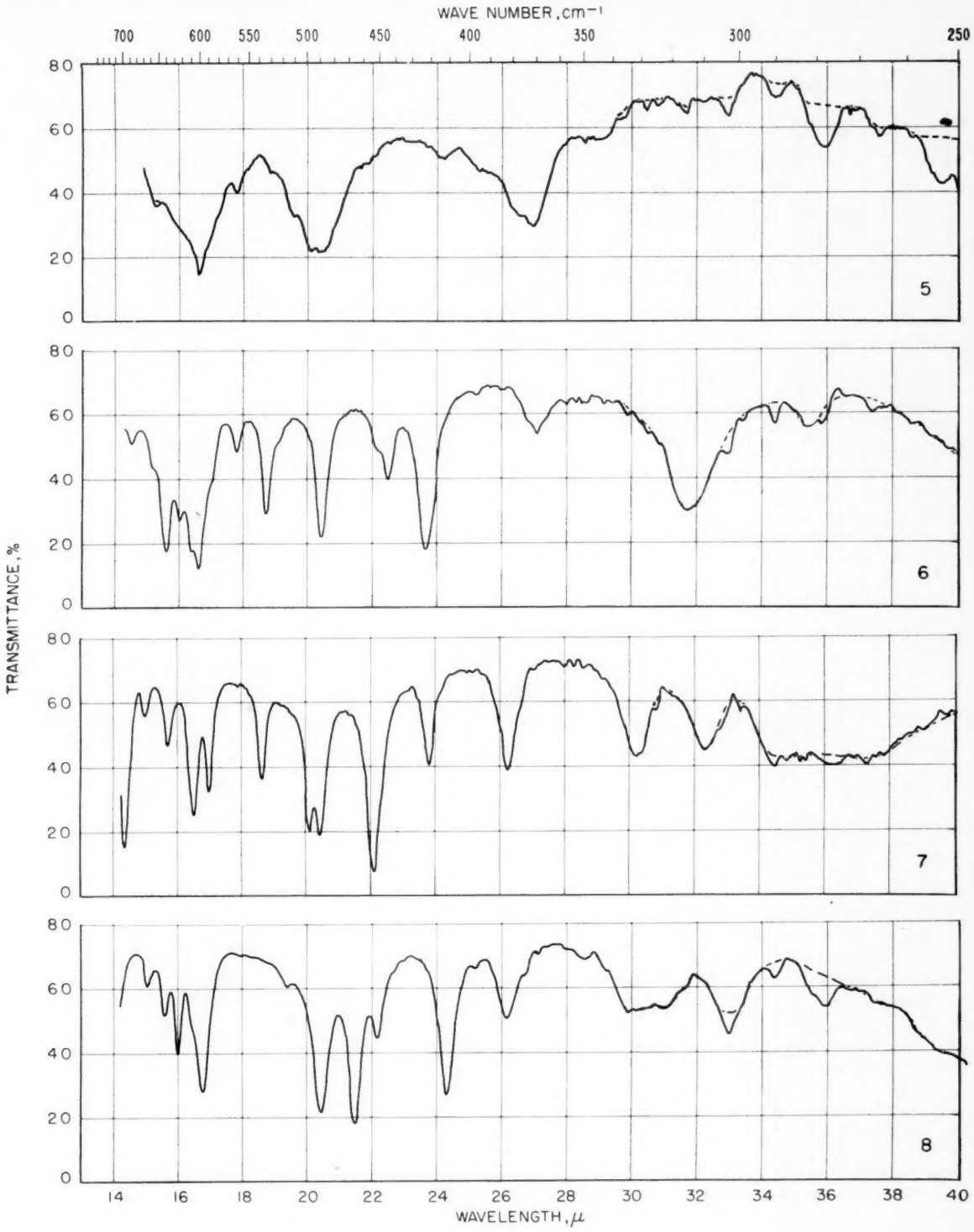

FIGURE 4. *Spectrograms of materials in potassium iodide pellets.*—Continued

5, methyl β-D-glucopyranosyl-(1→6)-β-D-glucopyranoside heptaacetate; **6**, methyl D-*glycero*-β(?)-D-*ido*-heptopyranoside pentaacetate; **7**, methyl α-D-lyxopyranoside triacetate; **8**, methyl β-D-lyxopyranoside triacetate.

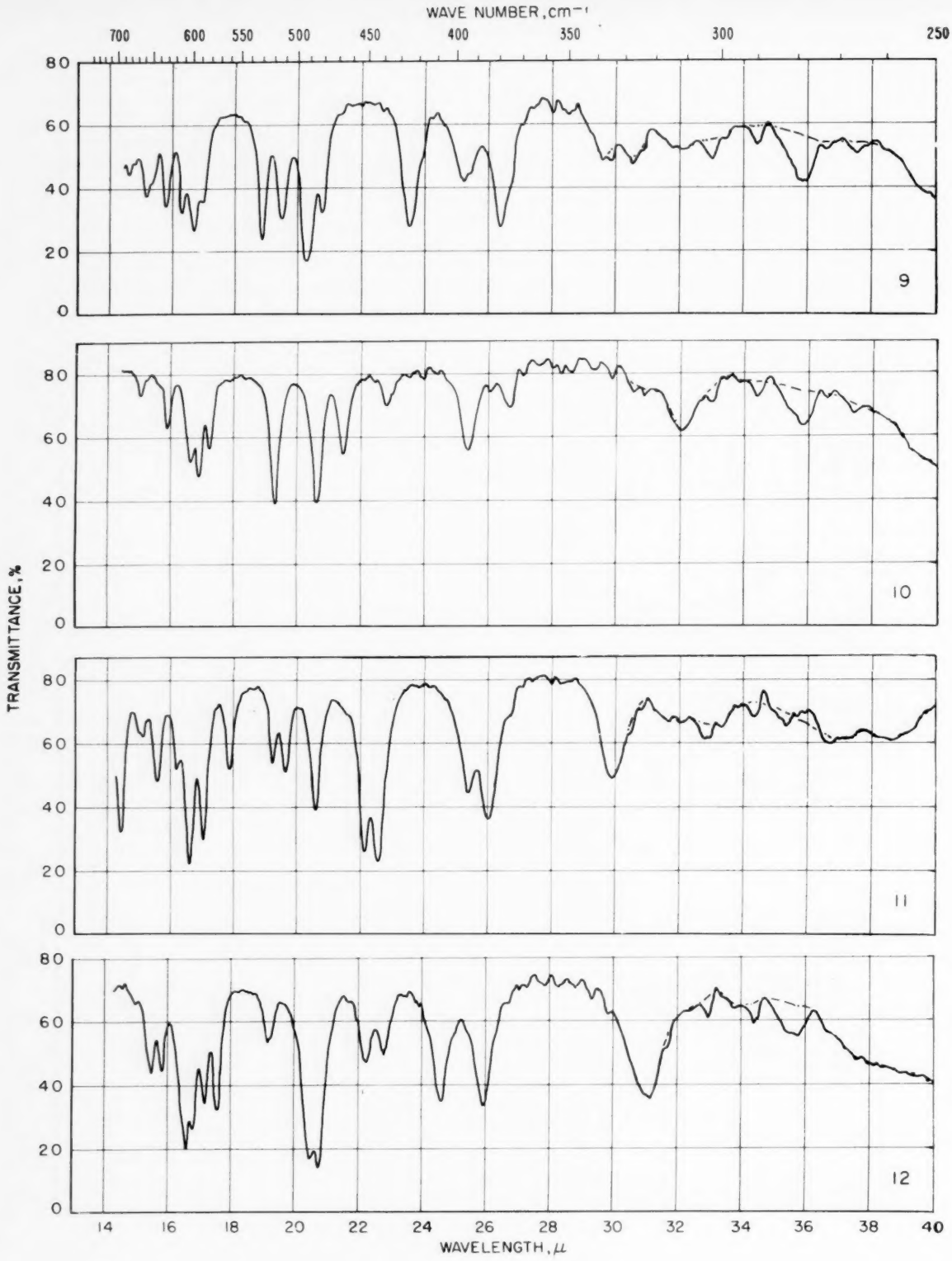

FIGURE 4. *Spectrograms of materials in potassium iodide pellets.*—Continued

9, methyl 6-deoxy-α-L-mannopyranoside triacetate; **10,** methyl 6-deoxy-β-L-mannopyranoside triacetate; **11,** methyl α-D-mannopyranoside tetraacetate; **12,** methyl β-D-mannopyranoside tetraacetate.

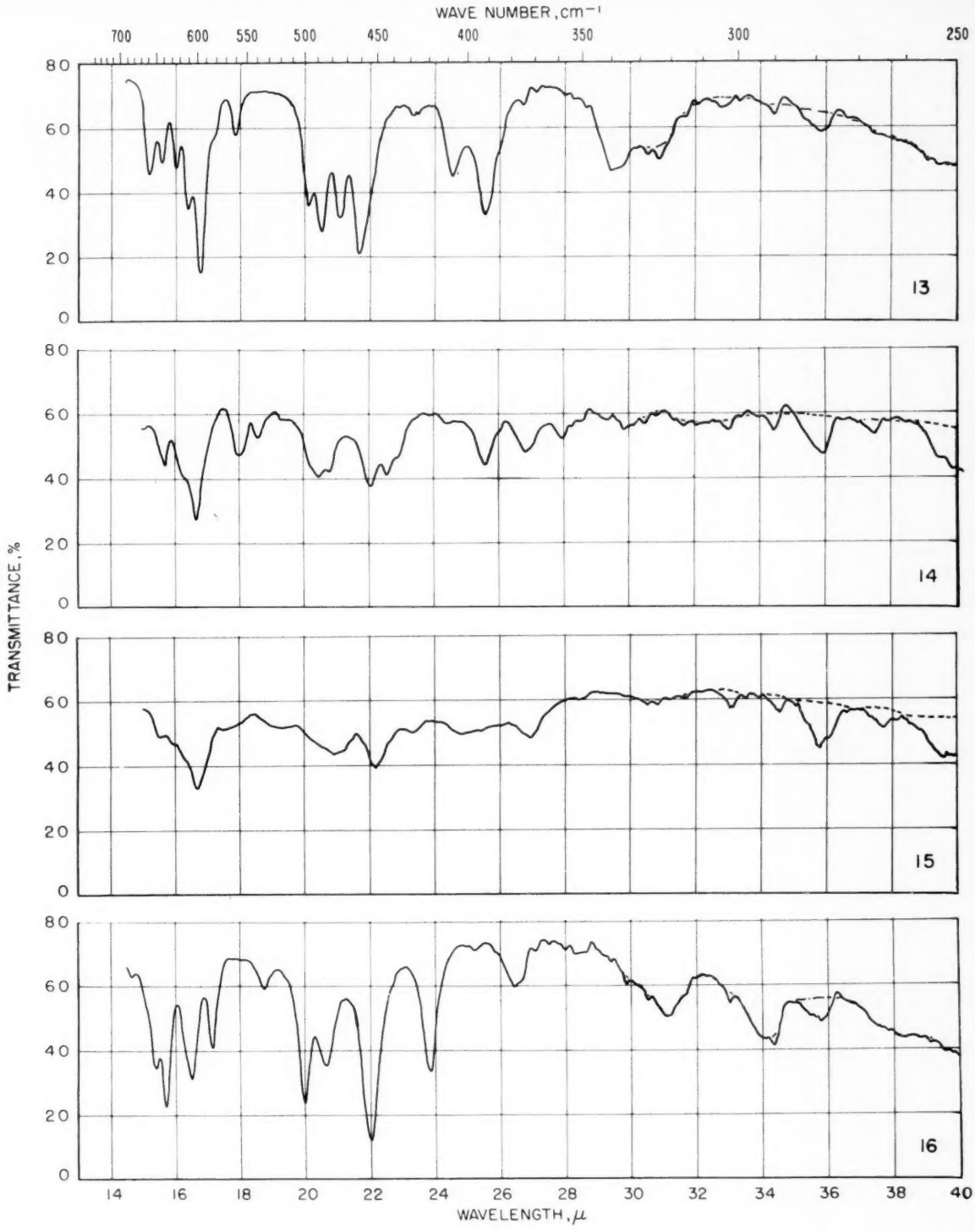

FIGURE 4. *Spectrograms of materials in potassium iodide pellets.*—Continued

13, methyl D-(*glycero*-β-L-*manno*-heptopyranoside pentaacetate; **14,** methyl β-D-glucopyranosyl-(1→4)-α-D-mannopyranoside heptaacetate; **15,** methyl β-D-glucopyranosyl-(1→4)-β-D-mannopyranoside heptaacetate; **16,** methyl α-D-gulopyranoside tetraacetate.

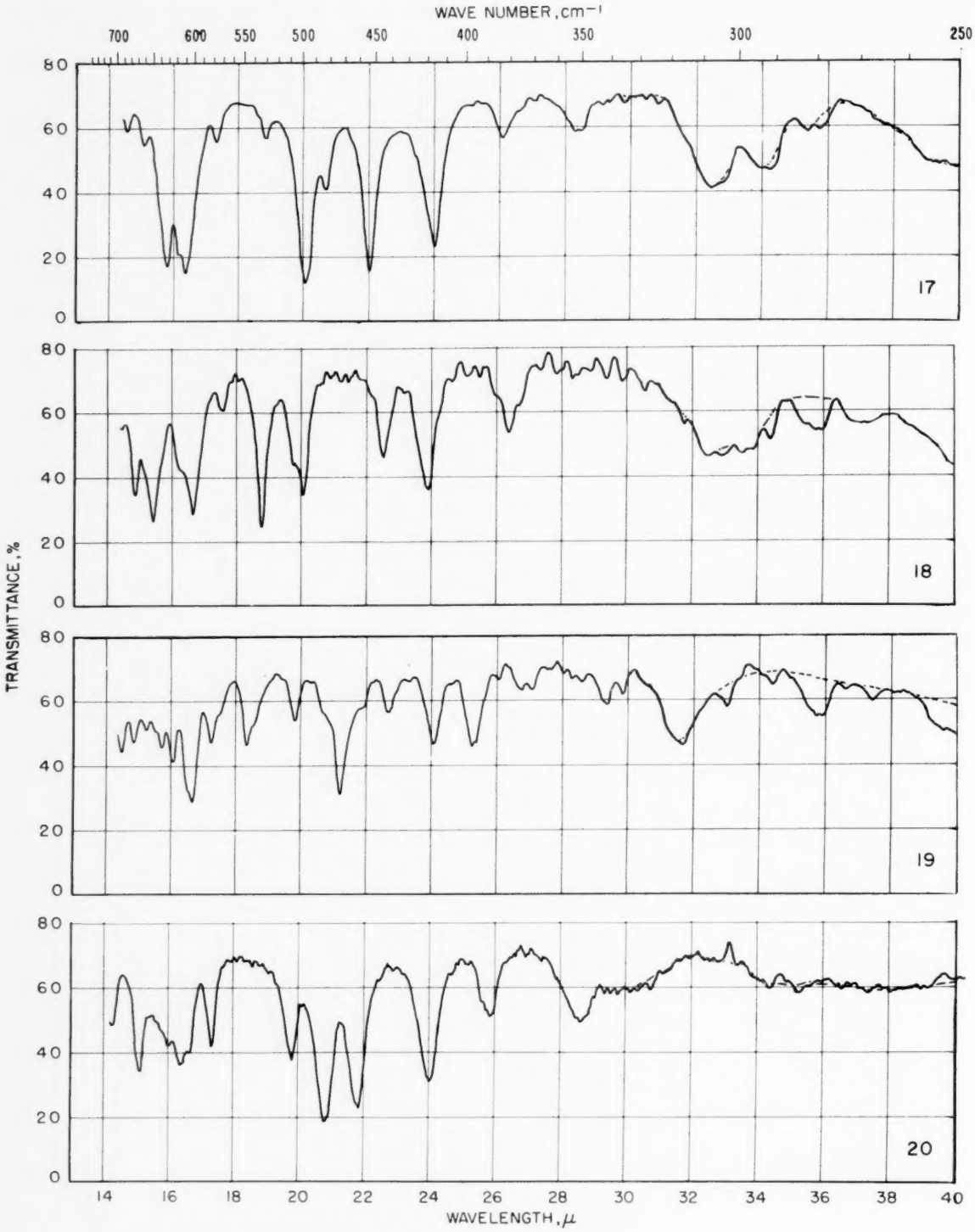

FIGURE 4. *Spectrograms of materials in potassium iodide pellets.*—Continued

17, methyl D-*glycero*-α-D-*gulo*-heptopyranoside pentaacetate; **18,** methyl D-*glycero*-β-D-*gulo*-heptopyranoside pentaacetate; **19,** cyclohexyl D-*glycero*-β-D-*gulo*-heptopyranoside pentaacetate; **20,** methyl β-L-arabinopyranoside triacetate.

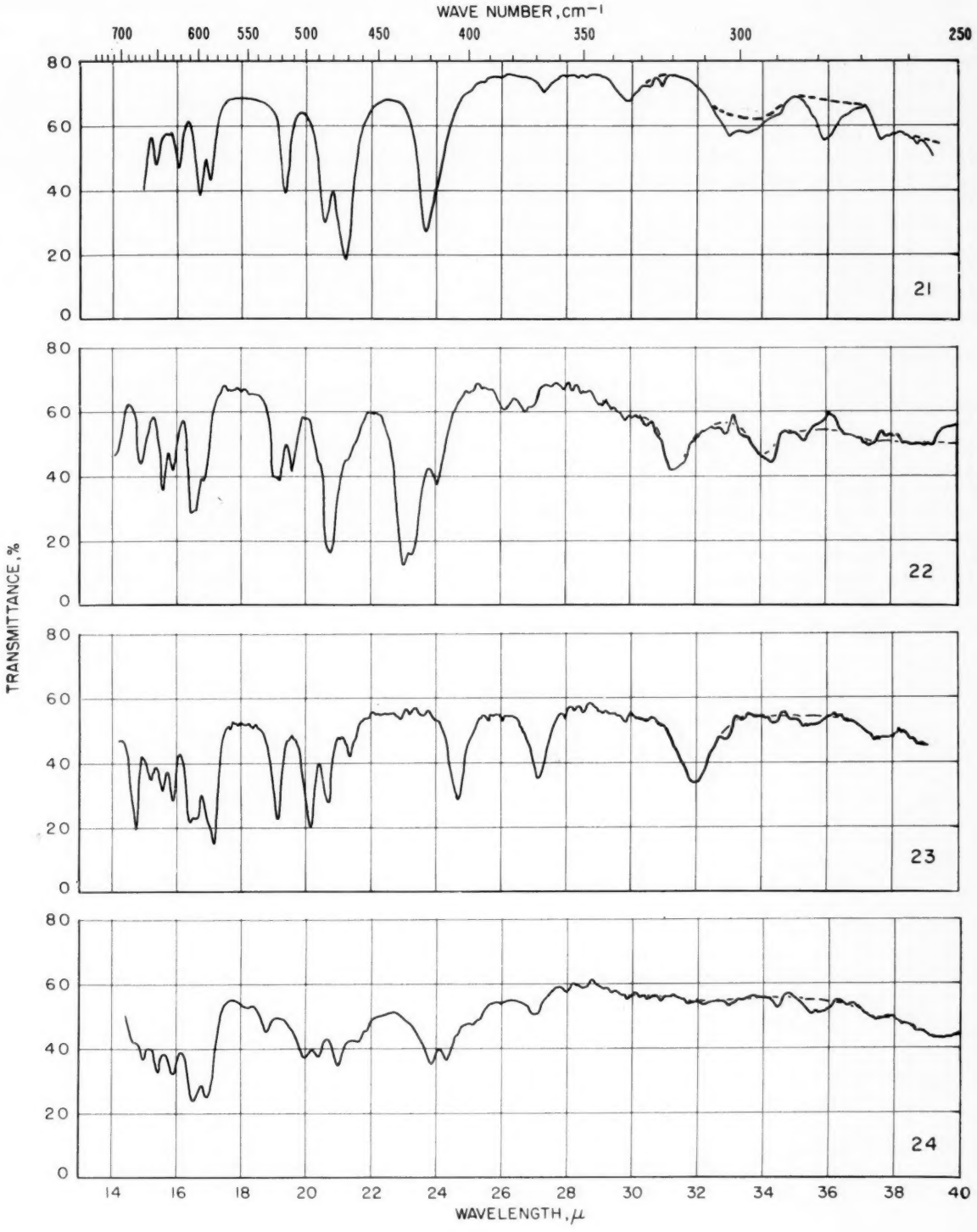

FIGURE 4. *Spectrograms of materials in potassium iodide pellets.*—Continued

21, methyl 6-deoxy-α-L-galactopyranoside triacetate; **22,** methyl α-D-galactopyranoside tetraacetate; **23,** methyl β-D-galactopyranoside tetraacetate; **24, methyl** β-D-galactopyranosyl-(1→4)-β-D-altropyranoside heptaacetate.

6.3. Measurement of Infrared Absorption

The spectrograms are shown in figures 3 and 4. Those in figure 3 for compounds 5 and 15 were recorded with a Beckman Model IR4 (double-beam) spectrophotometer equipped with prisms of sodium chloride. The others were recorded with a Perkin-Elmer Model 21 (double-beam) spectrophotometer equipped with a prism of sodium chloride (for the range of 5,000 to 667 cm^{-1}) and of cesium bromide (for the range of 667 to 250 cm^{-1}), as previously described [11].

Some absorption attributable to water (in the compound, the alkali halide, or both) was observed at 3,448 and 1,639 cm^{-1} and, attributable to atmospheric water vapor, in the far-infrared curves. These regions are drawn on the spectrograms with dashed lines which merely indicate uncertainty and are not to be interpreted quantitatively.

6.4. Spectra Measured Under Different Conditions

The spectra of 13 of the acetylated aldopyranosides (compounds 1 to 4, 7, 9 to 12, 18, 20, 22, and 23) had previously been measured [3] in carbon tetrachloride and in either carbon disulfide, dioxane, or chloroform. As has previously been mentioned, the infrared absorption spectra of crystalline materials show more bands than the spectra of the same compounds in solution. As a result, a larger number of bands were available for correlations than in the previous study [3].

The authors express their gratitude to Harriet L. Frush and J. D. Moyer for preparing and purifying many of the compounds used in this study, and to J. E. Stewart, J. J. Comeford, and F. P. Czech for recording the infrared absorption spectra.

7. References

[1] L. P. Kuhn, Anal. Chem. **22,** 276 (1950).
[2] H. S. Isbell, F. A. Smith, C. Creitz, J. D. Moyer, and H. L. Frush, Infrared spectra of sugar acetates and related compounds (informal communication).
[3] H. S. Isbell, F. A. Smith, E. C. Creitz, H. L. Frush, J. D. Moyer, and J. E. Stewart, J. Research NBS **59,** 41 (1957) RP2772.
[4] R. L. Whistler and L. R. House, Anal. Chem. **25,** 1463 (1953).
[5] S. A. Barker, E. J. Bourne, R. Stephens, and D. H. Whiffen, J. Chem. Soc. **1954,** 3468.
[6] R. S. Tipson and H. S. Isbell, J. Research NBS **64A,** 239 (1960).
[7] R. E. Reeves, J. Am. Chem. Soc. **71,** 215, 1737 (1949); **72,** 1499 (1950).
[8] H. S. Isbell, J. Research NBS **57,** 171 (1956) RP2707.
[9] H. S. Isbell and R. S. Tipson, Science **130,** 793 (1959).
[10] H. S. Isbell and R. S. Tipson, J. Research NBS **64A,** 171 (1960).
[11] R. S. Tipson, H. S. Isbell, and J. E. Stewart, J. Research NBS **62,** 257 (1959) RP2960.
[12] H. B. Henbest, G. D. Meakins, B. Nicholls, and A. A. Wagland, J. Chem. Soc. **1957,** 1462.
[13] J. E. Page, J. Chem. Soc. **1955,** 2017.
[14] H. S. Isbell and H. L. Frush, J. Research NBS **24,** 125 (1940) RP1274.

WASHINGTON, D.C. (Paper 64A5–65)

JOURNAL OF RESEARCH of the National Bureau of Standards—A. Physics and Chemistry
Vol. 64A, No. 5, September–October 1960

Dissociation Constant of 4-Aminopyridinium Ion in Water From 0 to 50 °C and Related Thermodynamic Quantities

Roger G. Bates and Hannah B. Hetzer

(June 13, 1960)

The dissociation constant of 4-aminopyridinium ion in water at 11 temperatures from 0° to 50° C has been determined from electromotive force measurements of 19 approximately equimolal aqueous buffer solutions of 4-aminopyridine and 4-aminopyridinium chloride. Cells without liquid junction were used; the cell is represented as follows:

$$\mathrm{Pt;\ H_2}(g),\ \mathrm{H_2NC_5H_4N{\cdot}HCl}(m_1),\ \mathrm{H_2NC_5H_4N}(m_2),\ \mathrm{AgCl;\ Ag}$$

where m is molality.

Between 0° and 50° C, the dissociation constant (K_{bh}) is given as a function of temperature (T) in degrees Kelvin by

$$-\log K_{bh}=\frac{2575.8}{T}+0.08277+0.0013093\,T$$

The changes of Gibbs free energy ($\Delta G°$), of enthalpy ($\Delta H°$), of entropy ($\Delta S°$), and of heat capacity ($\Delta C_p°$) for the dissociation process in the standard state were calculated from the constants of this equation. At 25° C the following values were found:

$$-\log K_{bh}=9.114,\ \Delta G°=52{,}013\ \mathrm{j\ mole^{-1}},\ \Delta H°=47{,}090\ \mathrm{j\ mole^{-1}},$$
$$\Delta S°=-16.5\ \mathrm{j\ deg^{-1}\ mole^{-1}},\ \Delta C_p°=-15\ \mathrm{j\ deg^{-1}\ mole^{-1}}.$$

Thermodynamic constants for the basic dissociation of 4-aminopyridine at 25° C were also computed.

1. Introduction

The usefulness of 4-aminopyridine as a standard for the direct titration of acid solutions has been pointed out by Van Hall and Stone [1].[1] The base is a solid substance at room temperature, melting at 161° C. It is a monoprotic base with an equivalent weight of 94.119 and can be purified easily by recrystallization from toluene or benzene or by sublimation.

Conductivity data [2, 3] and potentiometric titrations [1, 4] indicate that the negative logarithm of the basic dissociation constant is approximately 4.8 to 4.9 at 20° to 25° C. 4-Aminopyridine is accordingly about as strong as ammonia and is consequently a strong enough base to yield a sharp inflection point when titrated with a solution of a strong acid. Furthermore, the equivalence point of the titration matches the pH of the color transformation of methyl red sufficiently closely that this convenient indicator can be effectively utilized [1]. The base is now available commercially in pure form. One company supplies material specifically intended for use as a reference standard in acidimetry.

It appears likely, therefore, that 4-aminopyridine will find increasing use in the research laboratory. An accurate knowledge of the acidic dissociation constant of 4-aminopyridinium ion over a range of temperatures will permit this acid-base system to be used for pH control in the region pH 8.5 to 9.5 where the undesirable side reactions of borate buffers often preclude the use of borax or boric acid. The mechanism of the acidic dissociation of the cation acids conjugate to weak bases is a subject of continuing interest in this laboratory (see for example, ref. [5,6,7]). The changes of entropy and heat capacity calculated from the temperature coefficient of the dissociation constant offer a possible means of assessing the relative importance of the several structural factors on which the extent of acidic or basic dissociation is known to depend [8].

2. Determination of the Dissociation Constant

The emf method, which has been described in some detail in earlier publications [5,9,10], makes use of a cell without liquid junction:

$$\mathrm{Pt;H_2}(g,1\ \mathrm{atm}),\ \mathrm{H_2NC_5H_4N{\cdot}HCl}(m_1),\ \mathrm{H_2NC_5H_4N}(m_2),\ \mathrm{AgCl;Ag},$$

where m_1 and m_2 represent respectively the molalities of 4-aminopyridinium chloride (BHCl) and the corresponding free base (B). The dissociation of

[1] Figures in brackets indicate the literature references at the end of this paper.

the 4-aminopyridinium ion can be formulated

$$BH^+ + H_2O = B + H_3O^+. \quad (1)$$

The thermodynamic dissociation constant is represented by the symbol K_{bh}.

Inasmuch as 4-aminopyridine is a stronger base than water, the point of equilibrium in reaction (1) lies rather far to the left. Indeed, the free base reacts with water (dissociates) to a sufficient extent that a small correction must be applied to m_1 and m_2 to obtain the true concentrations of BH^+ and B. The dissociation reaction is

$$B + H_2O = BH^+ + OH^-, \quad (2)$$

and the corrected concentrations of 4-aminopyridinium ion and 4-aminopyridine are given by

$$m_{BH^+} = m_1 + m_{OH} \quad (3)$$

and

$$m_B = m_2 - m_{OH}. \quad (4)$$

In order to relate K_{bh} in a useful way to the emf (E) of the cell, the mass-law expression for K_{bh} was combined with the Nernst equation for the cell. The resulting equations are as follows:

$$-\log K_{bh} - \beta m_1 = \frac{E - E^\circ}{2.3026RT/F} + \log \frac{m_1(m_1 + m_{OH})}{m_2 - m_{OH}} - \frac{2A\sqrt{m_1}}{1 + Ba^*\sqrt{m_1}} \quad (5a)$$

$$= pw\mathrm{H} + \log \frac{m_1 + m_{OH}}{m_2 - m_{OH}} - \frac{2A\sqrt{m_1}}{1 + Ba^*\sqrt{m_1}}. \quad (5b)$$

In deriving these equations, the concentrations of BH^+ and B were expressed by eq (3) and (4), the term $f_{BH^+} f_{Cl^-} \mathbf{a}_{H_2O} / f_B$ (where f is an activity coefficient on the molal scale and $\mathbf{a}_{H_2O}$ is the water activity) was expressed by an equation of the Hückel form containing two parameters, a^* and β, and the Debye-Hückel constants A and B [11], and the ionic strength was set equal to the molality of 4-aminopyridinium chloride.

For convenience, $(-\log K_{bh} - \beta m_1)$ is called $-\log K'_{bh}$. It is evident that K'_{bh} is an "apparent" or inexact value of the dissociation constant which, however, becomes equal to the true value of the thermodynamic constant K_{bh} when m_1 becomes 0, that is, at infinite dilution.

In eq (5a), E° is the standard potential of the hydrogen-silver chloride cell [12] and R, T, and F are, respectively, the gas constant per mole, the temperature in degrees Kelvin, and the faraday. The term pwH, a useful experimental quantity numerically equal to $-\log(f_H f_{Cl} m_H)$, was defined in an earlier publication [13]. Its equivalent in terms of the emf and chloride ion molality is readily apparent from a comparison of eq (5a) and (5b).

It has been shown [14] that the hydroxyl ion concentration can be obtained with the accuracy needed to correct the buffer ratio by

$$\log m_{OH} \approx \log K_w + pw\mathrm{H}, \quad (6)$$

where K_w is the ion product constant for water [9]. This approximation is quite satisfactory if the base is not too strong (i.e., when m_{OH} is not too large). It has been found to be adequate for the calculation of the dissociation constant of piperidinium ion ($m_{OH} \approx 0.002$) [7] but fails when applied to the treatment of the data for $CaOH^+$ ($m_{OH} \approx 0.02$) [15].

3. Experimental Procedures

Commercial, unpurified 4-aminopyridine was recrystallized from a mixture of benzene and alcohol.[2] It was then crystallized twice from water, crushed, and dried for four hours at 105° C as recommended by Van Hall and Stone [1]. A further drying for two hours at 110° C brought about some sublimation. The melting point was found to be 160° C at a heating rate of about 1° C min^{-1}.

Hydrochloric acid of reagent grade was diluted to about 6 M and distilled twice, the middle third being collected in each instance. The redistilled acid was diluted to make a stock solution with a molality about 0.1 which was standardized by a gravimetric determination of chloride as silver chloride. Two different stock solutions were used in the course of the work. On the average, replicate determinations of the molality agreed within ±0.02 percent.

The assay of the purified 4-aminopyridine was determined by titration with the standard solution of hydrochloric acid. The concentration of pyridinium salt at the endpoint was about 0.035 M, and the pH was adjusted to the calculated equivalence point (pH 5.3) with the aid of a glass-electrode pH meter. The material assayed 100.0±0.1 percent.

Four stock solutions composed of 4-aminopyridine and hydrochloric acid were prepared. Each of these was diluted with distilled water to make other cell solutions, but no more than five cell solutions were prepared from each stock solution. Dissolved air was removed from the solutions by passing purified hydrogen through them for about 2 hours before the cells were filled. The cell vessels were flushed with hydrogen; the solution was then admitted and the vessel filled and emptied twice before the final filling. The preparation of the electrodes has been described elsewhere [16].

The solubility of silver chloride in a 0.1-M solution of 4-aminopyridine was found to be 0.00104 mole l^{-1}, from which the equilibrium constant (K_f) for the formation of the complex ion AgB_2^+ is found to be 7×10^5. The 4-aminopyridine complex of silver ion is thus considerably less stable than the

[2] The authors are indebted to M. M. Davis and M. Paabo for the initia purification.

corresponding silver-ammonia complex, $Ag(NH_3)^+_2$, for which the formation constant (K_f) is about 1.6×10^7 [17]. Bates and Pinching [5] showed that the percentage increase in m_{Cl} due to solubility of silver chloride is nearly proportional to K_{sp} K_f, where K_{sp} is the solubility product constant. For buffer solutions containing equimolal amounts of ammonia and ammonium chloride this quantity amounts to about 0.003, but it is only 0.00011 for the 4-aminopyridine buffers studied here. Inasmuch as the largest correction applied to the ammonia results was about 0.002 in *pw*H [5], it is evident that a negligible error will be incurred by the formation of complexes between silver ion and 4-aminopyridine in the buffer solutions of the present study.

Bruehlman and Verhoek [18] have found that plots of log K_f for amine-silver complexes versus $-\log K_{bh}$ for the base in question consist of a series of straight lines, each characteristic of a different class of base. The data for pyridine and two of its homologues fall on the line of the primary amines rather than that of the tertiary amines. It is of interest to note that our result for 4-aminopyridine also lies close to the line characteristic of the primary amines.

The emf data were corrected in the usual way to a partial pressure of 1 atm of dry hydrogen. The values of the emf summarized in table 1 represent the average of two hydrogen-silver chloride electrode combinations in the same cell. At 25° C, the mean difference between pairs of electrodes in the same cell was 0.06 mv.

4. Results

The values of $-\log K'_{bh}$ were calculated by eq (5a) and (5b) with several different values of the parameter a^*. The best straight-line plots of $-\log K'_{bh}$ with respect to m_1 at each temperature were obtained with $a^*=0$. The plots of the data at 0°, 25°, and 50° C are shown in figure 1. The best rectilinear fit of the experimental results was obtained by the method of least squares. The intercepts of the lines at $m_1=0$ gave the values of $-\log K_{bh}$ and K_{bh}. These are summarized in table 2 along with σ_i, the standard deviation of the intercept, and K_b, the basic dissociation constant of 4-aminopyridine computed by the formula

$$K_b=K_w/K_{bh}. \tag{7}$$

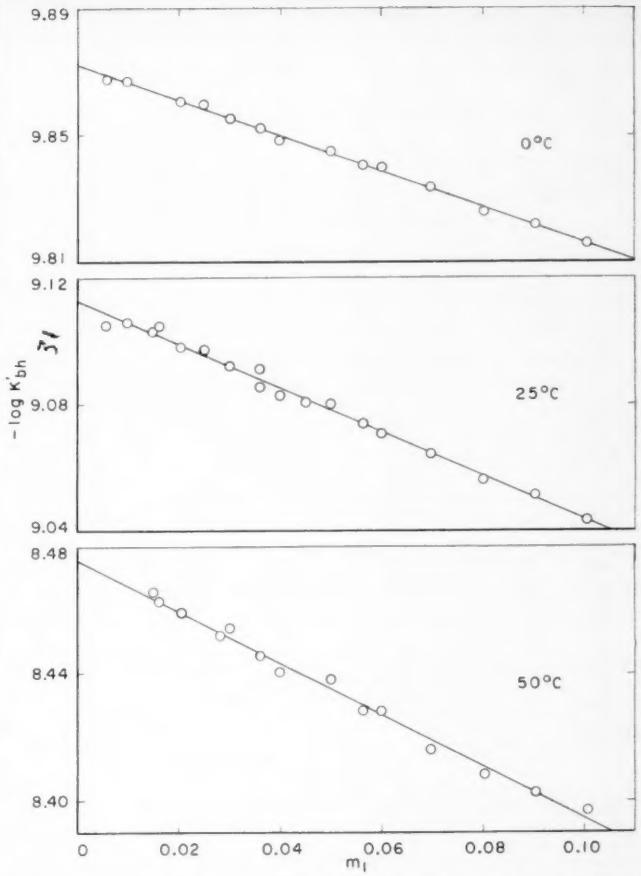

FIGURE 1. *Plots of* $-\log K'_{bh}$ *as a function of* m_1 *at 0°, 25°, and 50°C.*

TABLE 1. *Electromotive force of the cell:* Pt; $H_2(g, 1\ atm)$, $H_2NC_5H_4N\cdot HCl(m_1)$, $H_2NC_5H_4N(m_2)$, AgCl; Ag *from* 0° to 50° C, *in volts*

m_1	m_2	0°	5°	10°	15°	20°	25°	30°	35°	40°	45°	50°
0.10066	0.09914	0.83898	0.83849	0.83784	0.83704	0.83611	0.83499	0.83384	0.83255	0.83113	0.82960	0.82801
.09031	.08919	.84105	.84058	.83987	.83913	.83827	.83732	.83615	.83485	.83341	.83193	.83032
.08005	.07884	.84311	.84270	.84213	.84143	.84058	.83958	.83829	.83707	.83571	.83425	.83279
.06961	.06875	.84588	.84547	.84492	.84421	.84341	.84256	.84165	.84037	.83885	.83747	.83594
.05993	.05902	.84868	.84827	.84784	.84715	.84651	.84559	.84460	.84348	.84227	.84097	.83952
.05625	.05310	.84880	.84845	.84801	.84741	.84659	.84585	.84482	.84368	.84247	.84113	.83960
.04985	.04923	.85221	.85187	.85149	.85094	.85038	.84964	.84869	.84766	.84653	.84528	.84390
.04505	.04554						.85222	.85123				
.03986	.03926	.85635	.85618	.85589	.85542	.85482	.85406	.85325	.85229	.85109	.84987	.84858
.03604	.03402	.85741	.85722	.85689	.85645	.85584	.85512	.85436				
.03597	.03637						.85726	.85627	.85538	.85436	.85337	.85184
.02996	.02959	.86209	.86199	.86183	.86145	.86097	.86041	.85972	.85888	.85785	.85652	.85569
.02492	.02352	.86482	.86466	.86453	.86431	.86388	.86339	.86251	.86175	.86071	.85963	.85839
.02466	.02493						.86534	.86437	.86358	.86268	.86181	
.02003	.019730	.87014	.87006	.86996	.86986	.86964	.86914	.86872	.86793	.86699	.86583	.86498
.016111	.016289						.87492	.87435	.87360	.87291	.87238	.87102
.014963	.014126						.87468	.87403	.87334	.87269	.87189	.87104
.009766	.009646	.88520	.88529	.88562	.88576	.88575	.88556	.88561	.88504	.88437		
.005725	.015405	.89551	.89582	.89630	.89655	.89669	.89667					

TABLE 2. *Summary of the dissociation constants of 4-aminopyridinium ion and 4-aminopyridine from 0° to 50° C*

Temperature	$-\log K_{bh}$	σ_i	$K_{bh}\times10^{10}$	$-\log K_b$	$K_b\times10^8$
°C					
0	9.8731	0.0005	1.339	5.070	0.851
5	9.7043	.0006	1.976	5.030	.934
10	9.5486	.0006	2.827	4.986	1.03
15	9.3979	.0006	4.000	4.948	1.13
20	9.2524	.0006	5.592	4.915	1.22
25	9.1141	.0007	7.690	4.882	1.31
30	8.9783	.0012	10.51	4.855	1.40
35	8.8455	.0010	14.27	4.834	1.47
40	8.7170	.0013	19.19	4.818	1.52
45	8.5941	.0014	25.46	4.802	1.58
50	8.4768	.0014	33.36	4.785	1.64

It should be noted that K_b is the equilibrium constant for the process

$$B+H_2O=BH^++OH^-. \tag{8}$$

The values of $-\log K_{bh}$ from the present investigation are compared with earlier determinations in table 3.

TABLE 3. *Comparison of $-\log K_{bh}$ with earlier determinations at 4 temperatures*

Authors; method	5.4° C	20° C	25° C	35° C
Tropsch [2]; conductance			9.11	
Van Hall and Stone [1]; potentiometric titration			9.11	
Hansson [3]; conductance		9.24		
Albert, Goldacre, and Phillips [4]; potentiometric titration		[a] 9.29		
Elliott and Mason [20]; potentiometric titration	9.74			8.93
This investigation; emf	9.692	9.252	9.114	8.845

[a] Corrections for dilution applied in the manner prescribed by the authors.

5. Thermodynamic Quantities

The method of least squares was used to express $-\log K_{bh}$ as a function of absolute temperature by an equation of the form suggested by Harned and Robinson [19], namely

$$-\log K_{bh}=\frac{A}{T}+B+CT. \tag{9a}$$

Between 0° and 50° C, $-\log K_{bh}$ is given by

$$-\log K_{bh}=\frac{2575.8}{T}+0.08277+0.0013093T. \tag{9b}$$

The constants of this equation were determined by the IBM704 computer. The average difference between "observed" and "calculated" values at the 11 temperatures is 0.0014.

By the application of well-known thermodynamic relations, the standard changes of Gibbs free energy ($\Delta G°$), enthalpy ($\Delta H°$), entropy ($\Delta S°$), and heat capacity ($\Delta C_p°$) for the dissociation process, eq (1), in the standard state were derived from the constants of eq (9b). The resulting expressions for these quantities are as follows:

$$\Delta G°=49{,}313+1.585\ T+0.02507\ T^2\ (j\ \text{mole}^{-1}) \tag{10}$$
$$\Delta H°=49{,}313-0.02507\ T^2\ (j\ \text{mole}^{-1}) \tag{11}$$
$$\Delta S°=-1.58-0.0501\ T\ (j\ \text{deg}^{-1}\ \text{mole}^{-1}) \tag{12}$$
$$\Delta C_p°=-0.050\ T\ (j\ \text{deg}^{-1}\ \text{mole}^{-1}). \tag{13}$$

The values obtained by these equations are summarized in table 4. The estimated uncertainties at 25°C are as follows: $\Delta G°$, ±6 j mole $^{-1}$; $\Delta H°$, ±100 j mole $^{-1}$; $\Delta S°$, ±0.5 j deg $^{-1}$ mole $^{-1}$; and $\Delta C_p°$, 5 j deg^{-1} mole^{-1}.

TABLE 4. *Thermodynamic quantities for the acidic dissociation of 4-aminopyridinium ion from 0° to 50° C*

t	$\Delta G°$	$\Delta H°$	$\Delta S°$	$\Delta C_p°$
°C	*j mole*$^{-1}$	*j mole*$^{-1}$	*j deg*$^{-1}$ *mole*$^{-1}$	*j deg*$^{-1}$ *mole*$^{-1}$
0	51,616	47,440	−15.3	−14
5	51,693	47,370	−15.5	−14
10	51,771	47,300	−15.8	−14
15	51,851	47,230	−16.0	−14
20	51,931	47,160	−16.3	−15
25	52,013	47,090	−16.5	−15
30	52,097	47,010	−16.8	−15
35	52,181	46,930	−17.0	−15
40	52,267	46,860	−17.3	−16
45	52,354	46,780	−17.5	−16
50	52,442	46,700	−17.8	−16

Elliott and Mason [20] have calculated the heat and entropy of ionization of 4-aminopyridinium ion from values of $-\log K_{bh}$ at three temperatures, namely 5.4°, 20°, and 35° C. Their results are as follows:

$\Delta H°(20°\ C)=45{,}000$ j mole^{-1}; $\Delta S°(20°\ C)=-24$ j deg^{-1} mole^{-1}.

The equation for the variation of $-\log K_b$ with absolute temperature (T) is obtained, as suggested by eq (7), by subtracting the equation for $-\log K_{bh}$ (eq (9b)) from the corresponding equation for $-\log K_w$ given by Robinson and Stokes [11]. In this way, one obtains

$$-\log K_b=\frac{1895.53}{T}-6.1674+0.015744T. \tag{14}$$

From the constants of this equation, thermodynamic quantities for the basic dissociation of 4-aminopyridine (B) at 25° C were calculated, with the following results:

Process: $B+H_2O=BH^++OH^-$ at 25° C

$\Delta G°=27{,}880$ j mole^{-1}
$\Delta H°=9{,}490$ j mole^{-1}
$\Delta S°=-61.7$ j deg^{-1} mole^{-1}
$\Delta C_p°=-180$ j deg^{-1} mole^{-1}.

6. Discussion

Recent studies [20 to 22] indicate clearly that it is the nuclear, or pyridine, nitrogen of 4-aminopyridine which has much the greater attraction for the

proton. Indeed, Hirayama and Kubota [21] found that the proton does not add in significant amounts to the amino nitrogen even in 50-percent sulfuric acid. They estimated $-\log K_{bh}=-6.55$ for the dissociation of the bivalent cation acid, $^{+}H_3NC_5H_4NH^{+}$, in 95-percent sulfuric acid.

Pyridine itself is a very weak base ($-\log K_{bh}$ about 5.2) and aniline is still weaker ($-\log K_{bh}=4.6$). It is of interest to inquire into the reasons for the ten-thousandfold increase in basicity of the nuclear nitrogen atom when an amino group is substituted on the carbon atom located in position 4. Albert, Goldacre, and Phillips [3], in their study of the strength of heterocyclic bases, attribute the increase to increased resonance in the structure of the ion. They point out that analogous compounds in the quinoline and acridine series also show a similar increase.

It is well understood that an uncharged base tends to add a proton if resonant structures imparting greater stability to the cation than to the free base itself exist [23]. The low basicity of aniline can be explained by the fact that the resonance energy of the neutral base is greater than that of the anilinium ion. The resonance structure which makes the strongest contribution appears to be the following:

In this resonance configuration, a flow of electrons toward the ring gives rise to a residual positive charge (δ^+) on the amino nitrogen, which in turn repels the proton. No similar resonance contribution is possible in anilinium ion.

On the other hand, the weakly basic nature of pyridine cannot be explained on the basis of resonance. Similar resonance structures can be written for both pyridine and pyridinium ion, so that resonance does not favor the molecular form, as is the case with aniline.

The weakness of pyridine as a base is presumably due to the fact that the nitrogen is doubly bonded to one of the adjacent carbon atoms in each of the Kekulé structures. It can be shown on theoretical grounds that an atom joined to another by a multiple bond holds its remaining electrons more firmly than usual [23]. The donor properties of the nitrogen atom are correspondingly lessened.

The greatly enhanced basicity of the nuclear nitrogen in 4-aminopyridine appears to be the result of a strong contribution of the resonance configuration to the structure of the free base [23, 24].

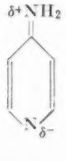

The increased density of charge on the ring nitrogen attracts protons, whereas the residual positive charge of the amino nitrogen repels them so effectively that almost no basicity in the usual sense remains. Resonance structures likewise stabilize the cation effectively.

A comparison of the dipole moments of aniline, pyridine, and 4-aminopyridine offers some support for the existence of the resonant structure in the free base [24]. A simple linear combination of the moments of aniline (1.90 Debye units) and pyridine (2.22 Debye units) in dioxane solution would lead to a moment of 4.12 if the vectors are all in the plane of the ring. The observed moment for 4-aminopyridine in dioxane is 4.36 Debye units, pointing to an appreciable contribution of the resonant configuration. Sidgwick [25] has suggested that 4-aminopyridine can exist in a tautomeric imine form, $HN=C_5H_4NH$.[3] The symmetry of this tautomer would, however, probably cause the molecule to exhibit only a small dipole moment; hence, the relatively large observed moment would appear to rule out the existence of this tautomer in significant amounts in dioxane solutions of 4-aminopyridine.

The interpretation of the changes of heat content, entropy, and heat capacity that accompany the dissociation of univalent cation acids should be somewhat simpler, in view of the equality of charge distribution among reactants and products, than the interpretation of the corresponding data for uncharged acids or anion acids.[4] It is nonetheless still exceedingly complex and, furthermore, is hampered by a lack of data for a group of several related, sterically similar, acids.

In terms of the Harned-Robinson equation, eq (9a), the difference between ΔS° and ΔC_p° for a given acid or base is constant and independent of temperature:

$$\Delta S^\circ - \Delta C_p^\circ = -2.3026RB = -19.1447B. \qquad (15)$$

The value of B is positive for the dissociation of most cationic acids (see appendix 12.1 of [11]), and hence ΔC_p° usually exceeds ΔS° for acids of this charge type. The B constant for the dissociation of 4-aminopyridinium ion is very small; hence, ΔS° and ΔC_p° are nearly equal. Nevertheless, these two quantities need not always have the same sign; for the dissociation of piperidinium ion [7], ΔS° at 25° C was found to be −34 j deg^{-1} mole^{-1} whereas ΔC_p° was 88 j deg^{-1} mole^{-1} at the same temperature. This decrease of entropy on dissociation, larger than has been found for other acids of this charge type, was attributed to steric exclusion of solvent from the immediate vicinity of the piperidinium ion. Consequently, the entropy-increasing effect of the release of water molecules on dissociation is absent. If it be assumed that the two free bases are equally solvated, it may be reasoned that the wider distri-

[3] The existence of the imine structure has also been suggested by Mason [26].

[4] As the Born equation shows, however, the electrostatic work of charging two spherical ions of the same charge is only equal when the radii of the ions are the same.

bution of charge possible with the existence of resonant forms permits more extensive solvation of 4-aminopyridinium ion than occurs with piperidinium ion.

If changes in solvent orientation play an important part in determining the sign and magnitude of the entropy change on dissociation, the same should be true of the heat capacity change: release of water from combination would be expected to bring about an increase in both entropy and heat capacity. Structural changes, however, sometimes result in an increase in one of these quantities and a decrease in the other. Unfortunately, no independent assessment of the degree of solvation of the acidic and basic forms is available, and our knowledge of the details of the geometry of the molecules and ions and their immediate surroundings is likewise incomplete. Thus, measurements of the entropies and heat capacities for dissociation reactions are as yet unable alone to provide an insight into the mechanisms of acid-base behavior.

7. References

[1] C. E. Van Hall and K. G. Stone, Anal. Chem. **27,** 1580 (1955).
[2] H. Tropsch, Monatsh. Chem. **35,** 775 (1914).
[3] J. Hansson, Svensk Kem. Tidskr. **67,** 256 (1955).
[4] A. Albert, R. Goldacre, and J. Phillips, J. Chem. Soc. 1948, 2240; A. Albert, J. Chem. Soc. 1951, 1376.
[5] R. G. Bates and G. D. Pinching, J. Research NBS **42,** 419 (1949) RP1982.
[6] R. G. Bates and G. D. Pinching, J. Research NBS **46,** 349 (1951) RP2205.
[7] R. G. Bates and V. E. Bower, J. Research NBS **57,** 153 (1956) RP2705.
[8] D. H. Everett, D. A. Landsman, and B. R. W. Pinsent, Proc. Roy. Soc. (London) [A] **215,** 403 (1952); D. H. Everett and B. R. W. Pinsent, Proc. Roy. Soc. (London) [A] **215,** 416 (1952).
[9] H. S. Harned and B. B. Owen, The physical chemistry of electrolytic solutions, 3d ed. (Reinhold Publishing Corp., New York, N.Y., 1958).
[10] R. G. Bates and S. F. Acree, J. Research NBS **30,** 129 (1943) RP1524.
[11] R. A. Robinson and R. H. Stokes, Electrolyte Solutions, 2d ed., p. 363, Appendices 7.1, 12.1 (Academic Press, New York, N.Y., 1959).
[12] R. G. Bates and V. E. Bower, J. Research NBS **53,** 283 (1954) RP2546.
[13] R. G. Bates, Chem. Revs. **42,** 1 (1948).
[14] R. G. Bates, G. L. Siegel, and S. F. Acree, J. Research NBS **31,** 205 (1943) RP1559.
[15] R. G. Bates, V. E. Bower, R. G. Canham, and J. E. Prue, Trans. Faraday Soc. **55,** 2062 (1959).
[16] R. G. Bates, Electrometric *p*H determinations, pp. 166, 167, 205, 206 (John Wiley and Sons, Inc., New York, N.Y., 1954).
[17] P. F. Derr, R. M. Stockdale, and W. C. Vosburgh, J. Am. Chem. Soc. **63,** 2670 (1941).
[18] R. J. Bruehlman and F. H. Verhoek, J. Am. Chem. Soc. **70,** 1401 (1948).
[19] H. S. Harned and R. A. Robinson, Trans. Faraday Soc. **36,** 973 (1940).
[20] J. J. Elliott and S. F. Mason, J. Chem. Soc. 1959, 2352.
[21] H. Hirayama and T. Kubota, J. Pharm. Soc. Japan **73,** 140 (1953).
[22] H. H. Jaffé and G. O. Doak, J. Am. Chem. Soc. **77,** 4441 (1955); H. H. Jaffé, J. Am. Chem. Soc. **77,** 4445 (1955).
[23] G. W. Wheland, Resonance in organic chemistry, pp. 178, 355–359 (John Wiley and Sons, Inc., New York, N.Y., 1955).
[24] D. G. Leis and B. C. Curran, J. Am. Chem. Soc. **67,** 79 (1945).
[25] N. V. Sidgwick, Organic chemistry of nitrogen, revised by T. W. J. Taylor and W. Baker, p. 529 (Oxford Univ. Press, Oxford, 1937).
[26] S. F. Mason, J. Chem. Soc. 1960, 219.

(Paper 64A5–66)

JOURNAL OF RESEARCH of the National Bureau of Standards—A. Physics and Chemistry
Vol. 64A, No. 5, September–October 1960

Tritium-Labeled Compounds VI. Alditols-*1-t* and Alditols-*2-t*[1]

Harriet L. Frush, Horace S. Isbell, and Alexander J. Fatiadi

(June 1, 1960)

By reduction of aldoses and aldonic lactones with lithium borohydride-*t*, the following 1-tritium-labeled alditols were prepared: D-arabinitol-*1-t*, D-lyxitol-*1-t*, D-ribitol-*1-t*, D-xylitol-*1-t*, D-galactitol-*1-t*, D-mannitol-*1(6)-t*, D-glucitol-*1-t*, D-talitol-*1-t*, L-gulitol-*1-t* (D-glucitol *6-t*), L-rhamnitol-*1-t*, D-*glycero*-D-*gulo*-heptitol-*1-t*, and 4-*O*-β-D-galactopyranosyl-D-glucitol-*1-t*. By reduction of ketoses with lithium borohydride-*t*, the following epimeric pairs of 2-labeled alditols were prepared and subsequently separated: D-mannitol-*2(5)-t* and D-glucitol-*2-t*; L-gulitol-*2-t* (D-glucitol-*5-t*) and L-iditol-*2-t*; D-galactitol-*2-t* and D-talitol-*2-t*; D-*glycero*-D-*gulo*-heptitol-*2-t* and D-*glycero*-D-*ido*-heptitol-*2-t*; and D-*glycero*-D-*galacto*-heptitol-*2-t* and D-*glycero*-D-*talo*-heptitol-*2-t*.

The yields of the epimeric alditols formed from ketoses were determined by an isotope-dilution technique. Stereomeric relationships are discussed for the labeled alditols and for the ketoses derivable from them by oxidation with *Acetobacter suboxydans*.

1. Introduction and Discussion

Tritium-labeled alditols are useful intermediates for synthesizing tritium-labeled ketoses and for studying a wide variety of chemical and biological reactions. As part of a program on the development of methods for synthesizing tritium-labeled carbohydrates [1, 2, 3, 4, 5, 6],[2] procedures have now been developed for preparing alditols position-labeled with tritium.

Nonradioactive sodium borohydride has been used for reducing aldoses [7] and lactones [8,9] to alditols. However, for the preparation of tritium-labeled materials, it was considered advantageous to use lithium borohydride-*t* (instead of the sodium analog), because it may be more easily prepared.[3] Hence, processes were developed for the use of lithium borohydride-*t* in preparing tritium-labeled alditols.

The experimental conditions under which lithium borohydride is used are critical, insofar as the extent and efficiency of the reduction are concerned. In the previous preparation of aldoses-*1-t* by the reduction of aldonic lactones [4], lithium borohydride-*t*, dissolved in anhydrous pyridine, was added to a solution of the lactone in water. The use of pyridine as a solvent avoids decomposition of the hydride and appears to suppress the further reduction of the aldose to the alditol. However, in the preparation of labeled alditols, better yields were obtained when tetrahydrofuran, instead pyridine, was used as the solvent.

Alditols may be prepared by the reduction of aldoses, aldonic lactones, or ketoses. Aldoses and lactones, on reduction, form alditols having, respectively, one and two atoms of hydrogen-*t* at C1. Thus, the product derived from the lactone has twice the specific activity of that derived from the aldose. Ketoses, on reduction, form epimeric pairs of alditols having one atom of hydrogen-*t* at C2; subsequent separation of the alditols is necessary.

Tables 1, 2, and 3 summarize the results obtained by the reduction of aldoses, aldonic lactones, and ketoses, respectively, to alditols. Yields of the alditols were determined by (a) radioactivity assay of the purified solutions and (b) isotope-dilution techniques. Table 3 gives the yields of the epimeric alditols formed from several ketoses, a subject of considerable theoretical interest.

Tritium-labeled products having high activities are subject to decomposition from self-radiation, and hence should not be held long in storage. The activities of the products listed in tables 1, 2, and 3 are adequate for most purposes, and decomposition over the course of several months has been slight. Position-labeled products of higher activity can be made, but these must be used within a relatively short time.

TABLE 1. *Reduction of aldoses with lithium borohydride-t*[a]

Aldose	Alditol-*1-t*	Specific activity	Radiochemical yield
		μc/mg	%
D-Arabinose	D-Arabinitol-*1-t*	59.8	94
D-Lyxose	D-Lyxitol-*1-t* (D-Arabinitol-*5-t*)	59.8	71
D-Ribose	D-Ribitol-*1-t*	59.8	80
D-Xylose	D-Xylitol-*1-t*	60.0	86
D-Galactose[b]	D-Galactitol-*1-t*	44	90
D-Glucose	D-Glucitol-*1-t*	50.0	81
D-Talose	D-Talitol-*1-t*	50.5	67

[a] Experimental details are given in section 4.1.
[b] Preparation reported earlier in ref [3]. The lithium borohydride had a specific activity different from that of the reductant used in other preparations.

[1] Part of a project on the development of met hods for the synthesis of radioactive carbohydrates, sponsored by the Division of Research of the Atomic Energy Commission. The tritium-labeled products described may be purchased from the National Bureau of Standards at a price of $10 per 100 microcuries.
[2] Figures in brackets indicate the literature references at the end of this paper.
[3] These materials can be prepared by tritium-hydrogen exchange, which occurs at about 200° C for lithium borohydride and at about 350° C for sodium borohydride [10]. The preparation of lithium borohydride-*t* is described in ref [3].

TABLE 2. *Reduction of aldonic lactones with lithium borohydride-t* [a]

Lactone	Alditol-*1-t* [b]	Radiochemical yield
		%
D-Arabono-γ-	D-Arabinitol-*1-t*	79.2
D-Xylono-γ-	D-Xylitol-*1-t*	80.0
D-Galactono-γ-	D-Galactitol-*1-t*	71.5
D-Glucono-δ-	D-Glucitol-*1-t*	70.8
D-Glucono-γ-	D-Glucitol-*1-t*	70.3
L-Gulono-γ-	L-Gulitol-*1-t* (D-glucitol-*6-t*)	66.6
D-Mannono-γ-	D-Mannitol-*1(6)-t* [c]	76.6
L-Rhamnono-γ-	L-Rhamnitol-*1-t*	75.5
D-*glycero*-D-*gulo*-Heptono-γ-	D-*glycero*-D-*gulo*-Heptitol-*1-t*	67.4
Lactobiono-γ-	4-*O*-β-D-Galactopyranosyl-D-glucitol-*1-t*	61.3

[a] Experimental details are given in section 4.2.
[b] The products had an activity of approximately 19 millicuries per millimole.
[c] The preparation of D-mannitol-*1(6)-t* from 2,3:5,6-di-*O*-isopropylidene-D-mannofuranose was described in an earlier publication [3].

TABLE 3. *Reduction of ketoses with lithium borohydride-t* [a]

Ketose	Alditol-*2-t*	Radiochemical yield [b]
		%
D-Fructose	D-Mannitol-*2(5)-t*	43.2
	D-Glucitol-*2-t*	42.1
L-Sorbose	L-Gulitol-*2-t*	27.9
	L-Iditol-*2(5)-t*	
D-Tagatose	D-Galactitol-*2-t*	22.9
	D-Talitol-*2-t*	59.5
D-*gluco*-Heptulose	D-*glycero*-D-*gluco*-Heptitol-*2-t*	22.6
	D-*glycero*-D-*ido*-Heptitol-*2-t*	32.1
D-*manno*-Heptulose	D-*glycero*-D-*galacto*-Heptitol-*2-t*	33.2
	D-*glycero*-D-*talo*-Heptitol-*2-t*	60.0

[a] Experimental details are given in section 4.3.
[b] Yields were determined by isotope dilution.

2. Nomenclature of Position-Labeled Alditols and Related Ketoses

The presence of an isotopic atom at a definite position in the molecule of an alditol gives rise to certain problems of nomenclature. An alditol that has *no axis or plane of symmetry* is related to two aldoses. If this alditol is position-labeled, the position of the label is designated differently in the two names. For example, the alditol obtained by reducing D-glucose-*1-*C^{14} may be named either D-glucitol-*1-*C^{14} or L-gulitol-*6-*C^{14}.

An unlabeled alditol that has a *plane of symmetry* is a *meso* compound derivable from either the D or the L form of an unlabeled aldose. However, this alditol is truly asymmetric if position-labeled, and is classified as D or L according to the configuration and the position of the label. Thus, D-galactitol-*1-t* is enantiomorphic with L-galactitol-*1-t*, but is identical with L-galactitol-*6-t*; similarly, D-xylitol-*1-*C^{14} may also be named L-xylitol-*5-*C^{14}.

An alditol that has an *axis of symmetry* is related to only one aldose. Because the two parts of the molecule are identical, the corresponding atoms or groups are indistinguishable. For instance, in D-mannitol, the structure and configuration are the same at C1 and C6 (as well as at C2 and C5, and at C3 and C4). Hence, if the alditol is labeled in one position of the molecule, it is labeled also in the corresponding position. Thus, for example, the alditol obtained by reducing D-mannose-*1-*C^{14} is D-mannitol-*1(6)-*C^{14}.

Certain of the alditols are oxidized to ketoses by *Acetobacter suboxydans*. This organism oxidizes a compound containing the structure 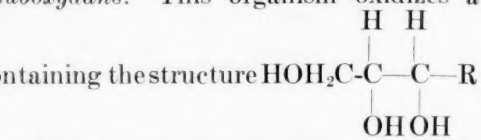 by converting the group at the penultimate carbon atom to -C- [11]. Table 4 lists the labeled ketoses that can be produced by *A. suboxydans* from 1-tritium-labeled alditols having six or fewer carbon atoms. D-Fructose-*1(6)-t* and L-sorbose-*6-t* have already been prepared. The latter sugar is an intermediate for the preparation of L-ascorbic-*6-t* acid.

3. Apparatus and Materials

The reductions were conducted in a closed system, in 50-ml flasks each having a rubber-capped side-arm for the injection of liquids. The flasks were attached to a vacuum manifold, which was part of the equipment previously described for collecting and handling tritium gas [3].

Lithium borohydride-*t* was prepared from nonradioactive lithium borohydride by hydrogen-tritium exchange. Solutions of lithium borohydride-*t* in dry tetrahydrofuran were then prepared by the procedure given in ref [3].

TABLE 4. *Tritium-labeled alditols and ketoses derivable from aldoses* [a]

Aldoses	Alditols-*t*	Ketoses-*t* [b, c]
D-Glycerose	D-Glyceritol-*1-t* (L-glyceritol-*3-t*)	Dihydroxyacetone-*1(3)-t*.
L-Glycerose	L-Glyceritol-*1-t* (D-glyceritol-*3-t*)	Dihydroxyacetone-*1(3)-t*.
D-Erythrose	D-Erythritol-*1-t* (L-erythritol-*4-t*)	L-*glycero*-Tetrulose-*4-t*.
L-Erythrose	L-Erythritol-*1-t* (D-erythritol-*4-t*)	L-*glycero*-Tetrulose-*1-t*.
D-Threose	D-Threitol-*1(4)-t*	
L-Threose	L-Threitol-*1(4)-t*	
D-Arabinose	D-Arabinitol-*1-t* (D-lyxitol-*5-t*)	D-*threo*-Pentulose-*5-t*.
L-Arabinose	L-Arabinitol-*1-t* (L-lyxitol-*5-t*)	
D-Lyxose	D-Lyxitol-*1-t* (D-arabinitol-*5-t*)	D-*threo*-Pentulose-*1-t*.
L-Lyxose	L-Lyxitol-*1-t* (L-arabinitol-*5-t*)	
D-Ribose	D-Ribitol-*1-t* (L-ribitol-*5-t*)	L-*erythro*-Pentulose-*5-t*.
L-Ribose	L-Ribitol-*1-t* (D-ribitol-*5-t*)	L-*erythro*-Pentulose-*1-t*.
D-Xylose	D-Xylitol-*1-t* (L-xylitol-*5-t*)	
L-Xylose	L-Xylithol-*1-t* (D-xylitol-*5-t*)	
D-Allose	D-Allitol-*1-t* (L-allitol-*6-t*)	L-Psicose-*6-t*.
L-Allose	L-Allitol-*1-t* (D-allitol-*6-t*)	L-Psicose-*1-t*.
D-Altrose	D-Altritol-*1-t* (D-talitol-*6-t*)	D-Tagatose-*6-t*.
L-Altrose	L-Altritol-*1-t* (L-talitol-*6-t*)	
D-Galactose	D-Galactitol-*1-t* (L-galactitol-*6-t*)	
L-Galactose	L-Galactitol-*1-t* (D-galactitol-*6-t*)	
D-Glucose	D-Glucitol-*1-t* (L-gulitol-*6-t*)	L-Sorbose-*6-t*.
L-Glucose	L-Glucitol-*1-t* (D-gulitol-*6-t*)	
D-Gulose	D-Gulitol-*1-t* (L-glucitol-*6-t*)	
L-Gulose	L-Gulitol-*1-t* (D-glucitol-*6-t*)	L-Sorbose-*1-t*.
D-Idose	D-Iditol-*1(6)-t*	
L-Idose	L-Iditol-*1(6)-t*	
D-Mannose	D-Mannitol-*1(6)-t*	D-Fructose-*1(6)-t*.
L-Mannose	L-Mannitol-*1(6)-t*	
D-Talose	D-Talitol-*1-t* (D-altritol-*6-t*)	D-Tagatose-*1-t*.
L-Talose	L-Talitol-*1-t* (L-altritol-*6-t*)	

[a] Relationships are illustrated for compounds having six or fewer carbon atoms.
[b] Ketoses derivable from sterically suitable alditols, through oxidation by *Acetobacter suboxydans*. The other alditols listed do not have the requisite configuration for attack by *A. suboxydans*.
[c] Systematic names are as follows: L-*ribo*-hexulose(L-psicose); D-*lyxo*-hexulose (D-tagatose); L-*xylo*-hexulose(L-sorbose); and D-*arabino*-hexulose (D-fructose).

Radioactivity assays were made with a 2π, windowless, gas-flow, proportional counter. Materials with low activity were counted in films of sodium *O*-(carboxymethyl)cellulose on 2-in. planchets [2]. Those with high activity were assayed as solutions in formamide. The procedure was essentially the same as that developed for the assay of carbon-14 [12], but was standardized with a sample having known tritium content. The counting efficiency is extremely low, but the precision of the method is excellent. Under the conditions used, one count per second is equivalent to 0.128 μc of tritium.

4. Procedures

4.1. Preparation of Alditols-*1*-*t* From Aldoses

A magnetic stirring bar and 4 millimoles of the aldose to be reduced were placed in a 50-ml reaction flask equipped with a rubber-capped side-arm. The flask was attached to the vacuum manifold and evacuated. The connection of the reaction flask to the manifold was closed, and the flask was cooled in a shallow ice-bath resting on a magnetic stirrer.

Five milliliters of ice-water containing 1 millimole (106 mg) of sodium carbonate was injected through the rubber cap by means of a hypodermic needle and syringe. The stirrer was started, and 2 ml of a solution containing 1.0 millimole (22 mg) of lithium borohydride-*t* in dry tetrahydrofuran was added by needle through the rubber cap; stirring was continued for 15 minutes. The solution was allowed to stand at room temperature for several hours (or overnight) and was then frozen in liquid nitrogen. The by-product hydrogen-*t*, formed by reaction of the lithium borohydride-*t* with water, was transferred to the manifold and either stored in a flask or converted to water-*t*. Finally, the connection to the manifold was closed and the flask was removed. The solvent (water and tetrahydrofuran) was evaporated in a rotary vacuum still equipped with a trap immersed in a dry-ice freezing bath. Water was added and the solution was again concentrated in the still; addition of water and concentration were repeated several times. Ultimately, the distillate in the trap was discarded as radioactive waste. The residue in the flask was dissolved in water, and the solution was passed through a column containing 10 ml of a cation-exchange resin. The effluent was evaporated to about 1 ml in the vacuum still; then, about 15 ml of methanol was added, and the solvent was again evaporated. Addition of methanol and evaporation were repeated several times in order to remove all boric acid as methyl borate. An aqueous solution of the residue was passed through a small column of mixed cation- and anion-exchange resins, and the effluent [4] was concentrated under reduced pressure. The residue was crystallized from hot ethanol or other suitable solvent, and the specific activity of the product was determined as described in section 3 and ref [2]. The alditol-*1*-*t* was recrystallized until the specific activity became constant.

4.2. Preparation of Alditols-*1*-*t* From Aldonic Lactones

The procedure for preparing 1-tritium-labeled alditols from aldonic lactones was the same as that described in section 4.1, except for the following changes: (a) 2 millimoles of the aldonic lactone were reduced in place of 4 millimoles of the aldose; (b) sodium carbonate was omitted in the reduction step; [5] and (c) 1.25 millimoles of lithium borohydride-*t* were used in place of 1 millimole.

4.3. Preparation of Alditols-*2*-*t* From Ketoses

The method for reducing ketoses with lithium borohydride-*t* was essentially the same as that given in section 4.1 for reducing aldoses. Two millimoles of the ketose were reduced with 0.5 millimole of lithium borohydride-*t* having an activity of approximately 9 mc per milliatom of hydrogen. The product was then treated as follows:

(a) The yields of the separate epimeric alditols-*2*-*t* were determined by an isotope-dilution technique. Aliquots of the solution containing approximately 5 μc of tritium were diluted with 100 mg of the nonradioactive alditol under investigation. The alditol carrier was then recrystallized repeatedly from a suitable solvent, ordinarily ethanol, until a product of constant activity was obtained. From the relative size of the aliquot used, the weight of the carrier taken, and the specific activity of the carrier after recrystallization, the total activity of the alditol in the parent solution was readily calculated.

(b) After removal of aliquots for analysis, the solution was concentrated and the epimeric alditols were separated by fractional crystallization, usually from ethanol. In most cases, one of the alditols crystallized more readily than the other; satisfactory separations were obtained by seeding the sirup with one epimer and removing the crystals of the substance before crystals of the other appeared. In some cases, the products were separated by addition of the nonradioactive alditol as carrier. The identity and purity of the alditol-*2*-*t* were confirmed by the following isotope-dilution technique:

A 1-mg sample of the purified alditol-*2*-*t* of known radioactivity was diluted with 100 mg of the pure, nonradioactive alditol. The carrier mixture was recrystallized three times, and the product was assayed for radioactivity. If A and B were, respectively, the specific activities of the alditol-*2*-*t* and the carrier mixture, then the purity of the alditol-*2*-*t* (in percent) was $(101B/A)\times 100$. All of the alditols reported in table 3 gave results within 4 percent of the expected value.

Appreciation is expressed to Joseph D. Moyer and Lorna T. Sniegoski, who conducted some of the laboratory work reported.

[4] The effluent, when tested with a conductivity meter, showed the absence of ionic impurities.

[5] Reduction of aldonic lactones to alditols is a two-step process, in the first of which the aldose is formed. Although an alkaline medium facilitates reduction of the aldose to the alditol, alkali tends to convert the lactone to the nonreducible salt. Hence, it was omitted in this reduction.

5. References

[1] NBS Tech. News Bul. **43,** 130 (1959); Chem. and Eng. News **37,** No. 39, 101 (1959).

[2] H. S. Isbell, H. L. Frush, and R. A. Peterson, J. Research NBS **63A,** 171 (1959).

[3] H. S. Isbell and J. D. Moyer, J. Research NBS **63A,** 177 (1959).

[4] H. S. Isbell, H. L. Frush, and N. B. Holt, J. Research NBS **64A,** 177 (1960).

[5] H. S. Isbell, H. L. Frush, and J. D. Moyer, J. Research NBS **64A,** 359 (1960).

[6] H. S. Isbell, H. L. Frush, and N. B. Holt, J. Research NBS **64A,** 363 (1960).

[7] M. Abdel-Akher, J. K. Hamilton, and F. Smith, J. Am. Chem, Soc. **73,** 4691 (1951).

[8] M. L. Wolfrom and H. B. Wood, J. Am. Chem. Soc. **73,** 2933 (1951); M. L. Wolfrom and K. Anno, J. Am. Chem. Soc. **74,** 5583 (1952).

[9] H. L. Frush and H. S. Isbell, J. Am. Chem. Soc, **78,** 2844 (1956).

[10] W. G. Brown, L. Kaplan, and K. E. Wilzbach, J. Am. Chem. Soc. **74,** 1343 (1952).

[11] R. M. Hann, E. B. Tilden, and C. S. Hudson, J. Am. Chem. Soc. **60,** 1201 (1938).

[12] A. Schwebel, H. S. Isbell, and J. D. Moyer, J. Research NBS **53,** 221 (1954) RP2537.

(Paper 64A5–67)

Publications of the National Bureau of Standards

Selected Abstracts

Electric polarizability of a short right circular conducting cylinder, T. T. Taylor, *J. Research NBS* **64B,** *No. 3, 135 (1960).*
A method similar to that employed by Smythe for calculating the capacitance of a freely charged short right circular conducting cylinder is used to calculate the electric polarizability tensor in the principal axis system for such a cylinder. Calculations to an accuracy of approximately five significant figures are carried out for cylinders with radius to half-length ratios of ¼, ½, 1, 2, and 4. The results are applicable to the design of artifical dielectrics.

Split Runge-Kutta method for simultaneous equations, J. R. Rice, *J. Research NBS* **64B,** *No. 3, 151 (1960).*
Consider two simultaneous first order differential equations $x'(t)=F(x, y, t), y'(t)=G(x, y, t)$. Runge-Kutta type integration methods are developed which allow different integration steps to be used for these equations. These methods retain the desirable properties of Runge-Kutta methods, namely the self-starting property and ease of change of integration step. Two different approaches are considered and extensive experimental work is reported upon. Experiments are done both in situations where these methods are advantageous and where they are not. It is seen that these methods are more efficient than the normal Runge-Kutta methods if they are at all applicable and in ideal situations they give the same accuracy with 90% less computation. These methods are applicable to six degree of freedom missile simulations, for which they were developed.

A reduction formula for partitioned matrices, E. V. Haynsworth, *J. Research NBS* **64B,** *No. 3, 171 (1960).*
A theorem of L. Goddard and H. Schneider, concerning square matrices A and B, of orders n and m respectively, which satisfy an equation $AX=XB$ for some $n\times m$ matrix X, is generalized here for rectangular matrices A and B, with dimensions $n_1\times n_2$, $m_1\times m_2$, which satisfy $AX_2=X_1B$, where X_i has dimensions $n_i\times m_i$ for $i=1,2$. This result is used to find reduction formulae for partitioned matrices with submatrices, A_{ij}, having dimensions $n_i\times n_j$, and satisfying equations $A_{ij}X_j=X_iB_{ij}$. The reduction formulae given here are also generalizations of a theorem by J. Williamson concerning partitioned matrices whose submatrices are all square and satisfy $AX=XB$, where B is triangular and X is square.

Phase angle master standard for 400 cycles per second, J. H. Park and H. N. Cones, *J. Research NBS* **64C,** *No. 3, 229 (1960).*
A continuously variable, 0 to 180 degree, phase shift standard for 400 c/s is described in detail. It consists of a π-section line made up of twelve 14.6° and three 4.3° sections to provide for two sizes of coarse steps and an RC circuit at the input to the line to provide for fine steps and a continuous fine control. A method for accurately adjusting the characteristic impedance of all π-sections to the same value, which is used as the termination, was devised. Under these conditions it is shown that the phase shift introduced by each π-section can be accurately computed from a measured value of inductance. The phase shift of each π-section was also determined by an experimental procedure dependent upon a 180° phase shift introduced by a toroidal transformer. The values obtained by these two independent methods agree to within 0.01 degree.

Disturbances due to the motion of a cylinder in a two-layer liquid system, L. H. Carpenter and G. H. Keulegan, *J. Research NBS* **64C,** *No. 3, 241 (1960).*
The disturbance created at the interface of a two-layer liquid system by the horizontal motion of a cylinder in the upper layer is studied for various sizes and shapes of cylinders, depths of the liquids, cylinder velocities, and density ratios. The disturbances fall into three categories. First, when the layers are of equal thickness, in most cases a train of progressive oscillatory waves is produced at the interface. Second, when the depth of the denser layer is much less than the depth of the fresh-water layer, the profile of the interface usually resembles that corresponding to positive internal solitary waves. Third, when the depth of the denser layer is much greater than the depth of the fresh-water layer, in most cases an internal hydraulic jump is produced. The characteristics of the disturbances in each category are related to the size of the cylinder, the depths of the liquids, the cylinder velocity, the density ratio, and the total distance of travel of the cylinder. A theoretical analysis is given for disturbances of the first category.

Microwave absorption in compressed oxygen, A. A. Maryott and G. Birnbaum, *J. Chem. Phys.* **32,** *No. 3, 686 (1960).*
Precise measurements of the absorption in oxygen resulting from the small magnetic dipole moment are reported at frequencies near 2.3, 9, and 23 kMc and at pressures in the range from 3 to 70 atoms. Up to 10 atmospheres the resonant contribution agrees with the Van Vleck-Weisskopf theory and the line width increases in proportion to the pressure. The line width (relaxation frequency) for the nonresonant contribution also increases in proportion to the pressure but is only about one-third as large as the resonant line width. Above 20 atmospheres the resonant absorption shows anomalous behavior resembling that previously noted in the case of the inversion spectra of NH_3 and ND_3. In particular, the resonant frequency appears to decrease rapidly while the line width changes much less rapidly than the pressure.

Studies of infrared absorption spectra of solids at high pressures, E. R. Lippincott, C. E. Weir, A. Van Valkenburg, and E. N. Bunting, *Spectrochim. Acta* **16,** *p. 58 (1960).*
Infrared spectra of solids were studied with a diamond pressure cell in the wavelength range 5–15 μ at pressures between 1 atm and 50,000 atm. The calibration of the cell at the 14,000 atm transition of $NaNO_2$ is described. Spectra were studied for aromatic organic compounds, inorganic hydrates, and ammonium halides. In general, band shifts produced by pressure were to higher frequencies and at most 10 cm^{-1}/10,000 atm. Many bands exhibited large changes in intensity. Occasionally bands increased in intensity or were unaffected but in general a decrease in intensity was observed at elevated pressure. Representative spectra are given, one to a pressure of 160,000 atm. Suggestions for the causes of the frequency shifts are given.

Nickel-aluminum alloy coatings produced by electrodeposition and diffusion, D. E. Couch and J. H. Connor, *J. Electrochem. Soc.* **107,** *No. 4, 272 (1960).*
Nickel-aluminum alloy coatings were produced by diffusion of aluminum electrodeposited over nickel. The aluminum was plated from baths operated at 25°–1000° C. The alloys were much harder than nickel and were superior to nickel coatings in salt spray, atmospheric exposure, and air oxidation tests. Attempts to codeposit the two metals were not successful.

Energy requirements of mechanical shear degradation in concentrated polymer solutions, A. B. Bestul, *J. Chem. Phys.* **32,** *No. 2, 350 (1960).*
Molecular weight decrease by mechanical shearing results when solutions of around 10% of polyisobutene having average molecular weights above 500,000 are forced through a capillary at nominal rates of shear above 10,000 sec^{-1}. Comparison of observed plots of shear load *vs* duration of shearing at fixed rates of shear during this degradation process with the corresponding estimated plots which would be expected to obtain if degradation did not occur provide a means of evaluating the amount of applied shearing energy

which is dissipated by the degradation process. The result is several hundred thousand kilocalories per mole of broken bonds, which is several thousand times the bond energy of carbon-carbon bonds. This finding is consistent with the hypothesis that whenever a bond breaks the system loses much of the free energy temporarily stored in bonds and macromolecular chains located in a comparatively large volume surrounding the broken bond, these bonds and chains having been involved in concentrating the required activation energy into the ruptured bond.

Low-temperature transport properties of commercial metals and alloys. II. Aluminums, R. L. Powell, W. J. Hall, and H. M. Roder, *J. Appl. Phys.* **31,** *496 (1960).*
The thermal conductivity, electrical resistivity, Lorenz number, thermoelectric force, and thermoelectric power are given in the temperature range 4°–120° K for ten aluminums and aluminum alloys: high-purity, 1100–F, 1100–O, 3003–F, 2024–T4, 5052–O, 5083–O, 5086–F, 5154–O, and 6063–T5. Four of the samples show a maximum in thermal conductivity, the others do not. For the four high-thermal conductivity samples the separate components in the electronic thermal resistivity are resolved; for the others, components in both the electronic and the lattice thermal resistivities are given. The residual electrical resistivities vary from 2.5×10^{-8} to 3.2×10^{-6} ohm-cm. The Lorenz numbers for the high-conductivity samples fall considerably below the Sommerfeld value 2.44×10^{-8} watt-ohm/°K^2; those for the low-conductivity samples are somewhat above the Sommerfeld value. The thermoelectric power of some of the alloys is positive with respect to the high-purity sample, for others it is negative. The various properties, methods of analysis, and separation of components are discussed in detail.

Low-temperature transport properties of commercial metals and alloys. III. Gold-cobalt, R. L. Powell, M. D. Buncb, and E. F. Gibson, *J. Appl. Phys.* **3,** *504 (1960).*
The thermal conductivity, electrical resistivity, and Lorenz number are given in the temperature range 4–100°K for the widely used thermocouple wire, gold-2.1 atomic percent cobalt alloy. The total thermal conductivity is relatively low: from 0.01 watt/cm°K at 4°K to 0.23 at 100°K. The lattice contribution to the total thermal conductivity is larger than the electronic contribution. The electrical resistivity is nearly independent of temperature, but does have a definite minimum of about 1.20×10^{-5} ohm-cm at 30°K. Because of the relatively large contribution of the lattice term to the total thermal conductivity, the Lorenz number is considerably above the electronic Sommerfeld value, 2.44×10^{-8} watt-ohm/°K^2.

Infrared studies of dense forms of ice, E. R. Lippincott, C. E. Weir, and A. Van Valkenberg, *Communication to Editor, J. Chem. Phys.* **32,** *No. 3, 612 (1960).*
Preliminary infrared studies in the water-ice system at high pressures have been conducted. Spectra in the 1μ–15μ range were obtained for liquid water, Ice I, and for ice at two elevated pressures at about −27°C. At 9,000 atm the run is in the Ice VI field and at 3,000 atm it is close to the II–III transition line. Although the exact phases cannot be specified because of uncertainties in equilibrium the spectra at elevated pressures differ markedly from Ice I. The details of the patterns are interpreted as indicating weak hydrogen bonding in dense ices with an O–H . . . O angle differing from 180°.

Several new methods to measure the thermal diffusivity of semiconductors, J. H. Becker, *J. Appl. Phys.* **31,** *No. 3, 612 (1960).*
The techniques suggested in this note are well suited for measurements of thermal diffusivity on small semiconducting samples. The thermal diffusivity is derived from changes in the steady-state temperatures when the front surface of the specimen is heated at a sinusoidally time-varying rate (ac) and in some cases with a nontime-varying component (dc). The temperature changes are usually deduced from thermal-electric effects produced in the samples. These effects include the *bolometric, Nernst,* and *Seebeck* effects. The bolometric effect depends upon the variation of the electrical conductivity with temperature ($d\sigma/dT$), while the Nernst and Seebeck effects depend upon the Nernst coefficient Q_n, and thermoelectric power θ , respectively.

Correlation effects in impurity diffusion, J. R. Manning, *Phys. Rev.* **116,** *No. 4, 819 (1959).*
Expressions are developed giving the correlation factor for an impurity diffusing in an otherwise pure lattice. These expressions will apply in general since, in the derivation, there is no requirement that there must be a large binding energy tending to create vacancy-impurity complexes. When this requirement is eliminated, accurate expressions can be obtained even for the nonclose packed lattices. Both vacancy and interstitialcy mechanisms are treated. A matrix method developed by LeClaire and Lidiard for the face-centered cubic lattice is applied to various lattices to obtain approximate expressions for the correlation factor. Then a correction is applied giving the effect of those dissociating vacancies (or interstitialcies) which return to the impurity. It is found that the effect is the same as if only a fraction of the dissociative jumps actually occurred. If it is assumed that the effect of an impurity is quite localized, the probability of return can be calculated in a very straightforward manner. It is shown that the effect of returning vacancies (or interstitialcies) can be quite important. The resulting expressions are used to estimate the correlation factor in nondilute alloys.

Cavity resonator dielectric measurements on rod samples, H. Bussey, *Insulation, p. 26 (Nov. 1959).*
Resonant cavity methods of measuring dielectric constant are especially valuable when the sample is in the shape of a rod. The rod is put on the axis of a circular cylindrical cavity. Some problems encountered in this method are the long and involved calculations, errors due to a hole in the cavity and plate for inserting a sample, the inconvenience of the necessary frequency changes when TM_{0m0} modes are used, and the difficulty of making accurate Q measurements. Solutions to all of these problems are available at 9000 Mc, and to some extent at other microwave frequencies. Based on experimental data and theory, hole corrections have been obtained both for TM_{0m0} and TE_{011} modes. These corrections are very small for the TE_{011} mode, and since this mode is tuneable, a simple measuring system without frequency shifts can be set up, with an accurate micrometer moving the end plate. Q measurements may be made with this micrometer too. Instead of measuring Q, however, the change in cavity transmission and a theoretical calculation of the change of iris coupling can be used to obtain the sample loss. The automatic computer is used to evaluate the raw data, or to form curves and tables to be used in making calculations. Measurements on sapphire rods have shown that the sensitivity for tan δ is about 3×10^{-5} at 9000 Mc.

A technique for reducing errors in permeability measurements with coils, B. L. Danielson and R. D. Harrington, *Proc. IRE* **48,** *No. 3, 365 (1960).*
A method is described for eliminating the majority of the errors associated with permeability measurements using coils containing toroidal magnetic materials of rectangular cross section. Data is given to support the technique, and it is shown that correct answers can be obtained even for a small number of turns on the coil.

Low temperature phase transition of colemanite, A. Perloff and S. Block, *Letter to Editor, Am. Mineralogist, p. 229 (1960).*
Precession photographs of the *hOl* and *Okl* reciprocal lattice nets of colemanite [$CaB_3O_4(OH)_3\cdot H_2O$] were taken at room temperature and at −30°C using Mo K_α radiation with a Zr filter. Within the limits of error there was no change in the cell dimensions, which agree with the published values, and no changes were observed on the *Okl* net. However, the low temperature *hOl* net contained very weak reflections from the $70\bar{1}$, $50\bar{2}$, $90\bar{5}$, and $70\bar{6}$ planes which establishes that the glide plane does not exist in the low temperature form. The transition between the room temperature $P2_1/a$ phase and the low temperature $P2_1$ phase is readily reversible.

Magnetic properties of polycrystalline materials, D. M. Grimes, R. D. Harrington, and A. L. Rasmussen, *J. Phys. Chem. Solids* **12,** *28 (1959).*
The variation of the magnetic Q with internal magnetization is discussed using both the domain rotation and the domain-wall motion model of magnetization change. The variation of the reversible susceptibilities with magnetic moment is reported on four samples, and the results are compared with results from the frequency spectra in the initial and remanent states. The distribution of magnetic moments in the system as a function of angle between individual and averaged moments is discussed in terms of an infinite series expansion in Legendre polynomials. The coefficients of the first four terms can be measured. Experimental data are given for the first three.

Low angle X-ray diffraction of fibrous polyethylene, A. S. Posner, L. Mandelkern, C. R. Worthington, and A. F. Diorio, *J. Appl. Phys.* **31,** *No. 3, 536 (1960).*
Highly axially oriented fibers of linear polyethylene are shown to display four orders of well defined, meridionally directed diffraction maxima corresponding to a fundamental spacing of 408 A. An interpretation of the low angle X-ray pattern is given in terms of the fiber morphology and the Hess-Kiessig postulate as to the origin of the periodic variation in electron density. The relative macroscopic length of the fibers was systematically altered both by thermal treatment and by crosslinking, melting, and recrystallization. The magnitude of the spacings observed does not bear any direct relation to the change in length incurred, but reflects the change in crystallite size that develops because of annealing, partial melting or the introduction of crosslinks. It is also shown that in a completely shrunken fiber, where wide-angle X-ray diffraction shows that the crystallites are randomly arranged relative to one another, discrete diffraction maxima are observed at about 255 A. These maxima are, however, circular in shape. Intermediate types of line shapes are also observed, which depend solely on the crystallite orientation and not on the method by which the orientation is developed.

The source-function in a non-equilibrium atmosphere. IV. Evaluation and application of the net-radiative-bracket, R. N. Thomas, *Astrophys. J.* **131,** *429 (1960).*
The net rate of a radiative transition between two atomic energy levels depends upon the local radiation field through a factor which we define as the Net Radiative Bracket (NRB). The results of previous papers in this series are applied to show that NRB depends only upon the ratio of radiation absorbed in the line to the local value of the source function in the line and to evaluate this ratio as a function of optical depth in the line. These results may also be applied to the question of the local energy balance in a chromosphere-type atmosphere and to the problem of radiative stability.

The melting temperature of natural rubber networks, D. E. Roberts and L. Mandelkern, *J. Am. Chem. Soc.* **82,** *No. 5, 1091 (1960).*
The isotropic melting temperatures, T_m^i, of natural rubber networks which were formed either by chemical reaction or by the action of ionizing irradiation were determined by dilatometric techniques. Substantial depression of the melting temperature with increasing amounts of crosslinking was observed for networks formed from randomly coiled chains irrespective of the method by which the crosslinks were introduced. It is also found that the melting temperatures of networks formed from highly ordered chains are substantially greater than corresponding networks formed from random chains. The difference in melting temperatures for these two types of networks can be quantitatively attributed to the decrease in configurational entropy of the former type networks which occur as a consequence of the chain disposition at the time of their formation.

Ionic charges of glass surfaces and other materials, and their possible role in the coagulation of blood, D. Hubbard and G. L. Lucas, *J. Appl. Physiol.* **15,** *No. 2, 265 (1960).*
Some observations on the physicochemical role played by glass surfaces in accelerating the "normal" coagulation rate of blood have been made, in light of the nonmigratable negative ionic charge which appears on leached glass surfaces and the orientation of the positively charged calcium ions of the blood at the fluid-glass interface. Numerous other materials, including artificial arteries, heart valves, bandages and "live" skin, have been investigated with respect to the ionic nature of their surfaces and their effect on blood coagulation. An effort was made to establish the ionic charge of the endothelial layer of the circulatory system; however, the procedure used in this investigation does not lend itself to *in vivo* or even convincingly to *in vitro* determinations. The ionic nature of the materials was determined from the uneven distribution of $Ag(NH_3)_2^+$ and Br^- ions in full-strength aqueous ammonia, caused by the nonmigratable ionic charge characteristic of the surfaces. Such data appear to be qualitatively acceptable provided the material does not form any compound with either $Ag(NH_3)_2^+$ or Br^- ions which is more insoluble than AgBr, or does not have an isoelectric point between pH 7 and pH 13.3.

Emission spectra of N_2, O_2, and NO molecules trapped in solid matrices, H. P. Broida and M. Peyron, *J. Chem. Phys.* **32,** *No. 4, 1068 (1960).*
Molecular systems are observed in emission in solid products from a gas discharge trapped at liquid helium temperature. Previous tentative molecular assignments have been checked with the help of isotopic substitutions of oxygen and nitrogen. The Herzberg system (A bands) of oxygen ($A^3\Sigma_u^+ - X^3\Sigma_g^-$) is analyzed and the molecular constants are derived for a molecule trapped in a nitrogen matrix. Another system (M bands) is attributed to the NO molecule ($^4\pi - X^2\pi$).

Correction for systematic wavelength shifts in atomic beam devices, R. L. Barger and K. G. Kessler, *J. Opt. Soc. Am.* **50,** *No. 4, 352 (1960).*
Light emitted or absorbed by atoms in an atomic beam is shifted in frequency relative to the frequency for a stationary atom if the light ray is not normal to the trajectory of the atom. When photoelectric measurements are made by observing, on the optical axis, the central spot of an interference pattern, this shift is caused by any non-orthogonality between the atomic beam axis and the optical axis. When an interference pattern is photographed, an additional shift is present which varies in magnitude along the radius of the pattern. The magnitude of the shift is calculated for each case, and devices which correct for this effect are described. These devices, consisting of a spherical mirror or a system of plane mirrors with a beam splitter, combine light from both sides of the atomic beam. This gives one positive and one negative shift which compensate to give the true frequency. For photoelectric recording of interference fringes, complete compensation can be achieved. In the case of photographic recording, it is shown that the residual relative frequency shift $\delta\nu/\nu$ is normally less than about one part in 10^{12}.

Theory of the magnetic and spectroscopic properties of neptunium hexafluoride, J. C. Eisenstein and M. H. L. Pryce, *Proc. Roy. Soc.* **A255,** *181 (1960).*
The magnetic properties and the optical absorption spectrum of NpF_6 are interpreted on the basis of an appropriate model for the molecule. The theory, in its simplest form, is not in perfect accord with all the available data. Consequently various physical effects such as covalence, vibronic interaction, the coriolis force on the unpaired electron, and the John-Teller effect which might affect the agreement of theory and experiment are discussed in a qualitative or semi-quantitative way. It is pointed out that the g-value may vary with temperature so that one must be cautious when comparing the paramagnetic resonance and susceptibility data with theoretical predictions. Numerous experiments which would help to clarify the interpretation are suggested.

High pressure form of analcite and free energy change with pressure of analcite reactions, H. S. Yoder, Jr., and C. E. Weir, *Am. J. Sci.* **258-A,** *420 (1960).*
The compressibility of four natural analcites has been obtained up to 10,000 atm. at 25° C. All specimens show abnormal compressibility and one exhibits a reversible tran-

sition at about 8,400 atm. Abnormal increase of compressibility with pressure usually precedes a transition, and it is concluded that a similar transition lies at higher pressures than those investigated for the three remaining specimens. The compressibility and density data were used with previously obtained data to compute the volume change and free energy change with pressure for the reactions 2 analcite $\rightleftharpoons$ nepheline + albite + 2 water, analcite $\rightleftharpoons$ jadeite + water, and analcite + quartz $\rightleftharpoons$ albite + water. The volume change for all the reactions is negative for all pressures investigated at 25° C.

The increase in birefringence after compression in the analcite which exhibited the transition is attributed to either strain induced by the volume discontinuity or by retention of a possible lower symmetry of the high-pressure form. Lower symmetry in a high-pressure form is not uncommon in previously investigated substances.

Class of nonlinear dielectric materials, P. H. Fang, R. S. Roth, and H. Johnson, *J. Am. Ceram. Soc.* **43,** *No. 3, 169 (1960).*

A class of non-linear dielectric materials has been found, the members of which are formed by the reaction of a $BaNb_2O_6$ and a perovskite-type phase. At low temperature, dielectric hysteresis loops appear, similar to usual ferroelectric loops. Since one component of these new materials can be a transition element, it may be possible to find materials which are both ferroelectric and ferrimagnetic.

Bremsstrahlung linear polarization, J. W. Motz and R. C. Placious, *Nuovo Cimento* **15,** *Series X, 571 (1960).*

This work presents a general quantitative description of the bremsstrahlung linear polarization on the basis of original experimental data and available theoretical calculations. The results give the dependence of the polarization on (a) the initial electron kinetic energy, T_0, in a range from 10^{-2} to 10^3 Mev, (b) the photon energy in a range from 0.1 T_0 to T_0, (c) the photon emission angle in a range from 0 to 180 degrees, and (d) the atomic number of the target in a range from 4 to 79. The experimental data were obtained for a range of electron energies from 0.05 to 1.0—Mev with beryllium, aluminum, and gold targets. Theoretical estimates of the polarization were calculated from the Sommerfeld-Kirkpatrick-Wiedmann results for the nonrelativistic energy region, the Olsen-Maximon results for the extreme relativistic energy region, and the Gluckstern-Hull (Born approximation) results for the intermediate energy region. Final results are expressed in terms of the peak polarization and the corresponding peak angle as a function of the electron and photon energies, and the most accurate estimates of the polarization are given on the basis of the combined experimental and theoretical data.

Chemically induced vibrational excitation: hydroxyl radical emission in the 1–3 micron region produced by the H+O_3 atomic flame, D. Garvin, H. P. Broida, and H. J. Kostkowski, *J. Chem. Phys.* **32,** *No. 3, 880 (1960).*

A detailed investigation has been performed in the 1- to 3-μ wavelength region on the radiation emitted by the hydroxyl radical from a low-pressure flame of ozonized oxygen and atomized hydrogen. Wavelengths and photon intensities have been obtained for about 300 lines in the OH vibration-rotation bands V–V–ΔV where $\Delta V=3$, $V=9$ to 5, and for $\Delta V=2$, $V=9$ to 2. Relative photon band intensities have been determined from the overdetermined set of data by a method of successive approximations using an IBM 650 computer. Dipole moment parameters have been calculated using the above data and Morse oscillator transition probabilities.

Approximate rotational and vibrational Boltzmann distributions exist with an average rotational "temperature" of 560° K for the P branches, 460°K for the R and Q branches, and a vibrational "temperature" of 9250°K for the $\Delta V=2$ and 3 bands. The absence of radiation from levels $V>9$ confirms the nonthermal character of the excitation and its dependence on the energetics of the reaction $O_3+H\rightarrow OH+O_2$. Moreover, flux calculations based on the assumption that in this case collisional deactivation transition probabilities are proportional to the radiation probabilities show that there is an appreciable OH production in all levels $V\leq 9$ and the main flux of OH through any population level is via $\Delta V=1$ transitions. Possible causes for the large changes in line intensity with pressure and smaller but significant changes with flows or concentrations are discussed.

Photographs of the high-altitude nuclear explosion "Teak," W. R. Steiger and S. Matsushita, *J. Geophys. Research* **65,** *No. 2, 545 (1960).*

A sequence of four photographs of the August 1, 1958, high-altitude nuclear explosion "Teak" near Johnston Island in the Pacific is shown. These photographs were taken from Maui, Hawaii, at an altitude of 3050 meters and 1300 km from the explosion. Three main features of these photographs are evident and are discussed: an auroral arc directed southward; an expanding envelope; and an airglow cloud. The auroral arc extending southward from the explosion is interpreted as the glow produced by a stream of β-decay electrons directed along the earth's magnetic field. This arc apparently extended into the southern hemisphere and was observed from Apia, Samoa. The expanding envelope is interpreted as an excitation-recombination phenomenon produced by an expanding shock front. By assuming an average speed of propagation of 1.3 km/sec of the shock front, the times at which the photographs were taken are estimated. The airglow cloud is interpreted as a residue of ionized material having a lifetime estimated at 15 to 30 minutes. Assuming an electron density of 10 times the normal F_2-region value, an effective recombination coefficient of 10 times the normal F_2 value is obtained. The airglow cloud ascended at a rate of approximately 1000 m/sec and expanded horizontally at a rate of approximately 300 m/sec.

Appraisal of Land's work on two-primary color projections, D. B. Judd, *J. Opt. Soc. Am.* **50,** *No. 3, 254 (1960).*

An analysis of the results of Land's experiments with two-primary color projections has been carried out in terms of the known phenomena of object-color perception. It is shown that no new theory is required for the prediction of Land's result that two-primary color projections can produce object-color perceptions of all hues; nor for his result that many choices of pairs of primaries yield substantially the same object-color perceptions. Land's hypothesis that when the colors of the patches of light making up a scene are restricted to a one-dimensional variation of any sort, the observer usually perceives the objects in that scene as essentially without hue, is new; several special cases of it are supported by previous work as well as Land's. This hypothesis deserves the serious attention of research workers in object-color perception.

Other NBS Publications

Journal of Research, Section 64B, No. 3, July–September 1960. 75 cents.

Electric polarizability of a short right circular conducting cylinder. T. T. Taylor. (See above abstract.)
Distribution of quantiles in samples from a bivariate population. M. M. Siddiqui.
Split Runge-Kutta method for simultaneous equations. J. R. Rice. (See above abstract.)
A reduction formula for partitioned matrices. E. V. Haynsworth. (See above abstract.)
Selected bibliography of statistical literature, 1930 to 1957: III. Limit theorems. L. S. Deming.

Journal of Research, Section 64C, No. 3, July–September 1960. 75 cents.

A new method of measuring gage blocks. J. B. Saunders.
Gage blocks of superior stability: initial developments in materials and measurement. M. R. Meyerson, T. R. Young, and W. R. Ney.

Variation of resolving power and type of test pattern. Francis E. Washer and William P. Tayman.
A multiple isolated-input network with common output. C. M. Allred and C. C. Cook.
Phase angle master standard for 400 cycles per second. J. H. Park and H. N. Cones. (See above abstract.)
Disturbances due to the motion of a cylinder in a two-layer liquid system. L. H. Carpenter and G. H. Keulegan. (See above abstract.)

Journal of Research, Section 64D, No. 5, September–October 1960. 70 cents.

ELF electric fields from thunderstorms. A. D. Watt.
Field strength measurements in fresh water. G. S. Saran and G. Held.
Electrical resistivity studies on the Athabasca Glacier, Alberta, Canada. G. V. Keller and F. C. Frischknecht.
Amplitude distribution for radio signals reflected by meteor trails. A. D. Wheelon.
Computation and measurement of the fading rate of moon-reflected UHF signals. S. J. Fricker, R. P. Ingalls, W. C. Mason, M. L. Stone, and D. W. Swift.
On the theory of wave propagation through a concentrically stratified troposphere with a smooth profile. H. Bremmer.
Polarization and depression-angle dependence of radar terrain return. I. Katz and L. M. Spetner.
Methods of predicting the atmospheric bending of radio rays. B. R. Bean, G. D. Thayer, and B. A. Cahoon.
Loss in channel capacity resulting from starting delay in meteor-burst communication. G. R. Sugar.
Elementary considerations of the effects of multipath propagation in meteor-burst communication. G. R. Sugar, R. J. Carpenter, and G. R. Ochs.
Use of logarithmic frequency spacing in ionogram analysis. G. A. M. King.
Guiding of whistlers in a homogeneous medium. R. L. Smith.
Propagation of microwaves through a magneto-plasma, and a possible method for determining the electron velocity distributions. A. L. Cullen.
On electromagnetic radiation in magneto-ionic media. H. Kogelnik.
Radiation and admittance of an insulated slotted-sphere antenna surrounded by a strongly ionized plasma sheath. J. W. Marini.
A contribution to the theory of corrugated guides. G. Piefke.
High-gain, very low side-lobe antenna with capability for beam slewing. A. C. Wilson.
Shielding of transient electromagnetic signals by a thin conducting sheet. N. R. Zitron.
Cylindrical antenna theory. R. H. Duncan and F. A. Hinchey.

Table of wavenumbers, 2000 A to 7000 A, C. D. Coleman, W. R. Bozman, and W. F. Meggers, NBS Mono. 3, Vol. I (1960) $6.00.
Mercury barometers and manometers, W. G. Brombacher, D. P. Johnson, and J. L. Cross, NBS Mono. 8 (1960) 40 cents.
Bibliography on molecular and crystal structure models, D. K. Smith, NBS Mono. 14 (1960) 15 cents.
Calibration of line standards of length and measuring tapes at the National Bureau of Standards, L. V. Judson, NBS Mono. 15 (1960) 15 cents (supersedes NBS Circ. 572).
Quarterly radio noise data—March, April, May 1959, W. Q. Crichlow, C. A. Samson, R. T. Disney, and M. A. Jenkins, NBS Tech. Note 18–2 (PB151377–2) (1960) $1.00.
Analog-digital conversion equipment for electrocardiographic data, L. Taback, NBS Tech. Note 42 (PB151401) (1960) $1.25.
A summary of VHF and UHF tropospheric transmission loss data and their long-term variability. D. A. Williamson, V. L. Fuller, A. G. Longley, and P. L. Rice, NBS Tech. Note 43 (PB151402) (1960) $2.25.
Tables for the statistical prediction of radio ray bending and elevation angle error using surface values of the refractive index, B. R. Bean, B. A. Cahoon and G. D. Thayer, NBS Tech. Note 44 (PB151403) (1960) 50 cents.
Operating instructions for ARN–2 auxiliary log-linear noise recorder, R. T. Disney and C. A. Samson, NBS Tech. Note 45 (PB151404) (1960) 50 cents.
Report on the IGY oblique-incidence sporadic *E* and *F*-scatter program, J. W. Finney and E. K. Smith, Jr., NBS Tech. Note 48 (PB151407) (1960) $2.50.
Dynamic measurements of the magnetoelastic properties of ferrites, V. E. Bottom, NBS Tech. Note 49 (PB151408) (1960) $1.00.
Isotopic abundance ratios reported for reference samples stocked by the National Bureau of Standards, F. L. Mohler, NBS Tech. Note 51 (PB161552) (1960) 50 cents.
Field strength calculations for E.L.F. radio waves, J. R. Wait and N. F. Carter, NBS Tech. Note 52 (PB161553) (1960) 50 cents.
Physical properties of synthetic-rubber-base dental impression materials, W. A. C. Miller, Jr., W. C. Hansen, G. Dickson, and W. T. Sweeney, J. Am. Dental Assoc. **60,** 211 (1960).
The effect of multipath distortion on the choice of operating frequencies for high-frequency communication circuits, D. K. Bailey, IRE Trans. Ant. Prop. **AP-7,** No. 4, 397 (1959).
Liquid hydrogen from chemical and nuclear rockets, R. B. Scott, Discovery **XXI,** No. 2, 74 (1960).
Phosphorescence of nitrogen and nitrogen-argon deposited films at 4.2° K, H. P. Broida and R. W. Nicholls, Letter to Editor J. Chem. Phys. **32,** No. 2, 623 (1960).
Peculiarities of the ionosphere in the far east: A report on IGY observations of sporadic *E* and *F*-region scatter, E. K. Smith, Jr., and J. W. Finney, J. Geophys. Research **65,** 885 (1960).
Detecting radiation, L. Costrell, Chem. Eng. News, p. 132 (1960).
Opportunities in dental research, G. C. Paffenbarger, J. Am. Dental Assoc. **60,** 413 (1960).
Departures of hydrogen from L.T.E. in a stellar atmosphere and the consequent structure of the solar chromosphere, S. R. Pottasch, Commun. Observ. Roy. Belgique No. 157, entitled The empirical determination of the stellar photospheric structure, Paper 11, 67 (1959).
Pilot plant data for hydrogen isotope distillation, T. M. Flynn, Chem. Eng. Progr. **56,** No. 3, 37 (1960).
VLF phase characteristics deduced from atmospheric waveforms, A. G. Jean, W. L. Taylor, and J. R. Wait, J. Geophys. Research **65,** 907 (1960).
Short-wave fadeouts without reported flares, H. DeMastus and M. Wood, J. Geophys. Research **65,** No. 2, 609 (1960).
On the propagation of ELF radio waves and the influence of a nonhomogeneous ionosphere, J. R. Wait, J. Geophys. Research **65,** No. 2, 597 (1960).
Precision Zeeman modulation microwave spectrometer, R. W. Zimmerer, Rev. Sci. Instr. **31,** 106 (1960).
Chemistry, food, and civilization, A. T. McPherson, J. Wash. Acad. Sci. **50,** No. 3, 1 (1960).
World maps of *F*2 critical frequencies and maximum usable frequency factors for use in making ionospheric radio predictions, D. H. Zacharisen and V. Agy, J. Geophys. Research **65,** 593 (1960).
Recent experimental evidence favouring the $pK_1(p)$ correlation function for describing the turbulence of refractivity in the troposphere and stratosphere, K. A. Norton, J. Atmospheric and Terrest. Phys. **15,** 206 (1959).
Prediction of sunspot numbers for cycle 20, W. B. Chadwick, Nature, p. 1787 (1959).
The melting of crystalline polymers, L. Mandelkern, Rubber Chem. and Technol. **XXXII,** No. 5, 1392 (1959).,
Sampling of leather, J. Mandel and C. W. Mann, J. Sci. and Ind. Research **18A,** No. 12, 575 (1959).
Atmospheric limitations on electronic distance measuring equipment, M. C. Thompson, Jr., H. B. Janes, and F. E. Freethey, J. Geophys. Research **65,** 389 (1960).
Weighted restricted partitions, M. Newman, Acta Arith. **V,** 371 (1959).
A continuous poker game, A. J. Goldman and J. J. Stone, Duke Math. J. **27,** No. 1, 41 (1960).

Proposed specification for impression material; synthetic rubber base, dental, W. A. C. Miller, Jr., W. C. Hansen, G. Dickson, and W. T. Sweeney, J. Am. Dental Assoc. **60,** 224 (1960).

Some results on the cross-capacitances per unit length of cylindrical three-terminal capacitors with thin dielectric films on their electrodes, D. G. Lampard and R. D. Cutkosky, Inst. Elec. Engrs. (London, England) Monograph No. 351M, 1 (1960).

A class of non-linear dielectric materials, P. H. Fang, R. S. Roth, and H. Johnson, J. Am. Ceram. Soc. **43,** 169 (1960).

The linear viscoelastic behavior of rubberlike polymers and its molecular interpretation, R. S. Marvin, Viscoelasticity: Phenomenological aspects, p. 27 (Academic Press, New York, N.Y., 1960).

Low-frequency solar bursts and noise storms, A. Boischot, R. H. Lee, J. W. Warwick, Astrophys. J. **131,** No. 1, 61 (1960).

Mass spectrometry, V. H. Dibeler and R. M. Reese, Anal. Chem. **32,** No. 5, 211 (1960).

The components of power appearing in the harmonic analysis of a stationary process, M. M. Siddiqui, presented at Symp. on Statistical Methods in Radio Wave Propagation, Univ. California, Los Angeles, June 18–20, 1958, reprinted from Statistical methods in radio wave propagation (Pergamon Press, New York, N.Y., 1960).

Mechanical and electromechanical properties of indium antimonide, R. F. Potter, J. H. Wasilik, and R. B. Flippen, Ch. 12, Mechanical properties of intermetallic compounds, p. 265 (John Wiley & Sons, Inc., New York, N.Y., 1960).

Electrometric pH determination, R. G. Bates, Chimia **14,** 111 (1960).

Measurement of radiation exposure at the walls of medical X-ray rooms for determining protective barrier requirements, S. W. Smith and J. R. Brooks, ATOMPRAXIS **6,** No. 3, 77 (1960).

Introduction—Can you measure it? L. V. Judson, Am. Soc. Tool & Mfgr. Engrs. Tech. Paper 239, Book 1, 60, 1 (1960).

Some fundamentals of modern dimensional metrology, I. H. Fullmer, Am. Soc. Tool & Mfgr. Engrs. Tech. Paper 240, Book 1, 60, 1 (1960).

The error in prediction of $F2$ maximum usable frequencies by world maps based on sunspot number, E. L. Crow and D. H. Zacharisen, sec. II, Radio propagation phenomenology, in Statistical methods in radio wave propagation, p. 248 (Pergamon Press, New York, N.Y., 1960).

The use of 2,2,4,4,6,8,8-heptamethylnonane as a primary diesel fuel, T. W. Mears, R. M. David, and F. L. Howard, ASTM Bul. No. 245, p. 75 (1960).

Sinn und bedeutung der strahlenschutznormen, L. S. Taylor, Rontgen-Blatter **XIII,** Heft 2, 33 (1960).

Geomagnetic disturbance and velocity of slow-drift solar radio bursts, M. B. Wood and C. S. Warwick, Nature **184,** No. 4697, 1471 (1959).

Thermoelectric effects, H. P. R. Frederikse and W. W. Scanlon, ch. 7.6, Methods of experimental physics, Vol. VI, p. 114 (Academic Press, Inc., New York, N.Y., 1959).

The outlook for machine translation, F. L. Alt, Proc. Western Joint Computer Conf., Vol. 17, p. 203, San Francisco, Calif. (May 1960).

Further evidence of a solar corpuscular influence on large-scale circulation at 300 Mb, N. J. MacDonald and W. O. Roberts, J. Geophys. Research **65,** No. 2, 529 (1960).

Method for measurement of E'/I' in the reciprocity calibration of condenser microphones, W. Koidan, J. Acoust. Soc. Am. **32,** No. 5, 611 (1960).

Microphone diaphragm null method for sound pressure measurements, W. Koidan, J. Acoust. Soc. Am. **32,** No. 4 505 (1960).

An evaluation of a cesium beam frequency standard, R. C. Mockler, R. E. Beehler, J. A. Barnes, Symp. Quantum Electronics—Resonance Phenomena, p. 127 (Columbia University Press, New York, N.Y.) 1960.

Publications for which a price is indicated (except for NPS Technical Notes) are available only from the Superintendent of Documents, U.S. Government Printing Office, Washington 25, D.C. (foreign postage, one-fourth additional). Technical Notes are available only from the Office of Technical Services, U.S. Department of Commerce, Washington 25, D.C. (Order by PB number.) Reprints from outside journals and the NPS Journal of Research may often be obtained directly from the authors.

UNITED STATES
GOVERNMENT PRINTING OFFICE
DIVISION OF PUBLIC DOCUMENTS
WASHINGTON 25, D.C.

OFFICIAL BUSINESS

PENALTY FOR PRIVATE USE TO AVOID PAYMENT OF POSTAGE, $300 (GPO)

JOURNAL OF RESEARCH of the National Bureau of Standards
A. Physics and Chemistry

Vol. 64A, No. 5 September–October 1960

Contents

Page

Infrared spectrum of hydrobromic acid. Earle K. Plyler. 377

Determination of the value of the faraday with a silver-perchloric acid coulometer. D. N. Craig, J. I. Hoffman, C. A. Law, and W. J. Hamer. 381

Systems silver iodide-sodium iodide and silver iodide-potassium iodide. G. Burley and H. E. Kissinger. 403

Conformations of the pyranoid sugars. III. Infrared absorption spectra of some acetylated aldopyranosides. R. Stuart Tipson and Horace S. Isbell. 405

Dissociation constant of 4-aminopyridinium ion in water from 0 to 50 °C and related thermodynamic quantities. Roger G. Bates and Hannah B. Hetzer. 427

Tritium-labeled compounds VI. Alditols-*1-t* and alditols-*2-t*. Harriet L. Frush, Horace S. Isbell, and Alexander J. Fatiadi. 433

Publications of the National Bureau of Standards. 437

For sale by the Superintendent of Documents, U.S. Government Printing Office. Washington 25, D.C. Price 70 cents (single copy). Subscription price: $4.00 a year; $0.75 additional for foreign mailing.

UNITED STATES GOVERNMENT PRINTING OFFICE, WASHINGTON : 1960